論文 / 著書情報
Article / Book Information

題目(和文)	
Title(English)	Study of single layer slotted waveguide arrays
著者(和文)	榊原久二男
Author(English)	Sakakibara Kunio
出典(和文)	学位:博士(工学), 学位授与機関:東京工業大学, 報告番号:甲第3180号, 授与年月日:1996年3月26日, 学位の種別:課程博士, 審査員:
Citation(English)	Degree:Doctor (Engineering), Conferring organization: Tokyo Institute of Technology, Report number:甲第3180号, Conferred date:1996/3/26, Degree Type:Course doctor, Examiner:
学位種別(和文)	博士論文
Type(English)	Doctoral Thesis

Doctoral dissertation

Study of
single layer slotted waveguide arrays

December 1995

Under the supervision of

Professor Makoto Ando

Presented by

Kunio Sakakibara

Department of Electrical and Electronic Engineering

Tokyo Institute of Technology

Contents

Chapter 1. Introduction

1.1 Planar antennas

Planar antennas are arrays which consist of many radiation elements on the aperture. They are low profile, high efficiency and high applicability in comparison with low cost parabolic reflector antennas. Patch antennas fed by microstrip, triplate and suspended lines are popular planar antennas [1-1]-[1-3]. RLSA (Radial Line Slot Antennas) [1-4], which are developed in our laboratory, RLH (Radial Line Helical Antennas) [1-5] and RLMSA (Radial Line Micro Strip patch Antennas) [1-6] are planar antennas fed by radial waveguides [1-7]. Figure 1.1 summarizes the state of the antennas for DBS reception (12 GHz band) [1-8]. The antenna gain is proportional to the aperture size. The parabolic reflector antennas are low-efficiency for small antennas due to the spillover and the shadowing by the feed horn and the arm. They are suitable for the large antennas. The antenna efficiency of the planar antennas decreases with increasing the aperture size due to the feeding loss. The feeding loss of the radial waveguide is extremely small since it is a waveguide structure. High efficiency is realized even for large aperture in the respect of the radial waveguide antennas. The result of the single layer slotted waveguide array for DBS reception in Japan is also in the figure. The gain is relatively low. However, high efficiency of 75 % is obtained [1-9].

The feeding loss of the microstrip line degrades the antenna efficiency seriously in higher frequency band. Figure 1.2 summarizes the resultant antenna efficiency for the frequency and the gain [1-10]-[1-15]. The antenna efficiency of the microstrip and the triplate patch antennas still remains in the lower level for higher gain and higher frequency. The efficiency of the single layer slotted waveguide antenna results 75.6 % for high gain of 35.9 dBi in 22 GHz band. Furthermore, the efficiency of 60 GHz band antenna results 58.8 % for 35.1 dBi gain. Such a high efficiency can not be realized by any other type antennas in this frequency and gain range. High efficiency planar antennas with simple structure can be realized in this research.

1.2 High frequency application of planar antennas

Lower spectrum have been crowding and higher frequency such as millimeter-wave is planed to use with development of new technologies in recent years. 59~60 GHz is assigned experimental frequency band and 59~64 GHz is to-be-developed band for broad applications in order to advance the domestic development activities in Japan [1-16]. By using these frequency bands, several application systems are considered and developed intensively, such as the indoor wireless LAN (Local Area Network), COMETS (COMmunications and broadcasting Engineering Test Satellite), the car collision avoidance radar. Figure 1.3 shows required antenna performance of each millimeter-wave band application. The automotive radar requires highest antenna performance which covers the other use of the technology. One of the objectives of this dissertation is to realize the antenna performance for this use. The preceding trial is the development of the antenna for the entrance radio relay system which requires high-gain antenna in lower frequency band of 22 GHz than the millimeter-wave band.

1.2.1 Entrance radio relay system (22 GHz band)

Mobile communication is becoming popular and the number of base stations is growing rapidly. A lot of base stations have been connected to the central one by wired communication. High cost for installation of cables is serious problem for setting up the base stations on the top of the tall buildings. The entrance radio system is proposed for connecting base stations by wireless communication as is shown in Fig. 1.4 [1-17]. Three sizes of the antennas, 33, 39 and 45 dBi at 22.0 ~ 22.6 GHz and 22.6 ~ 23.2 GHz band, have been considered and the service has just started in Japan. High efficiency and low profile flat antennas are expected instead of parabolic antennas in order to install on the walls of the buildings. The first target is to realize the gain higher than 33 dBi in 600 MHz bandwidth at the 22 GHz band. The development of the antennas is located at the first step in order to apply to much higher frequency use.

1.2.2 Car collision avoidance radar (60 ~ 80 GHz band)

The radar technology for military use is adopt to the commercial use. In finding obstacles or other cars in forward direction, the system gives the information of their existence to the driver or brakes the vehicle automatically as is shown in Fig. 1.5 [1-18]-[1-21]. With an increasing in awareness of safety of vehicles and the background of public demand, the radar is becoming an important key-devices for protection from the car collision. The required characteristics of the radar antenna are as follows;

1. The beam width has to be small in order to obtain high angular resolution. The desired beam width is 2 degrees at half power points where the directional gain is 42 dBi.
2. The low side lobe and the large dynamic range up to 40 dB are necessary in order to suppress interference. A small sports car in the lane of operation and a large truck in the adjacent lane have to be distinguished.
3. Since the radar antenna is installed in front of a car, a low profile planar antenna is suitable.

This system requires high-gain, high-efficiency, low-profile antenna for high-frequency use. Two types of the systems; laser radar and millimeter-wave radar, are proposed. The development of the laser radar precedes the millimeter-wave antenna. The wavelength of the laser radar is shorter than that of the millimeter-wave radar. So, the laser radar is advantageous in terms of the cost and the size at present. However, the attenuation level of millimeter-wave is small in fog or dust compared with light. Furthermore, the antenna performances are degraded by adherence of mud or dirt on the antenna aperture of the laser radar. The millimeter-wave radar is extremely attractive for automotive use, considering that vehicles are intended to be driven in all types of weather.

1.3 Slotted waveguide planar antenna

A slotted waveguide planar antenna is an array of slots cut on the wall of the rectangular waveguide [1-22] [1-23]. Several types of slots are applied to the antenna as is shown in Fig. 1.6. Each of them is represented by an equivalent impedance, admittance or both. It depends upon the current direction the slot interrupts. For example, the longitudinal slot on the broad wall of the waveguide interrupts the

transversal current and is called as shunt slot. It is represented by parallel connected admittance in the equivalent circuit. The analysis which gives the equivalent admittance or impedance have been widely investigated [1-24]-[1-28]. The slotted waveguide arrays are substituted by the equivalent transmission model with the elements. In the design of the planar array, the transmission model includes the mutual coupling effects of the dominant mode in the waveguide, while the external mutual coupling has to be taken into account in the slot analysis [1-29]-[1-32].

In the conventional slotted waveguide antenna, even though it is the most simple one, a feed waveguide is attached at the back side of the radiation waveguides as is shown in Fig. 1.7. The radiation waveguides are fed from the feed waveguide by slot couplings. Since the structure of the antenna is complicated, it can not be applied to mass-production. Only military use have been the application of the antenna. Low cost and high efficiency are indispensable in order to adopt it to the commercial use. The antenna has to be mass-produceable with low transmission loss of the waveguide advantage.

1.4 Summary of this study

The single layer slotted waveguide arrays are extremely attractive in the respect of the simple structure. This dissertation fully investigate the characteristics of the single layer slotted waveguide array. We propose two types of single layer feed circuits. One is an in-phase feed circuit composed of π-junctions and another one is an alternating-phase feed circuit of T-junctions as is shown in Fig. 1.8. The T-junction is a new technology and is expected to be low loss. Most popular radiation slots are applied to both of the feed circuits in order to confirm its operation. Several types of slots; resonant shunt slots, cross slots and reflection canceling slot pairs, can be combined to these feed circuits according to the requirement as is shown in Fig. 1.9. Six types of the antennas are considered in combination of the two feed circuits and the three radiation slots. The combinations ①, ② and ④ are investigated in this dissertation.

Chap. 2 indicates the feature of the single layer slotted waveguide array. For higher frequency use of the antenna, scale model has the same characteristics with the original one proportional to the wavelength. However, the size of the structure such as the slot plate thickness, wall thickness and slot width are restricted in fabricating

limitations. For easy fabrication of the waveguide structure, this antenna consists of a slot plate and the groove structure. Close electrical contact between them is strongly required. Loss appear due to the incomplete contact between them by bonding and due to slot plate shrinkage by heating for welding or brazing. Such phenomena are observed in measurements and simulated by calculation. The alternating phase feed system is introduced in order to neglect the loss above mentioned. The basic operations are confirmed by the combination ④ in Fig. 1.9.

Chap. 3 presents the design applicable to any types of large arrays. The analysis in the design takes the mutual couplings from other slots in the infinite slot array into account by using Floquet's theorem. The slot parameters are related to the slot radiation by the analysis. In the array design, the desired radiation from each slots are assigned. Therefore all the slot parameters are determined systematically. The experiments and the calculation confirm that relatively large arrays can be simulated by the infinite slot arranging model.

Chap. 4 indicates the characteristics of the linearly-polarized shunt slot arrays (combination ①). The design of the array is systematically conducted as is mentioned in Chap. 3. The characteristics of the 22 and 60 GHz band slotted waveguide arrays are measured and calculated. The slot plate and the grooves are in contact by brazing. The peak gain and the antenna efficiency are 35.9 dBi and 75.6 % for 22 GHz band antenna and are 35.1 dBi and 58.8 % for 60 GHz band antenna, respectively.

Circularly-polarized cross slots are applied to the single-layer feed circuit (combination ②) in Chap. 5. The antenna is developed to use for the dual-polarization DBS in the United States. The antenna applied to the use of dual-polarization reception has two beams in different direction. One beam is right-hand circular polarization and another one is left-hand circular polarization. In order to obtain the identical characteristics of the two beams, the antenna structure has to be symmetrical. In this condition, the optimum distribution on the aperture is derived by the analysis of the calculus of variations. The slot structures are determined by the analysis of the method of moments for the desired slot excitation of the array. The basic characteristics of both operations are confirmed by experiments. The antenna efficiency of 71 % and 64 % for the right and left-hand circular polarization is obtained respectively, even though the aperture distributions are about 10 dB tapered.

Chap. 6 presents the advantages of the reflection-canceling slot pairs. The slot pair consist of two transversal slots located with spacing of a quarter of a guide wavelength on the broad wall of the rectangular waveguide. The reflections from the two slots are canceled because the path length difference corresponds to the phase difference of 180 degrees. Since the reflections are vanished in each element, traveling wave operation, strong coupling and array synthesis are expected. The measured and calculated characteristics of the one-dimensional array are compared with that of the resonant shunt slot array.

Chap. 7 summarizes the results of this study and presents the future studies of this work.

References

[1-1] Gupta, K. C., Garg, R., Bahl, I. J., *Microstrip lines and slotlines*, ARTECH, Chap. I

[1-2] Johnson, R. C. and Jasik, H., *Antenna Engineering Handbook*, New York McGraw-Hill, Chap. 9, 1984

[1-3] Pozar, D. and Schaubert, D., "Comparison of three series fed microstrip array geometries," *IEEE AP-S/URSI Sym. Digest*, pp. 728-731, June 1993

[1-4] Ando, M., Sakurai, K. and Goto, N., "Characteristics of a radial line slot antenna for 12 GHz band satellite TV reception," *IEEE Trans. on AP*, Vol. AP-34, No. 10, pp. 1269-1272, Oct. 1986

[1-5] Nakano, H., Takeda, H., Mimaki, H. and Yamaguchi, J., "A high-efficiency extremely low-profile helical array antenna," *1989 IEICE Natl. Conv. Rec.*, B-29, Oct. 1989

[1-6] Saito, S. and Haneishi, M., "Microstrip patch array fed by radial line," *IEICE Technical Report*, AP91-37, May 1991

[1-7] Marcuvitz, N., *Waveguide Handbook*, IEE Electromagnetic Waves Series 21, pp. 89-96

[1-8] Takahashi, M., "A study of single-layered radial line slot antennas," Doctoral dissertation, pp. 2-3, 15

[1-9] Hirokawa, J., Ando, M., Goto, N., Takahashi, N., Ojima, T. and Uematsu, M., "A single-layer slotted waveguide array antenna for mobile reception of direct broadcast

from satellite," *IEEE Trans. on VT*, Vol. 44, No. 3, Aug. 1995

[1-10] Weiss, M. A., " Microstrip antennas for millimeter waves," *IEEE Trans. on A.P.*, vol. AP-29, No. 1, pp. 171-174, Jan. 1981

[1-11] Huang, J., " A Ka-band circularly polarized high-gain microstrip array antenna," *IEEE Trans. on A.P.*, pp. 113-116, Jan., 1995

[1-12] Kado, S., Ohta, M., Hirao, M., Wakushima, S., Nozue, Y. and Haneishi, M., " Radiation properties of 22 GHz band triplate feed type patch antennas with parasitic elements," *IEICE Natl. Conv. Rec.*, B-53, March 1994

[1-13] Ohta, M., Ishizaka, H., Wakushima, S., Uesato, Y. and Haneishi, M., " Radiation properties of triplate-feed-type patch antennas at 60 GHz band," *IEICE Natl. Conv. Rec.*, B-114, Sep. 1993

[1-14] Ohta, M., Ishizaka, H., Kose, R., Saito, T., Okubo, N. and Haneishi, M., " Radiation properties of circularly polarized triplate-feed-type patch antennas at 60 GHz band," *IEICE Natl. Conv. Rec.*, B-115, Sep. 1994

[1-15] Kitao, S., Yamato, M., Ohmine, H., Aoki, H. and Haruyama, T., " Radiation properties of triplate line fed microstrip array antenna with polarization grid in the 60 GHz band," *IEICE Natl. Conv. Rec.*, B-60, Sep. 1995

[1-16] Millimeter-wave application system technology, *1995 Microwave Workshops and Exhibition Digest*, Dec. 1995, Yokohama, Japan

[1-17] *R.C.R. news*, No. 403, Research & Development Center for Radio Systems, May. 4, 1993

[1-18] Fukuhara, H., "Essential issues involved in radar based vehicle control systems," *APMC'94 Workshop Digest*, pp.91-95, Dec. 1994, Tokyo, Japan

[1-19] Meinel, H. H., "Commercial applications of millimeterwaves history, present status, and future trends," *IEEE Trans. on MTT*, Vol. 43, No. 7, pp. 1639-1653, July 1995

[1-20] "Crash avoidance FLR sensors," *Microwave Journal*, July 1994, pp.122-126

[1-21] "Low cost millimeter-wave radar systems for intelligent vehicle cruise control applications," *Microwave Journal*, Oct. 1995, pp.20-33

[1-22] Johnson, R. C. and Jasik, H., *Antenna Engineering Handbook*, New York McGraw-Hill, Chap. 9, 1984

[1-23] Collin, R. E. and Zucker, F. J., *Antenna theory*, Chap. 14, McGraw Hill, 1969

[1-24] Elliott, R. S. and Kurtz, L. A., "The design of small slot arrays," *IEEE Trans. on AP*, vol. AP-26, No. 2, pp.214-219, March 1978

[1-25] Elliott, R. S., "An improved design procedure for small arrays of shunt slots," *IEEE Trans. on AP*, Vol. AP-31, No. 1, pp. 48-53, Jan. 1983

[1-26] Oliner, A. A., "The impedance properties of narrow radiating slots in the broad face of rectangular waveguide Part I and II - Theory," *IRE Trans. on AP*, pp.4-20, Jan. 1957

[1-27] Josefsson, L. G., "Analysis of longitudinal slots in rectangular waveguides," *IEEE Trans. on AP*, Vol. AP-35, No. 12, Dec. 1987

[1-28] Yee, H. Y., "Impedance of narrow longitudinal shunt slot in a slotted waveguide array," *IEEE Trans. on AP*, pp.589-592, July 1974

[1-29] Edelberg, S. and Oliner, A. A., "Mutual coupling effects in large antenna arrays: Part I - Slot arrays," *IRE Trans. on AP*, pp.286-297, May 1960

[1-30] Wu, C. P. and Galindo, V., "Properties of a phased array of rectangular waveguides with thin walls," *IEEE Trans. on AP*, Vol. AP-14, No. 2, pp.163-173, March 1966

[1-31] Farrell, G. F., JR. and Kuhn, D. H., "Mutual coupling in infinite planar arrays of rectangular waveguide horns," *IEEE Trans. on AP*, Vol. AP-16, No.4, pp.405-414, July 1968

[1-32] Pozar, D. M. and Schaubert, D. H., "Analysis of an infinite array of rectangular microstrip patches with idealized probe feeds," *IEEE Trans. on AP*, Vol. AP-32, No. 10, pp.1101-1107, Oct. 1984

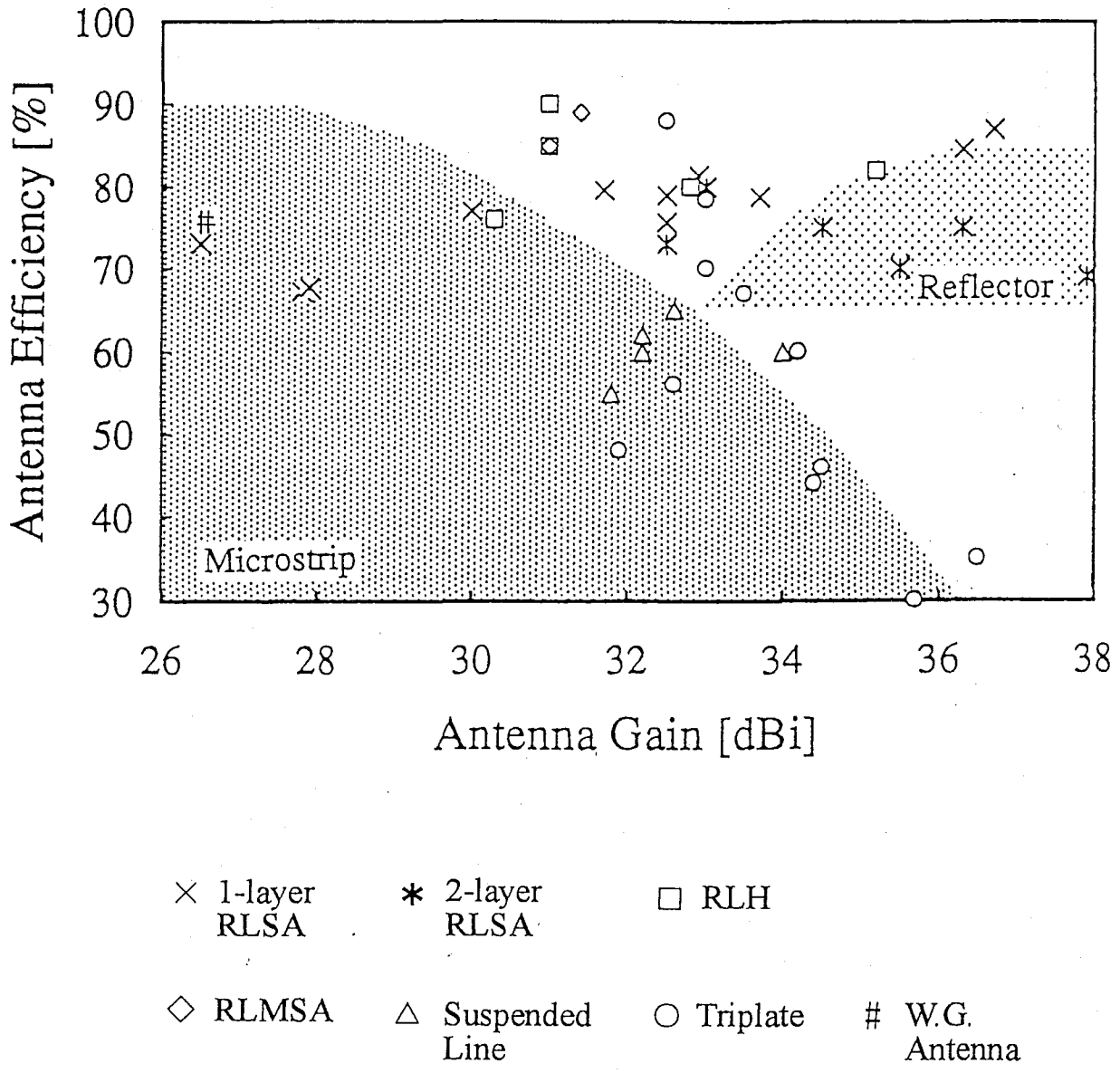

Fig. 1.1 Antenna efficiency of comercial DBS antennas

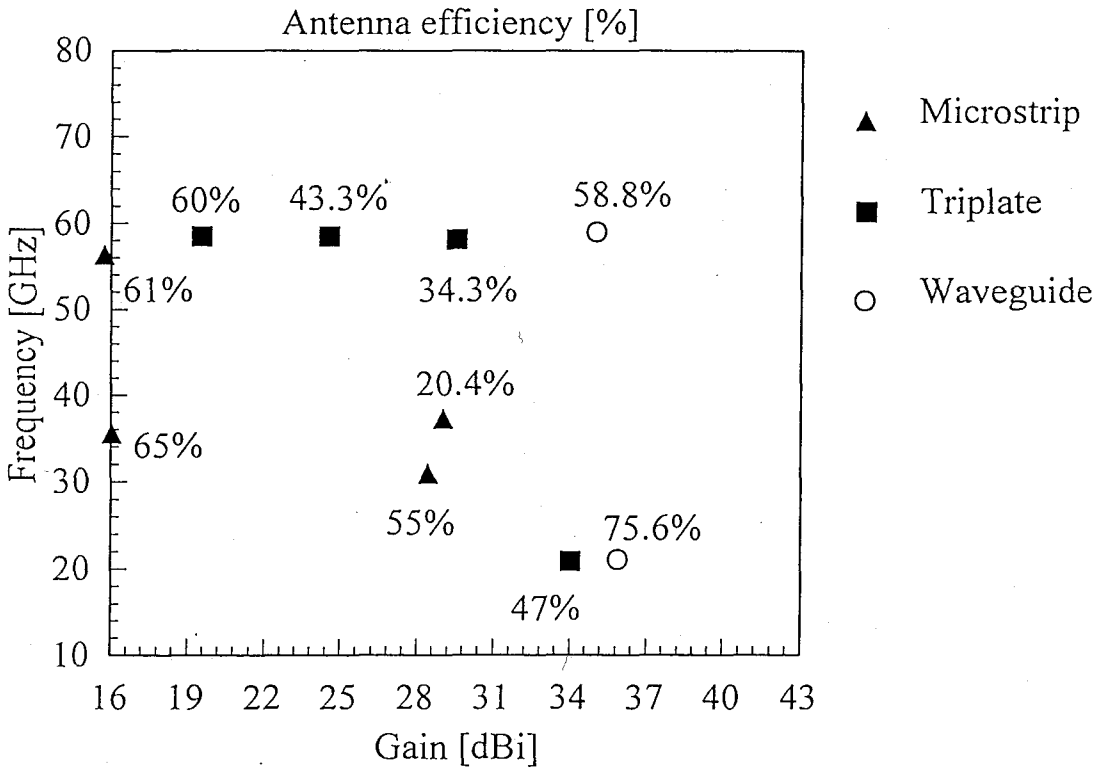

Fig. 1.2 Antenna efficiency of planar antennas related to frequency and gain

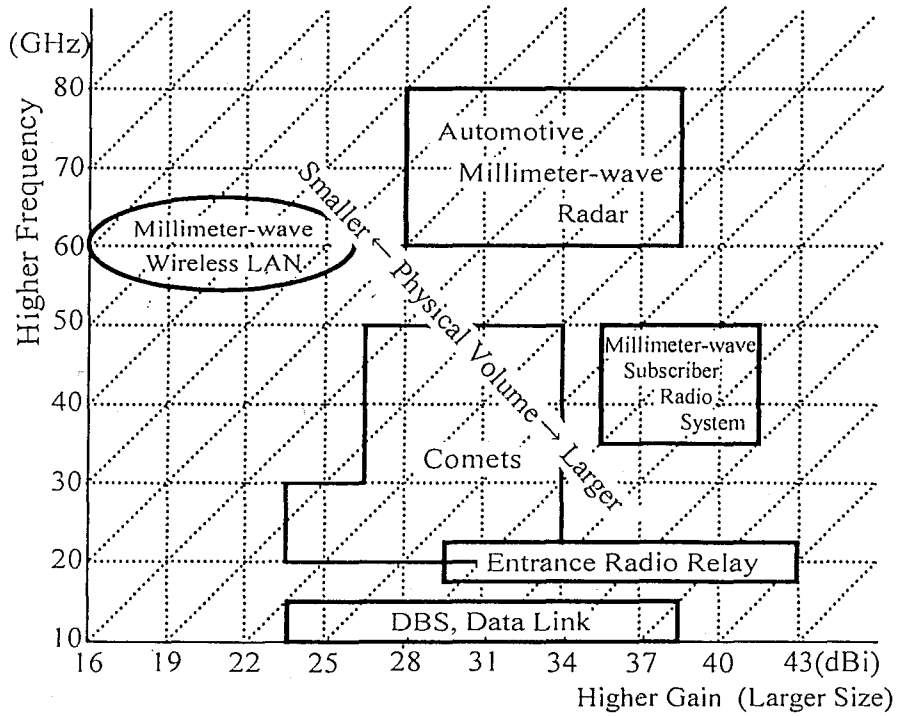

Fig. 1.3 Required antenna performance of millimeter wave applications

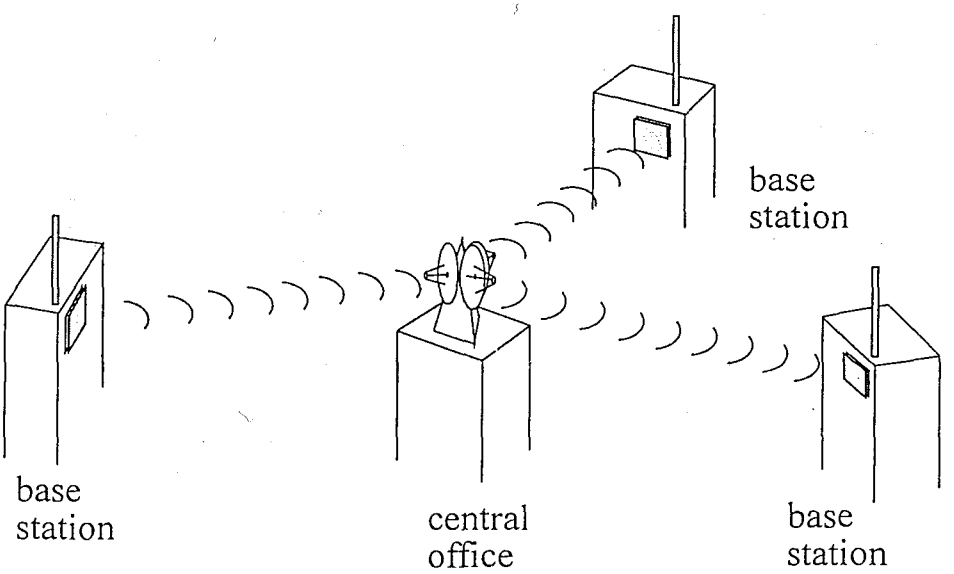

Fig. 1.4 Entrance radio relay system connecting base stations of mobile communincation

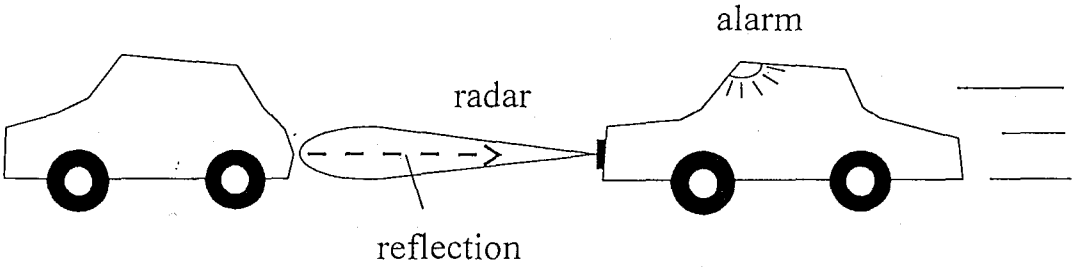

Fig. 1.5 Car collision avoidance radar

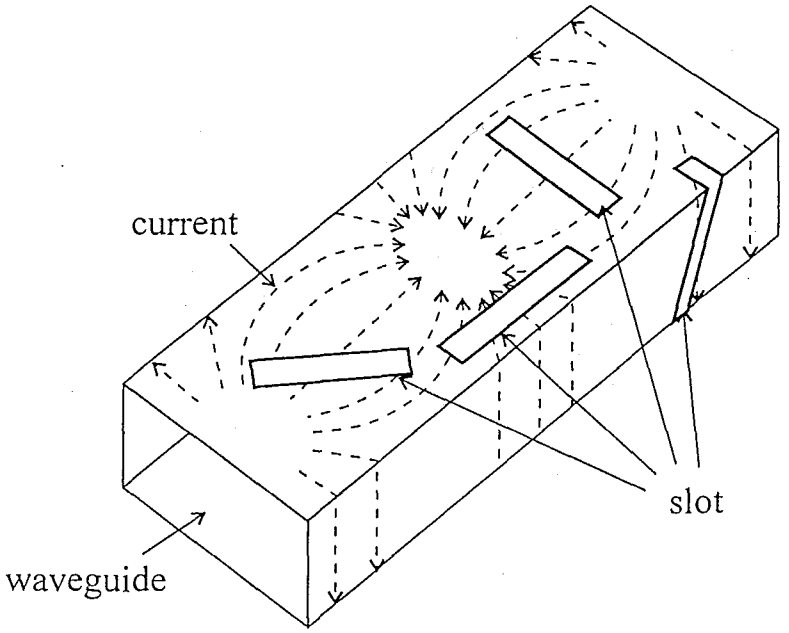

Fig. 1.6 Radiation slots on the waveguide

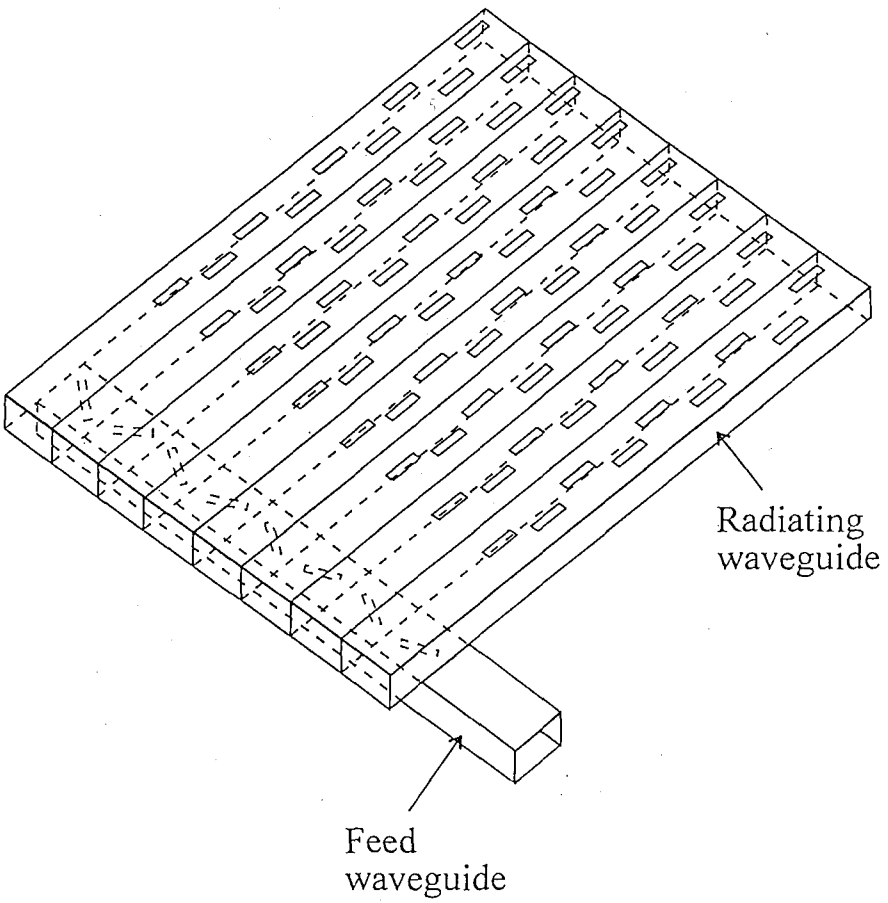

Fig. 1.7 Conventional slotted waveguide array

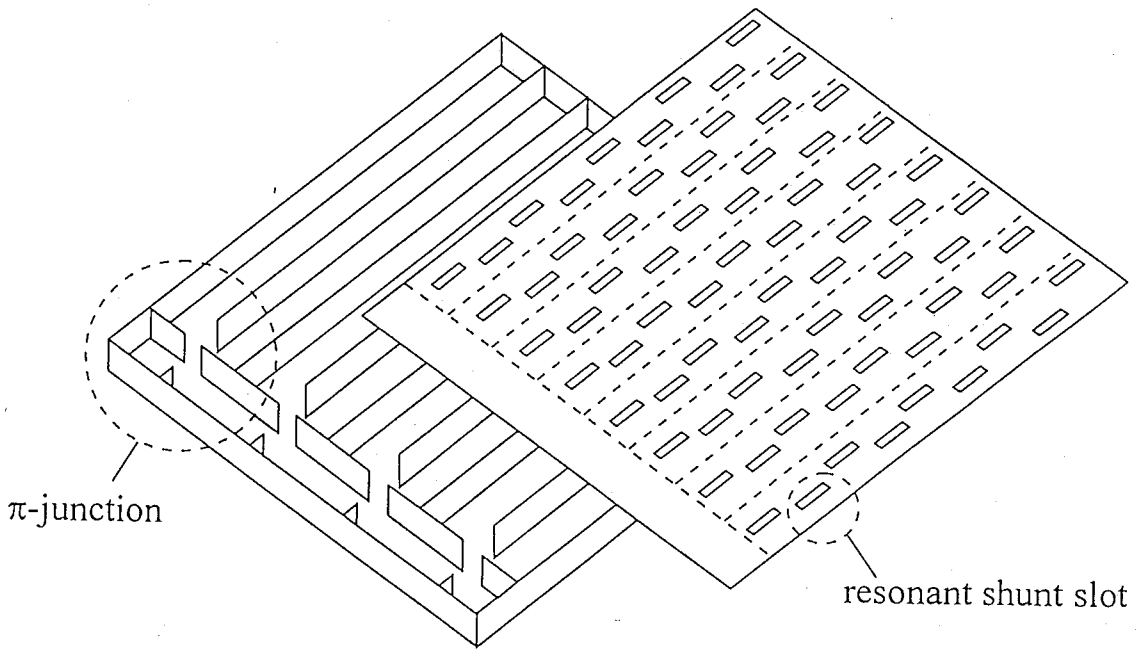

(a) In-phase feed circuit

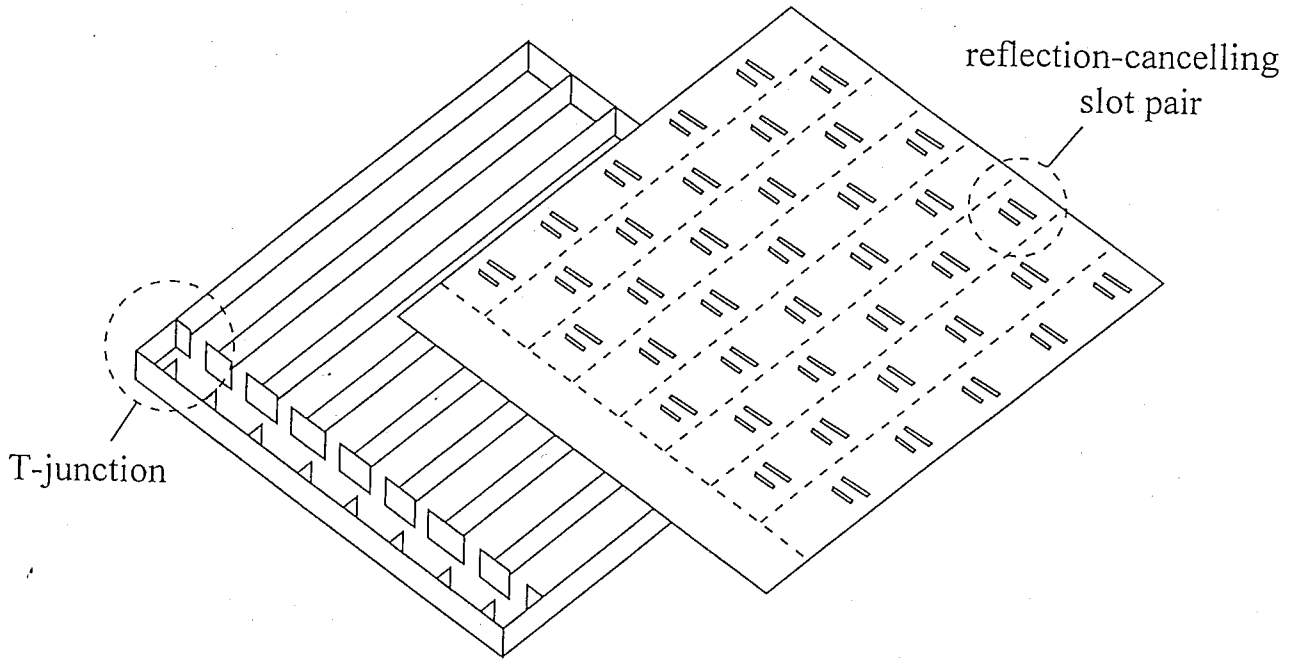

(b) Alternating phase feed circuit

Fig. 1.8 Single layer feed circuits

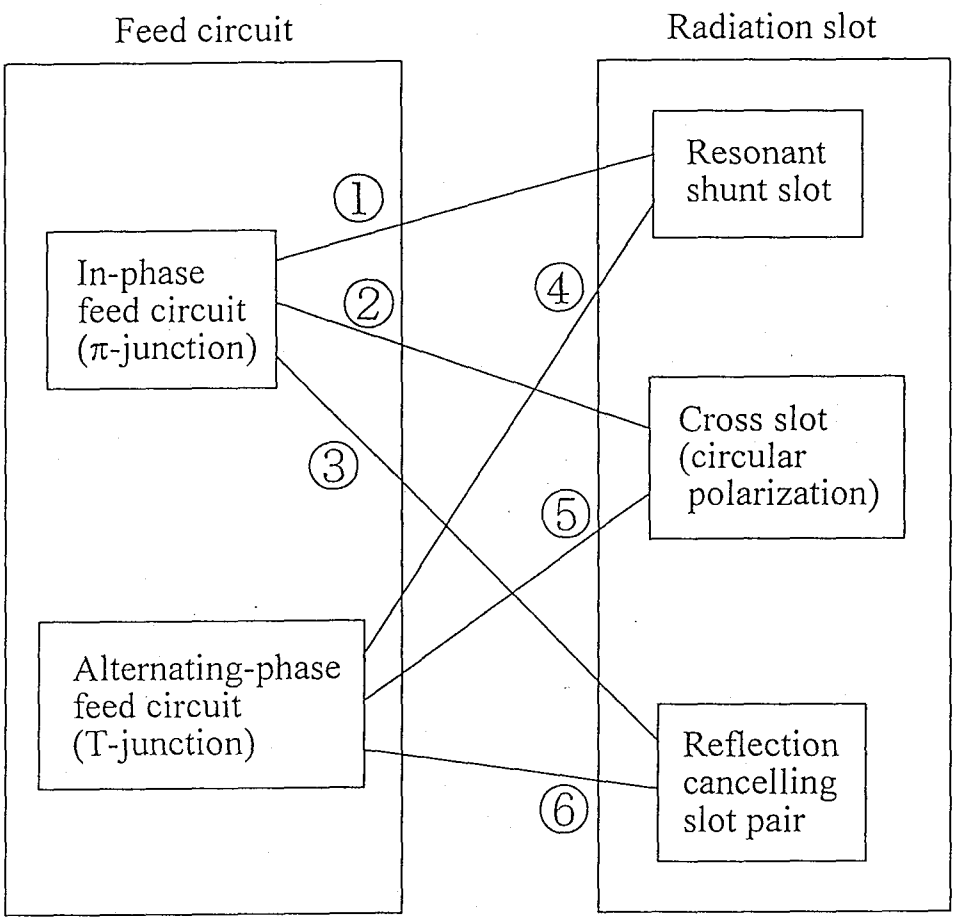

Fig.1.9 Combination of the feed circuit and radiation slot

Chapter 2. Single layer slotted waveguide array and key technology for higher frequency

2.1 Introductory remarks

Waveguide has an excellent characteristic of low transmission loss even in high frequencies such as K and Ka band. So, a slotted waveguide array is an attractive candidate of high efficiency planar antenna. However, it has not been used for commercial application in old days due to the complicated three-dimensional feed structure [2-1]. On the other hand, microstrip patch antennas are advantageous for cost reduction comparing with any other planar antennas due to the simple feed structure [2-2]–[2-4]. In high frequency use, insertion loss of the feed network can not be negligible. Low-profile single layer slotted waveguide arrays are developed in this dissertation [2-5] [2-6]. In the antenna, the feed waveguide is placed on the same layer of the radiation waveguide array. The antenna can be simply fabricated by placing the slotted plate on the groove feed structure. The structure is suitable for mass production and cost reduction. The slotted plate can be made by printing technology while the groove feed structure can be made by die casting. The fabrication has to be simplified without degrading the antenna efficiency. This chapter summarizes problems and possibility for higher frequency application. Resonant shunt slots are chosen for the radiation slots in this estimation.

It is one of key technologies to place the slotted plate on the groove feed structure in the accurate location and without the contact loss. This chapter investigate three ways to contact them; bonding, welding and brazing [2-7]. Test antennas sized 300 mm square are fabricated to compare the losses by measurements. Transmission loss exists in the waveguide of the bonding-type antenna. Shrinkage of the slot plate by heating in the welding-type antenna causes an error in slot location, which produces grating lobes. A frequency shift and a taper in the phase distribution along the feed

waveguide occur due to extension of the waveguide broad wall width and spacing of windows of the brazing-type antenna. It is because both plates are heated at the same time.

2.2 Structure of the single layer slotted waveguide antenna

Figure 2.1 shows the structure of a single-layer slotted waveguide array. The feed waveguide is attached on the same layer of the radiation waveguides. It is a cascade of π-junctions with an inductive walls. A window of the π-junction couples to two radiation waveguides in phase when the guide wavelength in the feed waveguide is set to be twice the width of the radiation waveguide including the wall thickness. All the radiation waveguides are fed in equal amplitude by controlling the widths of the windows in the π-junctions. Each π-junction is analyzed rigorously by Galerkin's method of moments [2-5] [2-6]. The coupling and reflection are estimated accurately and optimum parameters are obtained for dividing the power into equal amplitude and in phase.

Resonant shunt slots [2-8] are cut on a broad wall (slot plate) of the rectangular waveguide and are arranged parallel to the guide axis. The slot offset from the center of the waveguide is the parameter controlling amplitude of slot excitation, while slot spacing determines its phase. A slot with larger offset couples more strongly with magnetic field of TE_{10} mode; slot offset is small near the feed point and increases toward the termination, which results in a uniform aperture amplitude illumination. In order to avoid the growth of reflections at the feed point, a few degrees beam tilting θ_t is adopted by controlling slot spacing, as is usual with the case of general resonant slot arrays [2-9]. A matching slot consisting of a large slot with large offset and a short terminal is installed at the waveguide end in order to radiate all the residual power in the waveguide and quasi-traveling wave operation is realized.

2.3 Structural limitations in fabrication

2.3.1 Limitation of waveguide width

High frequency application is advantageous for downsizing the antenna. However, high accuracy is required in proportion to the wavelength. The dimension of each parts are limited by manufacturing accuracy. For example, ① The slot length has to be much larger than the slot width in order to suppress the cross polarization. ② The slot plate thickness should be much smaller than the slot length and width for enough slot coupling. The wall thickness h between the waveguides can not be small in order to contact the slot plate on the grooves. The slot spacing along the x-direction is expressed by

$$s_x = \frac{\lambda_f}{2} = a_g + h \qquad (2.1),$$

where λ_f and a_g are wavelength in the feed waveguide and broad width of the radiation waveguide, respectively. The slot spacing along the z-direction is expressed by

$$s_z = \frac{1}{\frac{2}{\lambda_g} - \frac{2}{\lambda_0}\sin\theta_t} \qquad (2.2),$$

where λ_0 and λ_g are wavelengths in free space and in the radiation waveguide, respectively. s_z is close to $\lambda_g/2$ when θ_t is small. The s_x and s_z should be smaller than λ_0 in order to suppress the grating lobes and to maintain the uniformity of the aperture distribution. Furthermore, when the guide wavelength is large, the waveguide has large conductor loss since the frequency is close to the cut off one. The relationship between λ_g and λ_f can be expressed from Eq. (2.1) and

$$a_g = \frac{\lambda_0}{2\sqrt{1-\left(\frac{\lambda_0}{\lambda_g}\right)^2}} \qquad (2.3)$$

by

$$\frac{1}{\lambda_g^2} + \frac{1}{\left(\lambda_f - 2h\right)^2} = \frac{1}{\lambda_0^2} \qquad (2.4)$$

The long line effects should appear equally along the feed and radiation waveguides. These wavelength λ_g and λ_f are chosen as almost the same with each other. Figure 2.2

shows the relationship between λ_g and λ_f expressed in (2.4) when frequency is 60 GHz and h = 1 mm. The region where both λ_g and λ_f are smaller than $2\lambda_0$ is small due to the large wall thickness.

2.3.2 Limitation of structure of T-junction at the input port

The antenna is fed from the T-junction at the center of the feed waveguide, which is advantageous in terms of long line effect. The structure of the T-junction of model 1 is shown in Fig. 2.3 (a). A matching inductive wall is installed at the opposite narrow wall of the feed waveguide against the input port. The wall is located on the axis of the waveguide center of the input port in order to divide the power equally. The structure is two-dimensional one and is analyzed by method of moments. Figure 2.4 shows the reflection characteristics with the optimum parameters for minimum reflection at 4 GHz band. Fine agreement is obtained between the measured and calculated ones. The reflection is lower than –20 dB in more than 25 % frequency bandwidth.

Reflection level is calculated as lower for thinner inductive wall. Reflection is about –12 dB for t = 10 mm although it is about –20 dB for t = 0.3 mm in 4 GHz as is shown in Fig. 2.4. The inductive wall is too thin to fabricate it in 60 GHz band. 0.3 mm in 4 GHz corresponds to 0.02 mm in 60 GHz band. In order to suppress the reflection even for thick inductive wall, iris is installed at the input port along the feed waveguide narrow wall of model 2 as is shown in Fig. 2.3 (b). Figure 2.5 shows the reflection characteristics with the optimum parameters at 4 GHz band for thick inductive wall. The reflection from the matched load is about –27 dB which is the limit of the experiment. Ripples are observed on the curves, which may be due to the reflection from the matched load. The frequencies which give minimum peaks of both measured and calculated curves agrees with each other. The optimum parameters are obtained at 60 GHz band by model 2 and are shown in Fig. 2.6. The reflection is lower than –29 dB in 2 GHz bandwidth.

2.4 Unique loss of the antenna with single layer feed structure

Two-dimensional slot arrays are fabricated for experiments in 22 GHz band. The test antenna consists of two parts; one is an slot plate and the other is a groove feed structure. Degradation of electrically and / or mechanically contact between the slot plate and the waveguide narrow walls is unique defect of a single layer slotted waveguide arrays. Three techniques to contact them; bonding (B), laser welding (W) and brazing (R), are tested. The design parameters are listed in Table 2.1 and are common in the three types of the antenna. Figure 2.7 shows frequency dependence of the gain. The peak gain of 35.9 dBi is obtained in the brazing-type antenna (R). The antenna efficiency is 75.6 %. The peak gains of the bonding-type (B) and the welding-type (W) antennas are 34.2 dBi (antenna efficiency: 62 %) and 34.9 dBi (53 %) which are about 1.0 dB and 1.7 dB lower than the brazing-type antenna (R), respectively. The reasons to degrade the gain are investigated by the following experiments.

2.4.1 Transmission loss in the bonding-type antenna (B)

In order to evaluate the quality of electrical contact, we measured the transmission loss of a groove covered with a metal plate by conducting adhesive. The waveguide is 275 mm long which is the same with the length of the radiation waveguide of the test antenna. The measured transmission loss of the waveguide is 0.65 dB which is much larger than the calculated conductor loss (0.10 dB) of a standard waveguide. The difference of 0.55 dB is regarded as a loss due to an imperfect contact by the adhesive. Such a loss occurs in both radiation and feed waveguides. Since matching walls and coupling windows exist in the feed waveguide, the contact in the feed waveguide is quite important for the expected antenna performance and the loss would affect more seriously.

2.4.2 Pattern degradation of the welding-type antenna (W)

Next we discuss the misalignment of the slot plate in the welding-type antenna which has better electric contact than the bonding-type antenna. Figure 2.8 shows H-

plane radiation patterns at 22.2 GHz. Two large grating lobes of about −12.5 and −15 dB appear at $\theta \cong -30°$ and +50°, respectively. Measured 2D-aperture amplitude distribution is shown in Fig. 2.9 (a). No ripples are observed on U-line. However, about 3 dB and 7 dB ripples are observed on T- and S-line, respectively. Spacings between ripples correspond to $2s$. Then the fabrication error in welding a slot plate and grooves is theoretically considered. All the observation suggests that only the slot plate shrinks in the x-direction during heating of aluminum, which causes slot location shift Δx (< 0) in the x-direction. This shift results in unwanted amplitude ripples in the aperture. Since the excitation intensity of slot is controlled by slot offset on the waveguide in the x-direction as in Fig. 2.1, slots with the offset of $-d_{(2n-1)} + \Delta x$ are excited strongly while those with the offset of $+d_{(2n)} + \Delta x$ are weakly compared with the design. As a result, slots at $z = 0, 2s, 4s, \ldots$ are strongly excited while those at $z = s, 3s, 5s, \ldots$ are weakly excited. This causes the measured ripples parallel to the x-direction in Fig. 2.9 (a). In this antenna, two components are welded along U-line first and S-line finally. The shrinkage of the slot plate in the x-direction seems to occur and the slot shift $|\Delta x|$ increases near S-line. This accounts for the increase of ripples near S-line. This phenomenon is simulated by the array analysis. The amount of slot shift $\Delta x(i)$ of the i-th radiation waveguide from S is assumed to be;

$$\Delta x(i) = \frac{\Delta x(1) - \Delta x(24)}{23}(24 - i)$$

where $\Delta x(1) = -0.25$ mm and $\Delta x(24) = 0$ are assumed on S- and U-line, respectively. Simulated distribution is given in Fig. 2.9 (b), which explains the general behavior of the measured distribution in Fig. 2.9 (a). Calculated radiation pattern from this simulated distribution is indicated by the dotted line in Fig. 2.8. It beautifully agrees with measured one in terms of grating lobes level. The reduction of directive gain estimated in this model is 0.9 dB and reasonably explains the 1.0 dB gain difference between (W) and (R). Consequently, the loss due to the alignment error of slot plate is dominant in model (W). Such a small error due to the shrinkage of 0.25 mm seriously degrade the antenna performance in this frequency range.

Table 2.2 summarizes the factors degrading the efficiency. The transmission loss is notable in the antenna (B) due to incomplete electrical contact. Grating lobes would not appear in the radiation patterns of (B) and (R) when the slot plate was placed

at the accurate location on the grooves. The slot plate shrinkage of (W) causes the grating lobes. The shifts of the center frequency occurs due to thermal extension in the model (R) and (W).

2.4.3 Frequency shift due to extension both of the slot plate and the grooves of brazing-type antenna (R)

The highest gain and efficiency of the three antennas are obtained in the brazing-type antenna which realizes perfectly electrical contact and reduction of fabrication error. However, the bandwidth of the gain is degraded as is shown in Fig. 2.7. We discuss the characteristics of the antenna for further enhancement of the efficiency and the bandwidth of gain.

Figure 2.10 shows the aperture distributions at the center frequency (22.2 GHz) and at the edge of the 600 MHz bandwidth (21.9 GHz and 22.5 GHz). In the phase distribution along the radiation waveguides, tapers corresponding to the beam tilting are compensated. In contrast with the prediction, a relatively large taper is observed in the phase distribution along the feed waveguide at 22.5 GHz in the measurements. The feed circuit is designed so that the antenna aperture would be uniform at 22.3 GHz. However, the aperture is actually uniform at 22.15 GHz. The frequency shift is due to the extension of the antenna. The extension of the broad width of the waveguide causes the wavelength change and the extension along the feed waveguide causes window spacing change. The phase taper appears at the design frequency 22.3 GHz. While in the radiation waveguides, since the extensions occur both in the slotted plate and in the groove feed structure, the slot location error is not serious and does not affect the slot excitation so much. However, because of shortening the guide wavelength, the amplitude distribution is uniform and the phase is tapered at the design frequency 22.3 GHz. It is confirmed by further experiments that the phase distribution is uniform at 22.1 GHz. In the Fig. 2.7, the black dots indicate the calculated gain including the measured phase taper along the feed waveguide. Its tendency agrees with the measured ones. It is confirmed that the bandwidth reduction of the gain is due to the unsymmetrical frequency shift between the phase distributions along the feed and radiation waveguides.

We discuss the antenna assembling in such a high frequency band. The most

important technology in this single-layer waveguide array is to achieve perfectly electrical contact between the slot plate and the grooves. Imperfect contact may degrade the efficiency seriously. Misalignment of the slot plate may cause the pattern degradation such as the grating lobe appearance. The guide wavelength changes due to the overall material extension by heating, which causes the frequency shift of the antenna operation. Table 2.2 summarizes the reasons to degrade the efficiency in the contact techniques we have discussed. The transmission loss exists only in the bonding-type antenna due to incomplete electrical contact. Grating lobes would not appear in the radiation patterns of the bonding-type antenna and the brazing-type antenna when the slot plate is set at the required location on the grooves. The slot plate shrinkage of the welding-type antenna causes the grating lobes. The frequency shift of antenna operation is due to heating the groove feed structure of the brazing-type antenna. It does not occur seriously in the welding-type antenna because of the partial heating.

These effects would be more serious in millimeter-wave band. The transmission loss of one waveguide is measured in 60 GHz band. The waveguide consists of a groove and an upper plate with no slots which are contact by soldering. Many holes exists on the upper plate along the narrow wall of the waveguide in order to flow the soldering paste into it as is shown in Fig. 2.11. The hole diameter is 0.5 mm. Four kinds of waveguide are fabricated for experiment. The pitch of the holes of each waveguide is 0.5, 1.0, 1.5 and 2.0 mm. The waveguide length is 500 mm. The waveguide is standard one of WRJ-60 and the size of the waveguide cross section is 3.76 × 1.88 mm. The transmission loss of them are measured as -3, -4, -15 and -35 dB, respectively, as is shown in Fig. 2.12. The loss increases rapidly for the pitch more than 1.5 mm. It shows that the pitch has to be smaller than 1.0 mm.

2.5 Alternating phase feed system

2.5.1 Principle of alternating phase feed system

Figure 2.13 shows the alternating phase feed circuits which can avoid the loss in contacting the slot plate and the grooves [2-10] [2-11]. The structure is single-layer and two-dimensional one. The feed waveguide is attached at the end of the radiation waveguides. Each one is fed from one window cut on the narrow wall of the feed

waveguide. Since the spacing between the adjacent windows are $\lambda_g/2$, the adjacent radiation waveguides are fed in 180 degrees out of phase. In order to excite all the radiation slots in phase, the slot arrangement of each waveguide is alternatingly different from each other. Figure 2.14 shows the directions of magnetic line of force and electric current in the cross sections of the waveguides fed with 180 degrees phase difference between the adjacent waveguides. Since the electric currents flowing from the two adjacent waveguide narrow wall into the slot plate is canceled each other, electric contact between them is not required in fabrication.

2.5.2 Experimental results

Two-dimensional arrays are manufactured for experiment. The design parameters are also shown in Fig. 2.13. The array consists of 24 waveguides each with 25 slots. The slot plate and the waveguide grooves are in contact by conducting adhesive. Design frequency is 22.3 GHz. Waveguide broad wall width a is 10 mm, narrow wall width b is 2 mm and guide wave length λ_g is 18.16 mm. Wave length in free space λ_0 is 13.44 mm. Aperture size of about 265 × 280 mm and antenna size of about 300 × 300 mm are required. The antenna is fed from an end of the feed waveguide.

Reflection characteristics are shown in Fig. 2.15. Reflection level is lower than −15 dB which is acceptable. Provided that the slot plate shifts to certain direction along the feed waveguide, the reflection characteristics of the adjacent one-dimensional arrays are different from each other, since slot arrangement becomes unsymmetrical with respect to the center of the two waveguides. Therefore, the ripples in the calculated curve are suppressed in the experiments. Figure 2.16 shows aperture distributions of antennas at 21.95, 22.25 and 22.55 GHz which are center and the edges of 600 MHz band. The results of (a) shows these along the radiation waveguides which indicate the distributions of one-dimensional arrays while (b) shows those along the feed waveguide which indicate the characteristics of feed circuits. Sufficiently uniform aperture distributions are obtained in center frequency. The phase tapers are observed due to the long line effect at the edge of the frequency bandwidth. Figure 2.17 shows radiation patterns at the center frequency 22.25 GHz. Fine agreement are obtained between experimental and calculated results in H-plane. Symmetrical radiation patterns of both antennas with low side lobes in E-plane are obtained. Figure 2.18 shows frequency

dependence of antenna gain. The reflection and radiation characteristics are sufficient. High efficiency is expected even though the slot plate and the grooves are in contact by bonding, since it does not require the close contact between the slot plate and the grooves. However, antenna efficiency results 45.7% for peak gain of 33.9 dBi at 22.25 GHz. The adhesive may interrupt the current flow on the grooves along the perpendicular direction of the radiation waveguides. The antenna efficiency is degraded by the transmission loss, but the basic operations are confirmed by experiments.

2.6 Concluding remarks

Two-dimensional single-layer feed circuit realizes mass-produceable simple structure which still has the waveguide advantages of the small transmission loss even in high frequency. The size of the antenna is small for high frequency uses, while several limitations appear in fabrication. Several types of contact between the slot plate and the grooves are investigated in experiment. The losses peculiar to this single-layer slotted waveguide antenna is estimated in high frequency for mass-production. Reduction of the loss without degrading the mass produceability is inevitable in the future study to fully demonstrate the superiority of a single-layer waveguide slot antenna. Alternating phase feed system is a new type of feed circuit which does not require the close contact between the slot plate and grooves. However, at the feed waveguide and at the edge of the slot plate, the electric current flows between them and they have to be in contact closely. The basic operations are confirmed by experiments.

References

[2-1] Collin, R. E., *Antennas and Radiowave Propagation*, New York McGraw-Hill, Chap. 1, pp. 6-7, 1985

[2-2] Weiss, M. A., " Microstrip antennas for millimeter waves," *IEEE Trans. on A.P.*, vol. AP-29, No. 1, pp. 171-174, Jan. 1981

[2-3] Huang, J., " A Ka-band circularly polarized high-gain microstrip array antenna," *IEEE Trans. on A.P.*, pp. 113-116, Jan., 1995

[2-4] Kado, S., Ohta, M., Hirao, M., Wakushima, S., Nozue, Y. and Haneishi, M., " Radiation properties of 22 GHz band triplate feed type patch antennas with parasitic

elements," *IEICE Natl. Conv. Rec.*, B-53, March 1994

[2-5] Hirokawa, J., Ando, M. and Goto, N., " A single-layer multiple-way power divider for a planar slotted waveguide array," *IEICE Trans. Commun.*, Vol. E75-B, No. 8, pp. 781-787, August 1992

[2-6] Takahashi, T., Hirokawa, J., Ando, M. and Goto, N., " The suppression of the reflection by an inductive wall of a power divider for a slotted waveguide array," *Tech. Rep. of IEICE*, AP-94-7, April 1994

[2-7] Sakakibara, K., Hirokawa, J., Ando, M. and Goto, N., " A slotted waveguide planar array antenna for entrance radio systems in mobile communication," *4th IEEE Int. Conf. on Universal Personal Commun.*, pp. 373-376, Tokyo, Nov. 1995

[2-8] Johnson, R. C. and Jasik, H., *Antenna Engineering Handbook*, New York McGraw-Hill, Chap. 9, 1984

[2-9] Collin, R. E. and Zucker, F. J., *Antenna Theory*, pt. 1, Sec. 14.8, McGraw-Hill, 1969

[2-10] Goto, N., " A waveguide-fed printed antenna," *Technical Report of IEICE*, AP 89-3, pp. 17-21, April, 1989

[2-11] Hirose, R., Ando, M. and Goto, N., " A design of a multiple-way power divider for a single layered slotted waveguide array," *Technical Report of IEICE*, AP 90-130, pp. 29-34, Feb. 1991

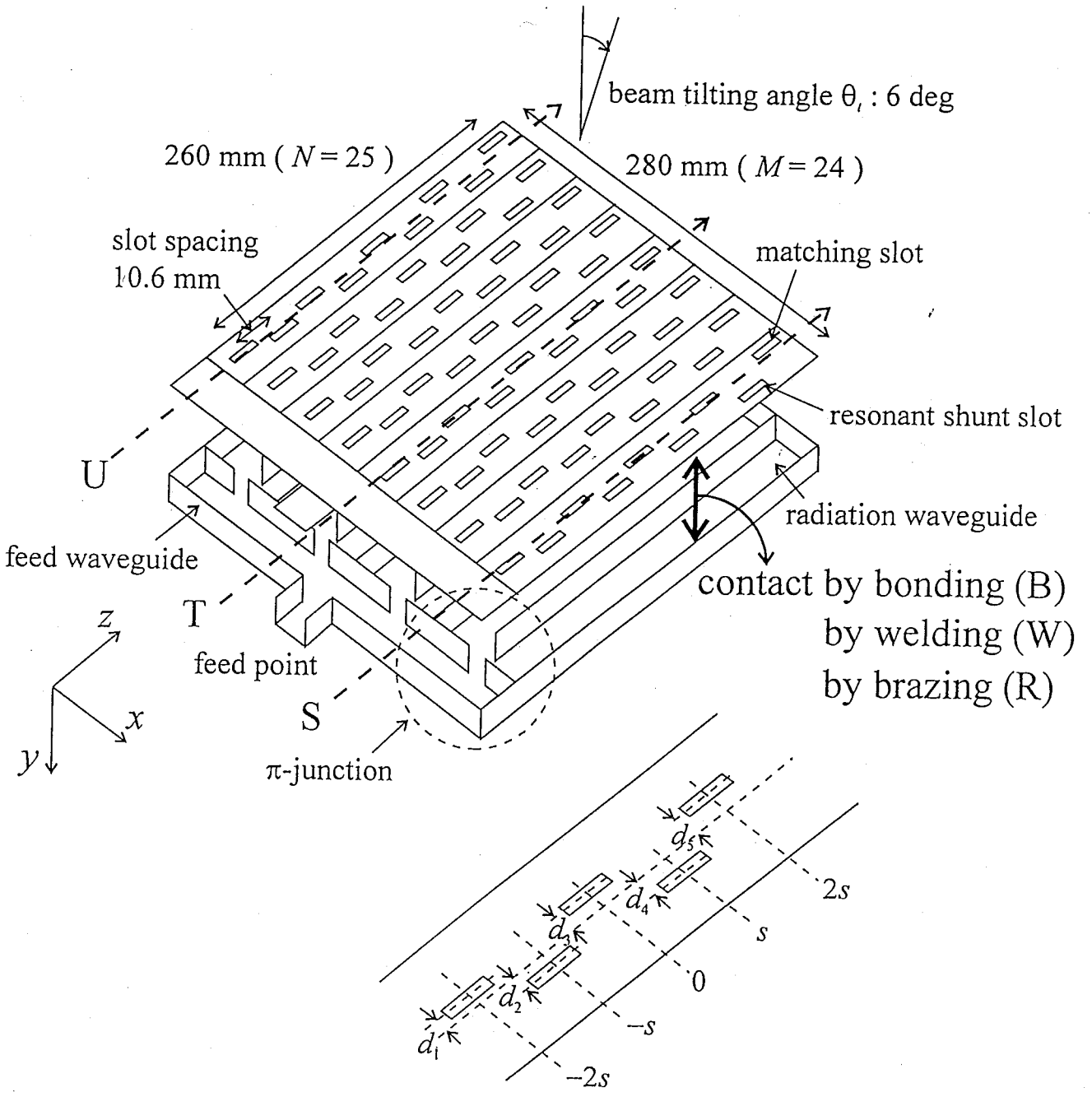

Fig. 2.1 Structure of the single layer slotted waveguide array

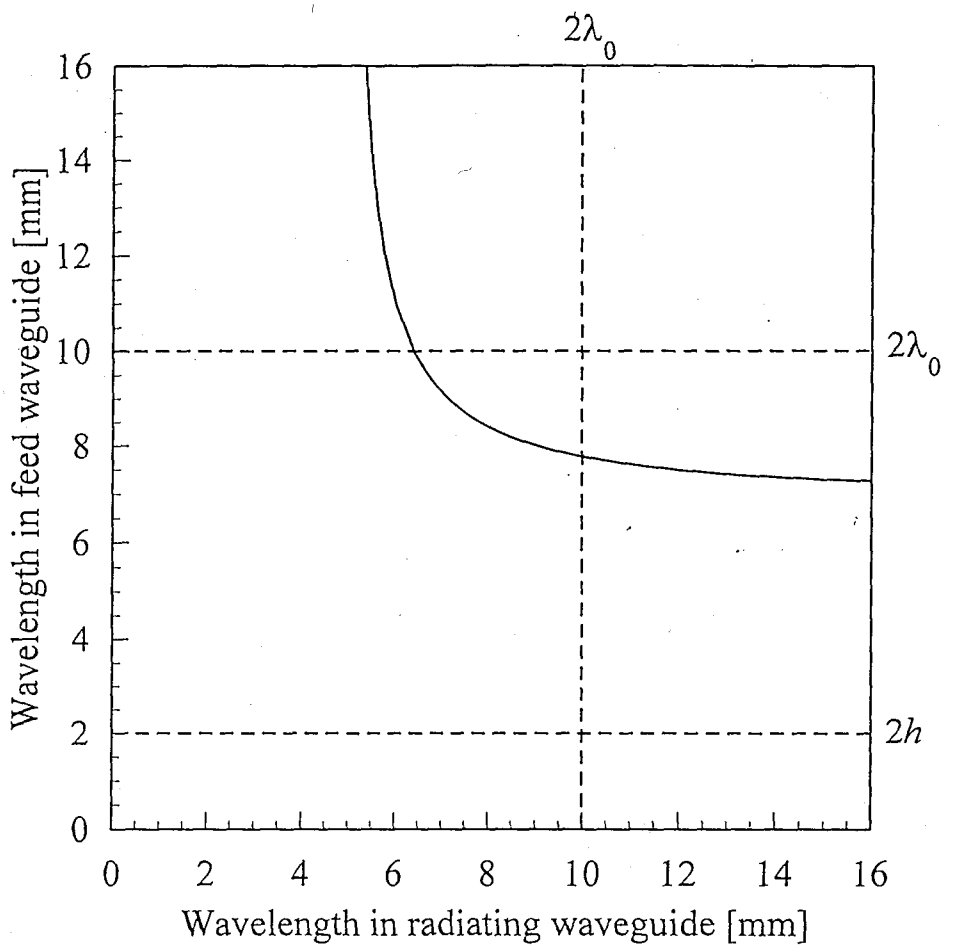

Fig. 2.2 Relationship between the wavelengths in the feed and radiation waveguides

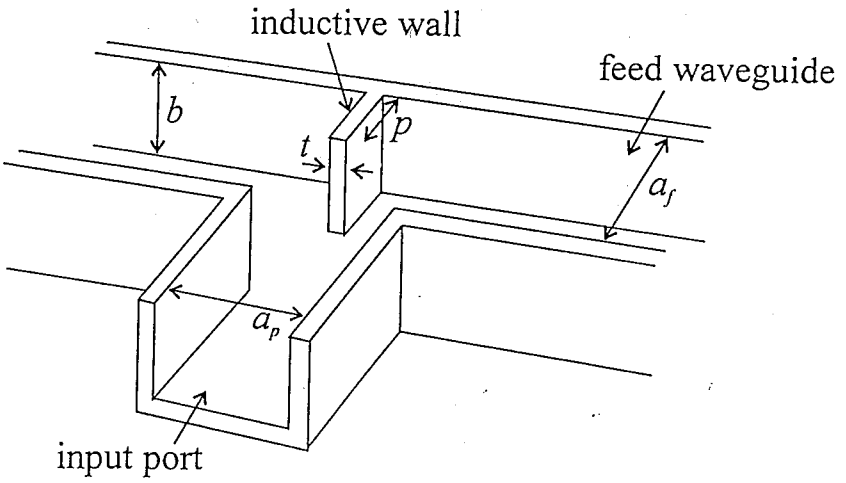

(a) T-junction without iris

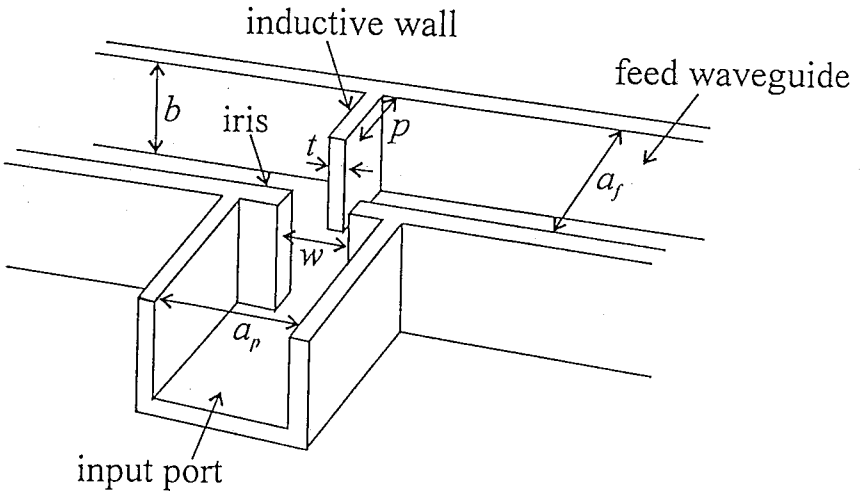

(b) T-junction with iris

Fig. 2.3 T-junctions at the input port

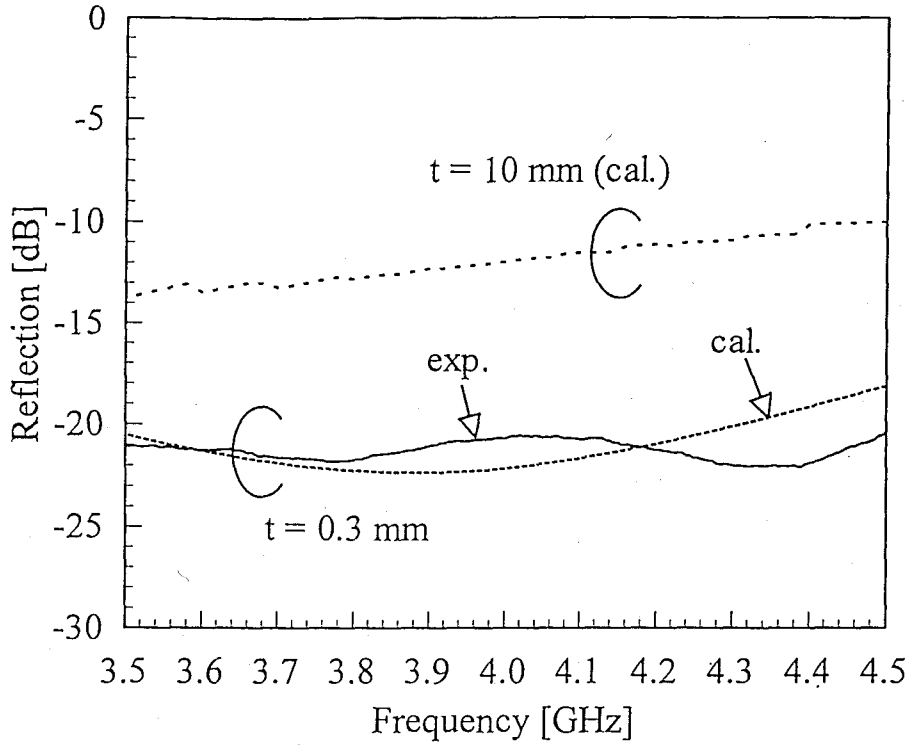

$a_f = a_p = 58.1$ mm
b = 29.1 mm
p = 29 mm

Fig. 2.4 Reflection characteristics of the model 1 without iris

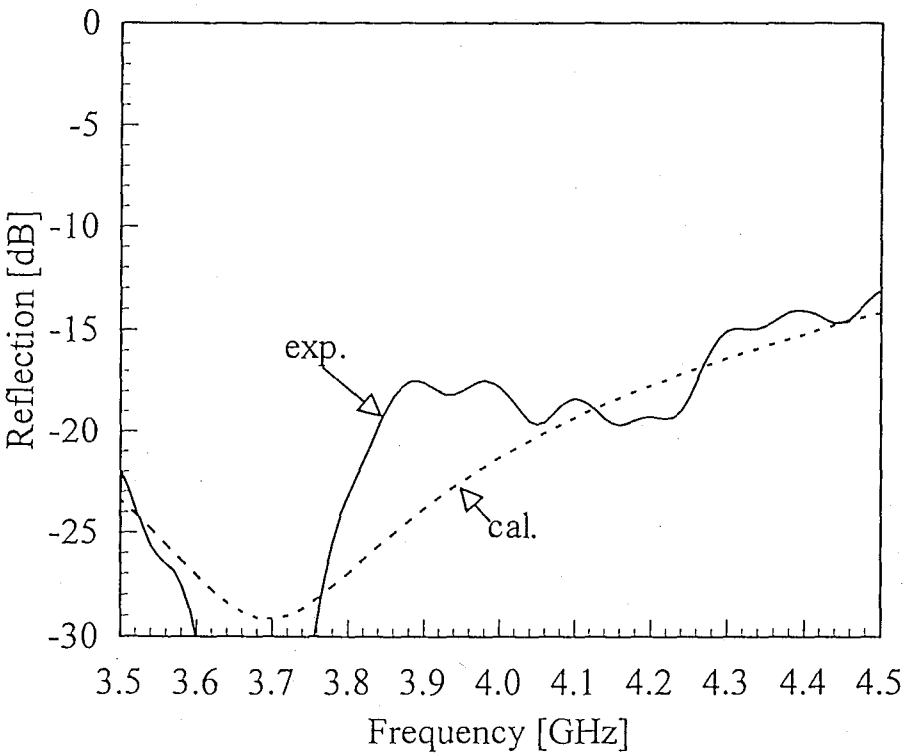

$a_f = a_p = 58.1$ mm
b = 29.1 mm
p = 24 mm
t = 10 mm
w = 45.3 mm

Fig. 2.5 Reflection characteristics of the model 2 with iris

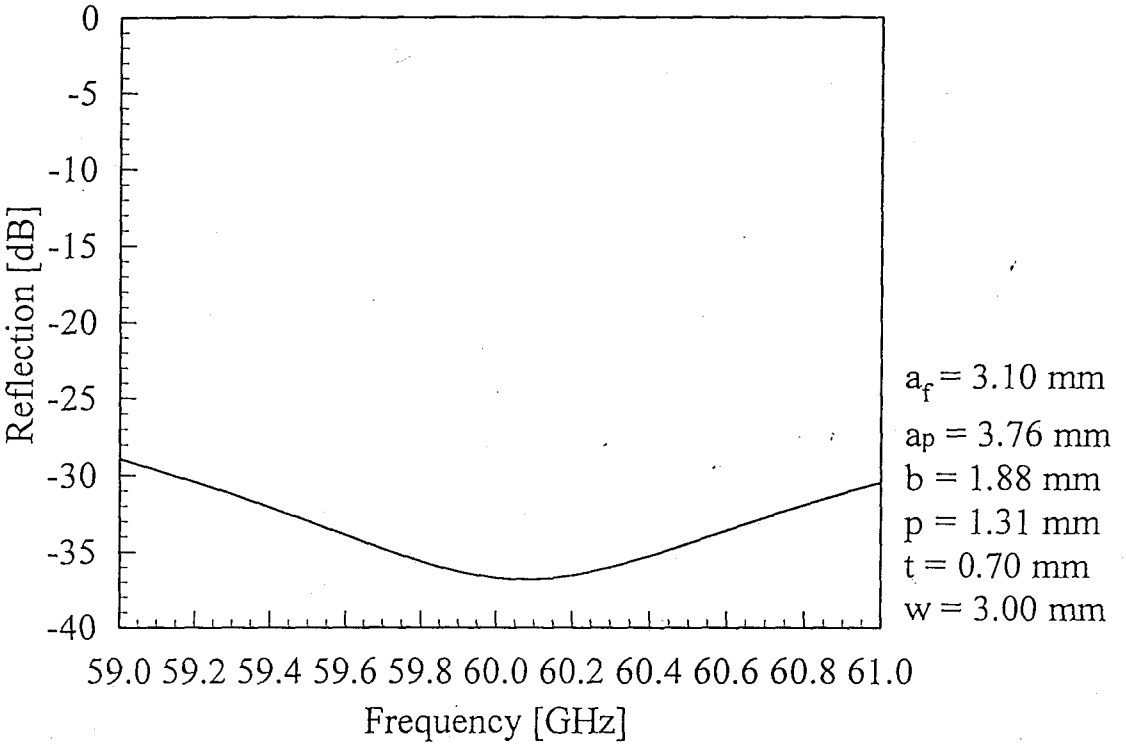

Fig. 2.6 Numerical reflection characteristics

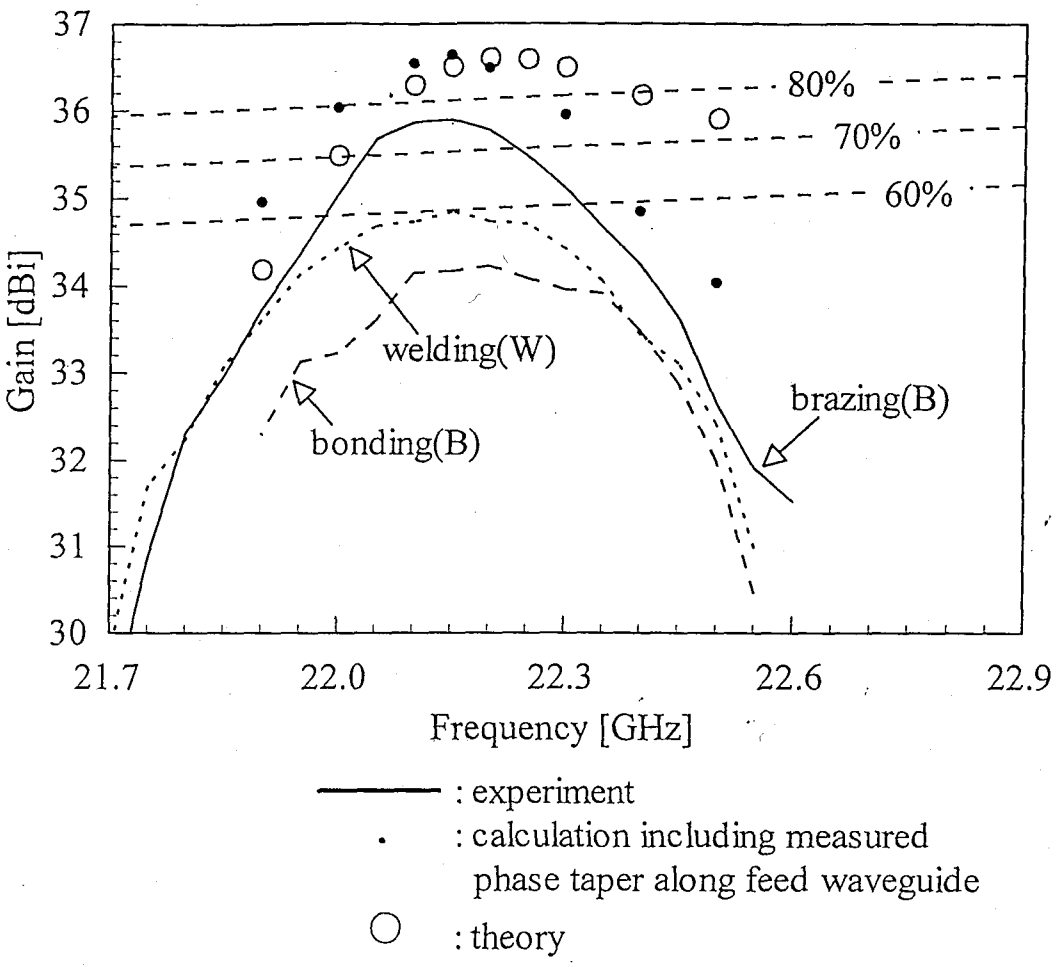

Fig. 2.7 Gain and antenna efficiency

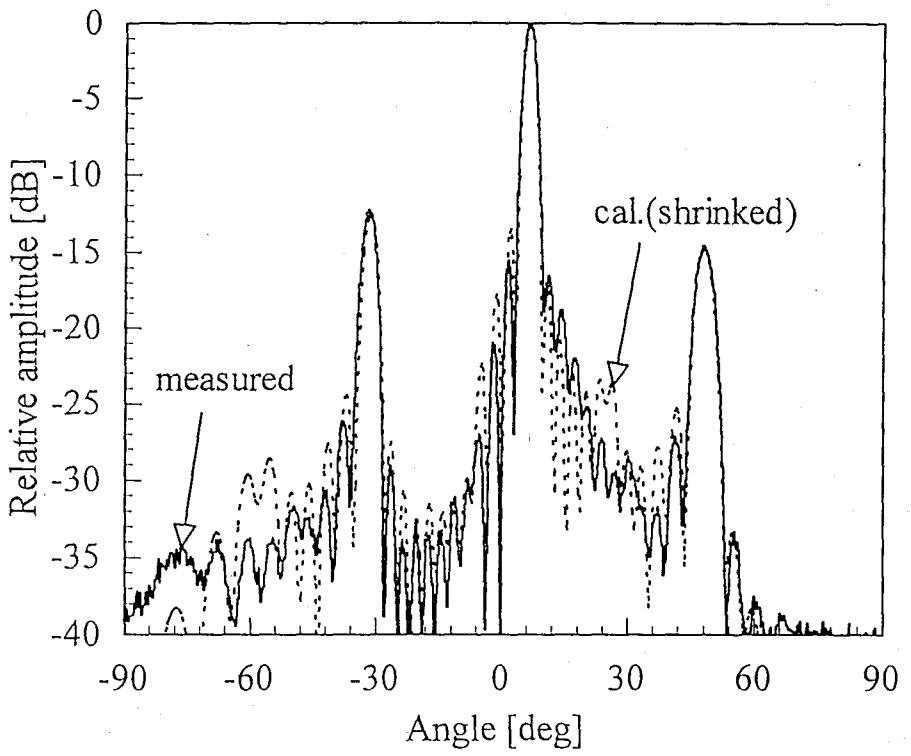

Fig. 2.8 Radiation pattern of the welding-type antenna (W) with shrinked slot plate

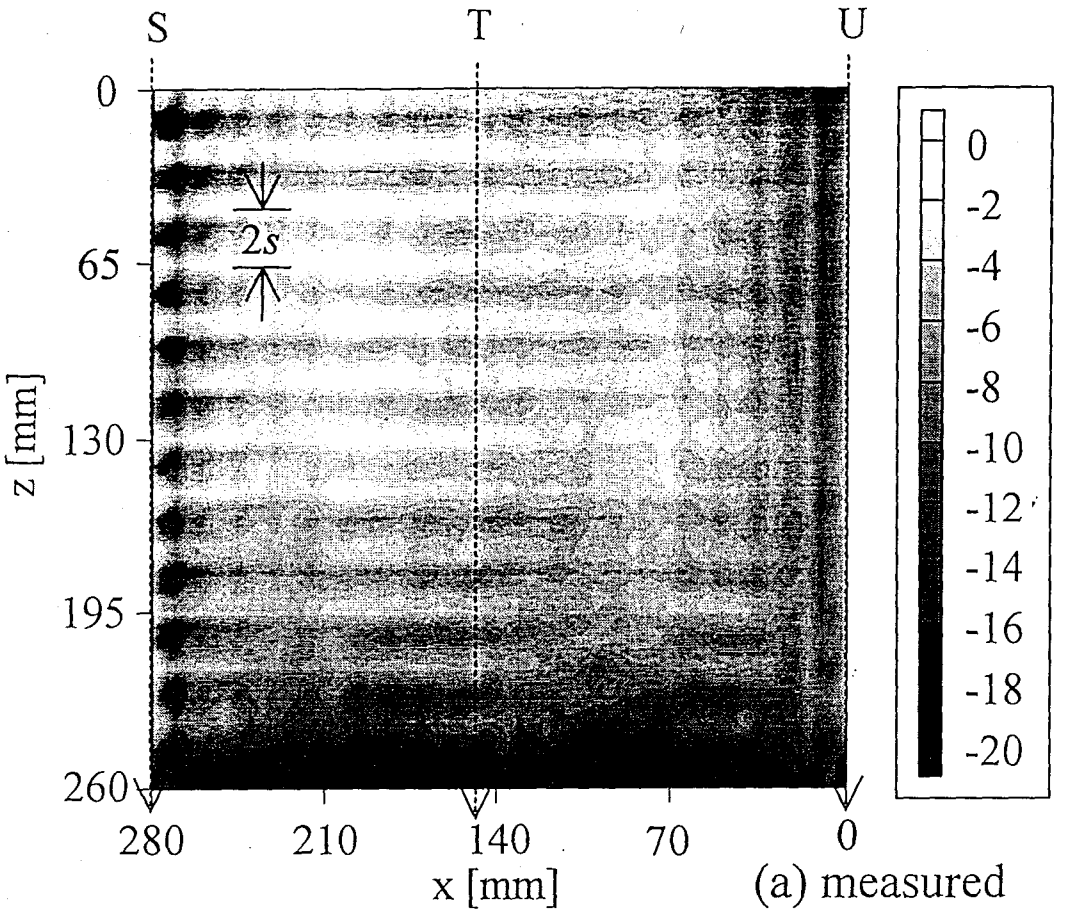

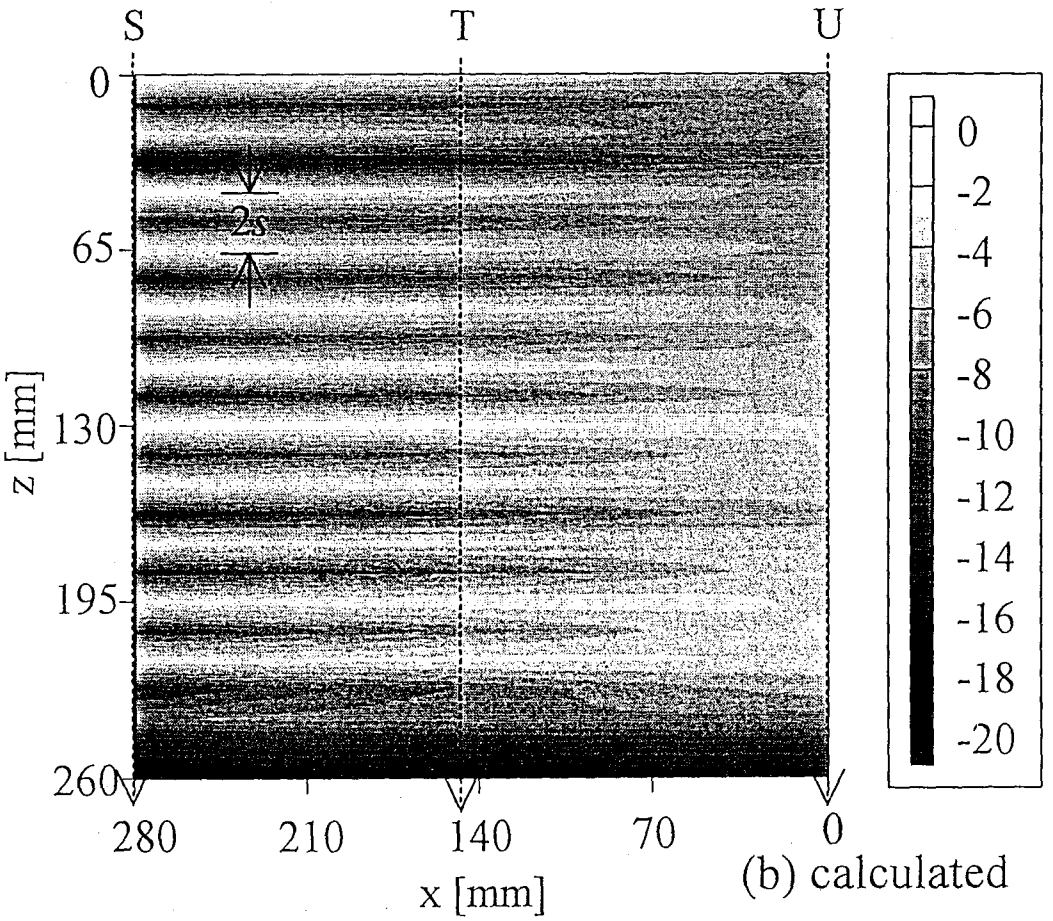

Fig. 2.9 Aperture distribution of model (W)

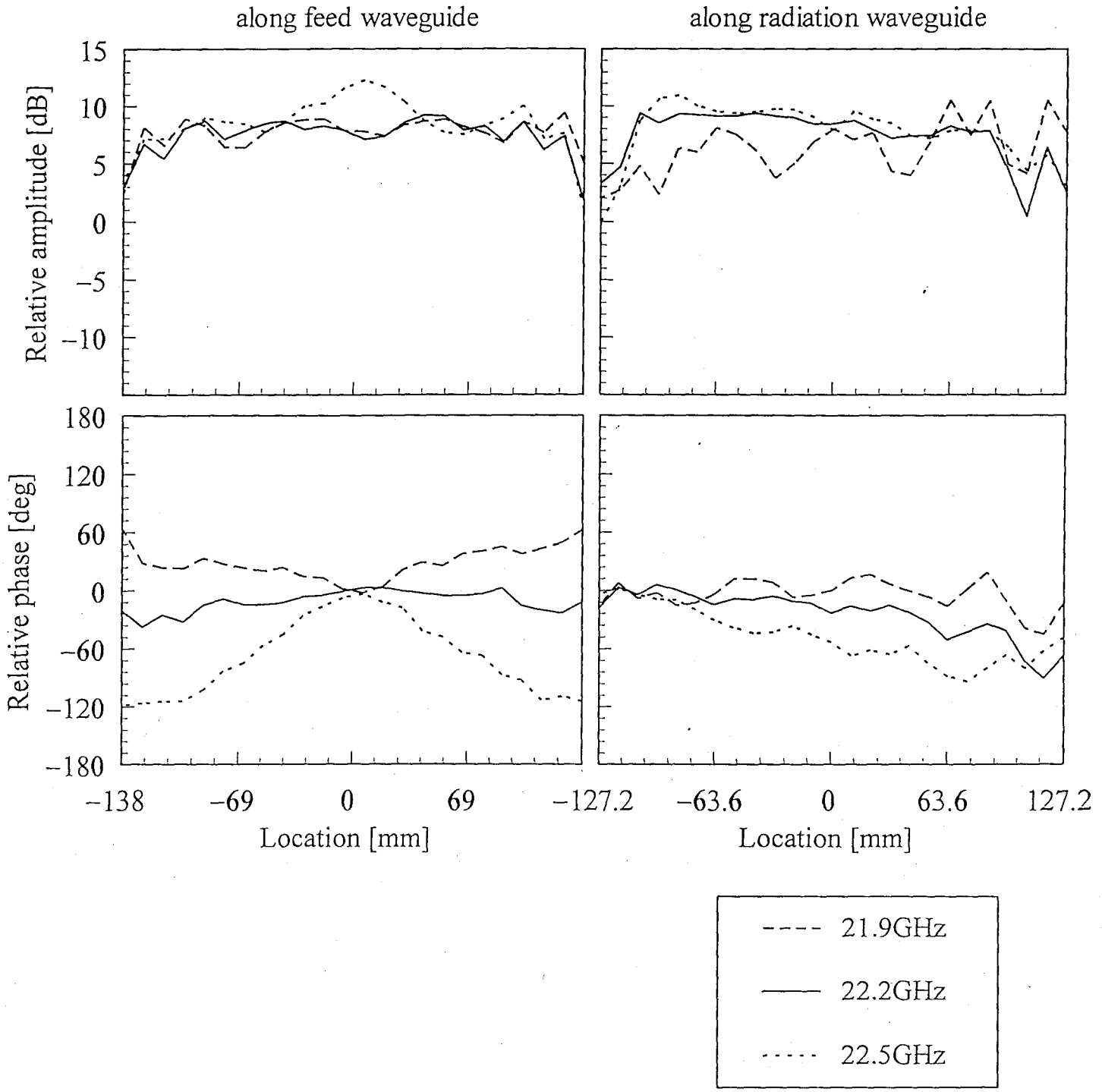

Fig. 2.10 Aperture distributions of brazing antenna (R)

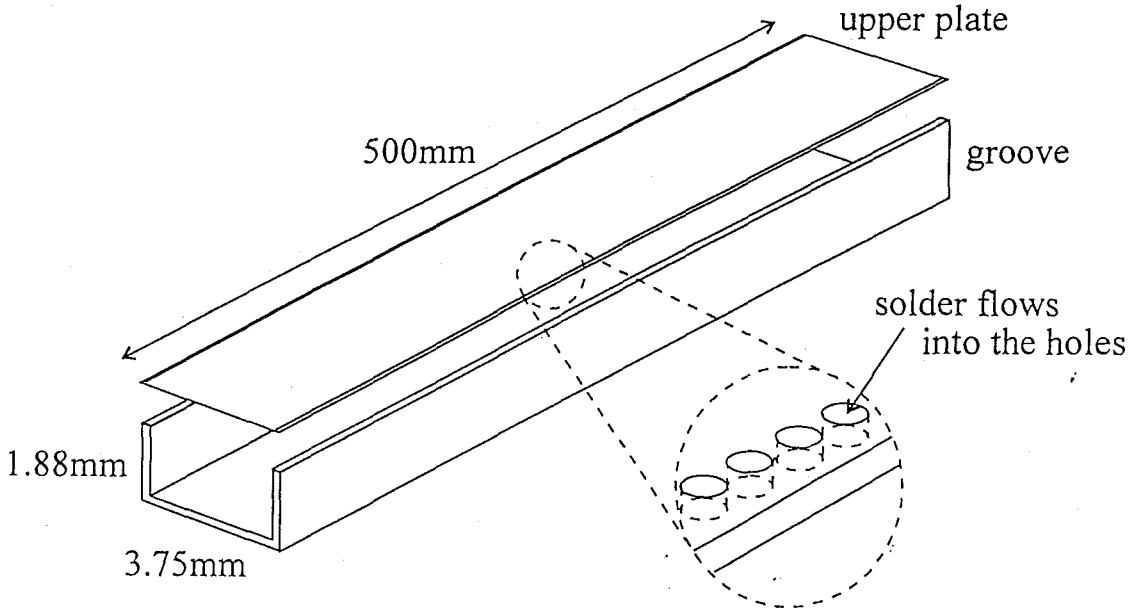

Fig. 2.11 Standard waveguide in contact by soldering

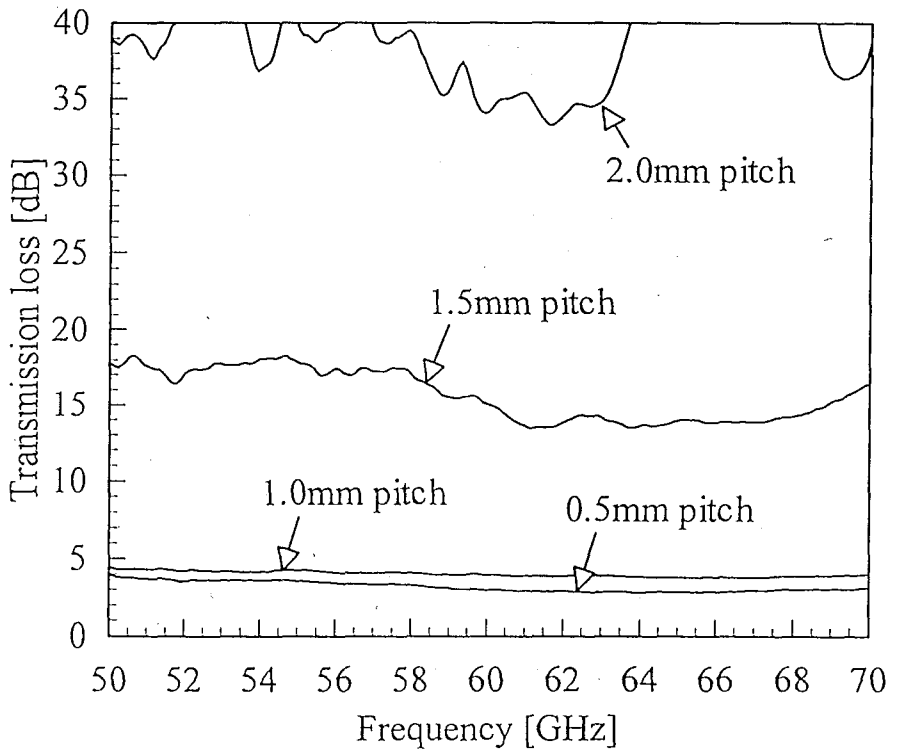

Fig. 2.12 Transmission loss in soldering contact waveguide

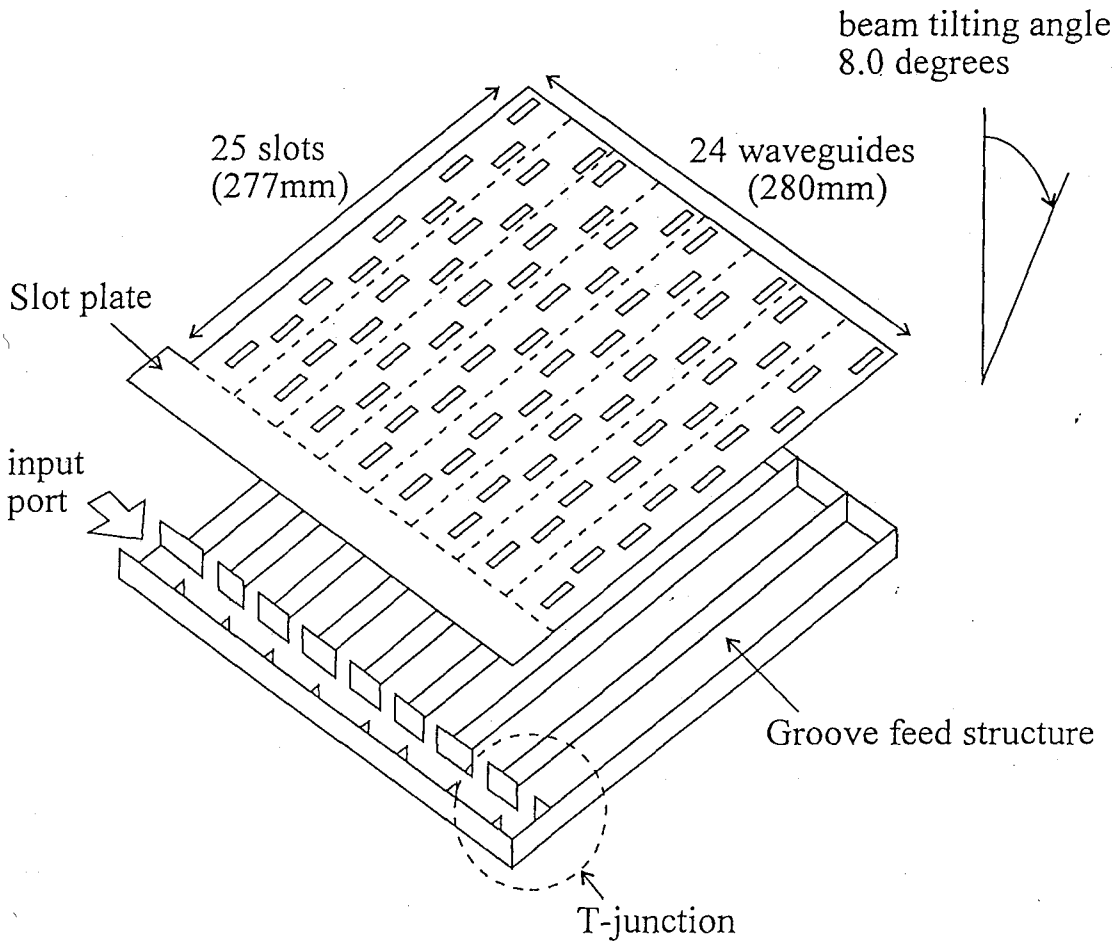

Fig. 2.13 Alternating phase fed antenna

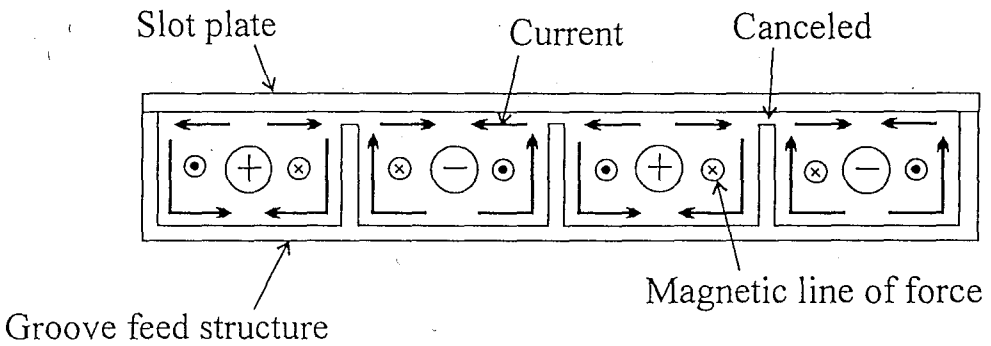

Fig. 2.14 Cross section of the alternating phase fed waveguides

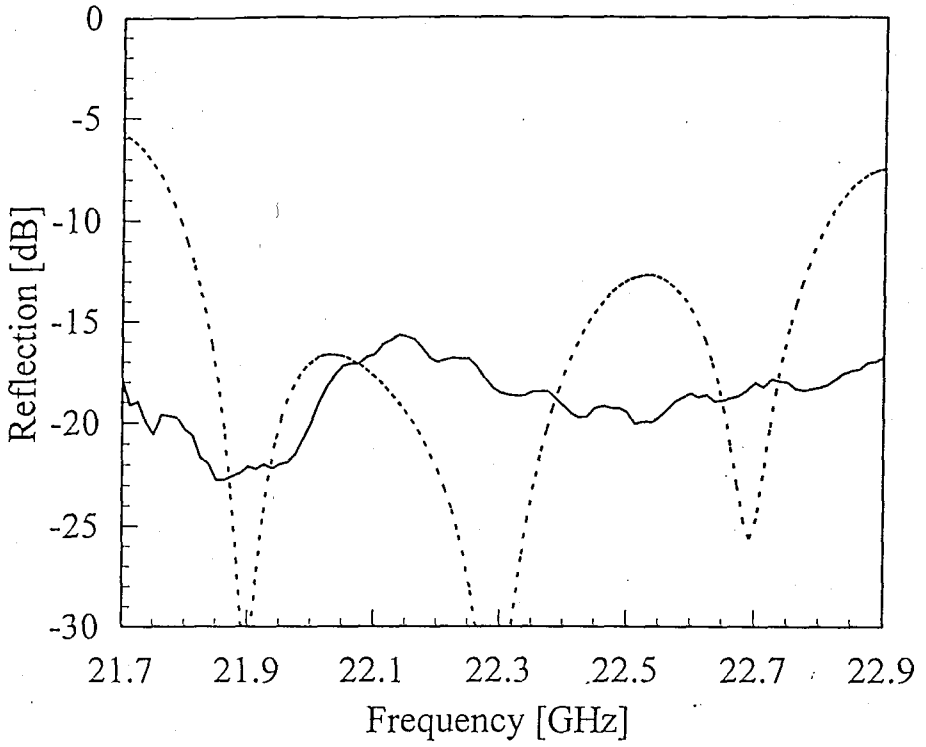

Fig. 2.15 Reflection characteristics

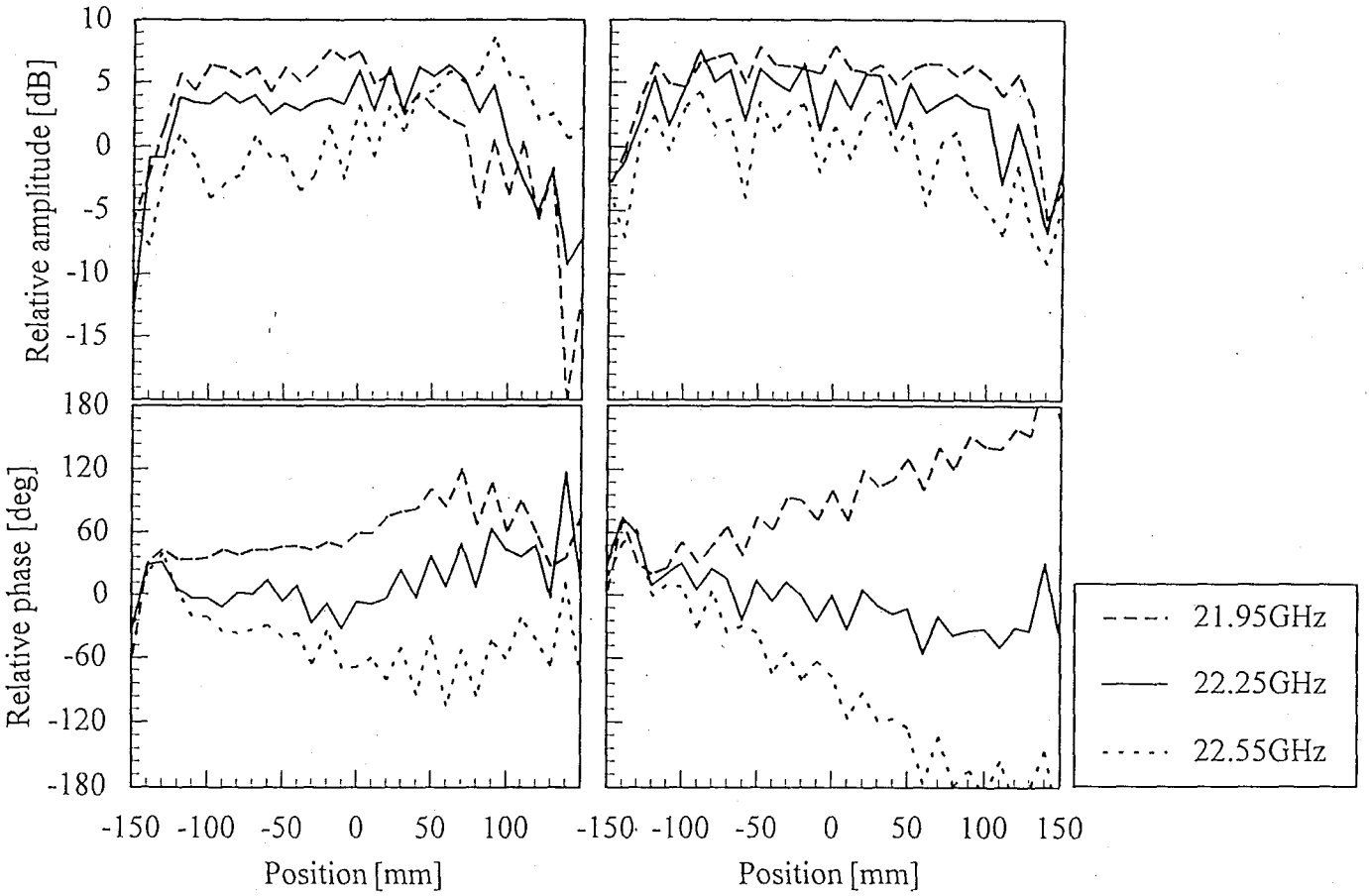

(a) Along radiation waveguides (b) Along feed waveguide

Fig. 2.16 Aperture distributions

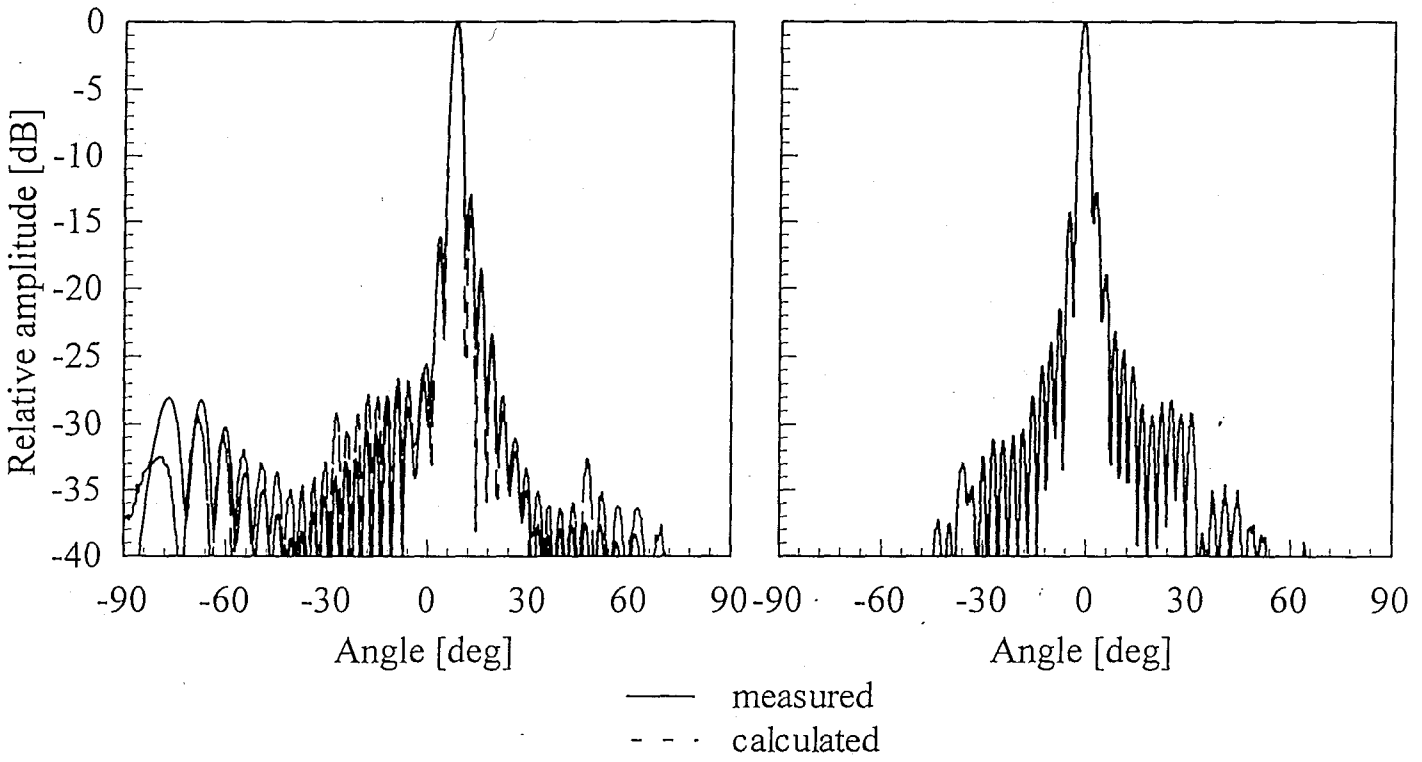

Fig. 2.17 Radiation pattern at 22.25 GHz

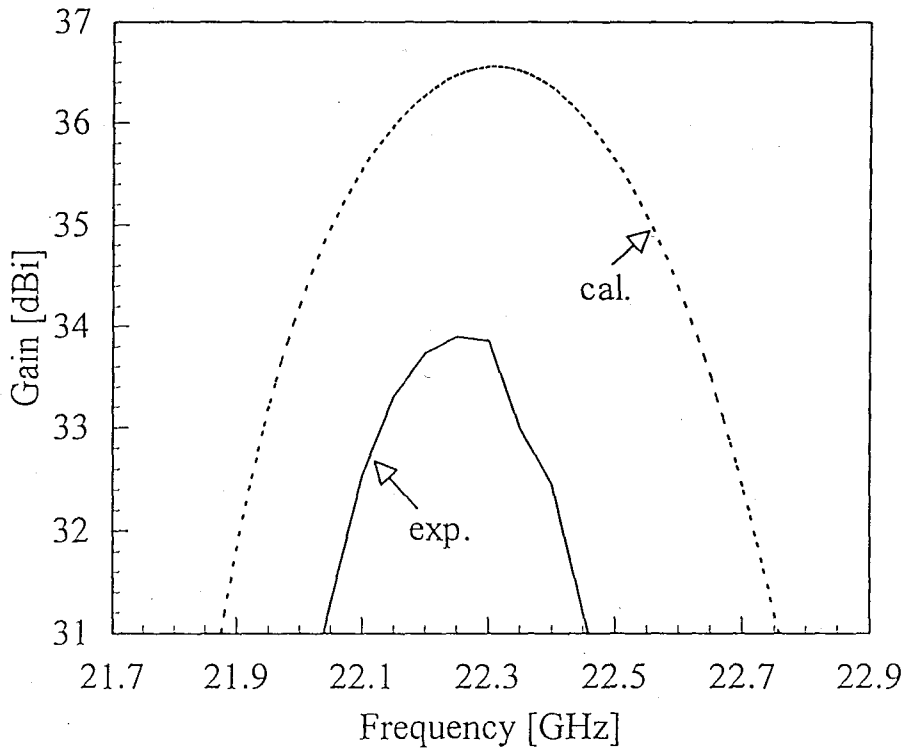

Fig. 2.18 Antenna gain

Table 2.1 Design parameters

Design frequency	22.2 GHz
Number of radiating waveguides	24
Number of slots (per waveguide)	25
Number of slots (all)	600
Array length (z)	260 mm
Array length (x)	280 mm
Broad guide width of feed waveguide a_f	8.1 mm
Broad guide width of radiating waveguide a_g	10.0 mm
Narrow guide width b	4.0 mm
Slot spacing (z)	10.6 mm
Beam-tilt angle	6 deg

Table 2.2 Techniques and loss for assembling the slot plate to the grooves

	Transmission loss due to incomplete contact between the two plates	Grating lobes due to misalignment of the slot plate on the grooves	Frequency shift due to overall antenna extension by heating
Bonding	×	△	○
Welding	○	×	△
Brazing	○	△	×

Chapter 3. Basic analysis and design of slots

3.1 Introductory remarks

High gain and high frequency planar antennas are required for various wireless communication systems mentioned in Chap. 1. Slotted waveguide arrays are the most attractive candidates for high efficiency antennas, since they are free from conductor loss. Unique demand in the design is high antenna efficiency in contrast with low sidelobe level specified in military use. Efficiency optimization generally results in the use of strongly coupled slots in the array as well as the use of termination slots. In addition, in higher frequency, waveguide wall thickness should be taken into account in the slot design. Efficient design method which reflects all these background is necessary for increasing use of slotted waveguide arrays.

A design of a resonant slotted waveguide array consists of two steps in parallel. One is the slot conductance analysis for various parameters, such as length and location of slots. Another one is the synthesis of desired aperture illumination. If the size of an array increases, the former is time-consuming due to the existence of mutual coupling between slots. The iterative methods of experiments or complicated analysis using high performance computer are conducted in general. One technique to remedy this difficulty is to introduce the periodic boundary condition into the full wave analysis of infinite arrays in order to simulate mutual couplings in large arrays [3-1]-[3-12]. Most of the previous works utilize the results of mutual coupling not for practical slots but in terms of complimentary dipole arrays based upon Babinet's principle [3-1]-[3-4] [3-12]; some parameters or effects such as slot offset and/or thickness of the wall were neglected there [3-1]-[3-9] [3-12]. Others, on the other hand, treat slots or open waveguide arrays with each element fed separately [3-5]-[3-9].

In this chapter, the design of arrays with uniform illumination is focused and extend the use of the periodic infinite array analysis [3-1] [3-4] for evaluating slot admittance which reflects all the important parameters of slot, such as length, width, wall thickness, offsets, etc. This fictitious boundary condition is applied to the design of

finite slotted waveguide arrays with staggered offsets in order to evaluate the external mutual coupling, assuming that edge effects are serious only in termination slots at the end of waveguides [3-4]. Periodic boundary walls surrounding two staggered slots (one period of slot arrangement) are assumed in external half free space, which approximately simulate the fields from adjacent slots in a large staggered slots array. Slot conductance is obtained by method of moments analysis for this model. The combination of periodic boundary wall, piece-wise sinusoidal functions for the slot aperture fields expansion and the concept of virtual cavity [3-13] as applied to the Green's functions in the waveguide leads us to the slot conductance in the explicit form in terms of parameters such as, waveguide dimensions, wall thickness, slot length, offset, etc. They are then applied to an equivalent transmission line model for synthesizing slot excitation distribution. In the final stage of the design, some iteration of full wave analysis is conducted for the infinite in *E*-plane and finite in *H*-plane model [3-4], to compensate the edge effects and to design termination slots. The effectiveness of this model even for arrays with relatively small number of waveguides is demonstrated by experiments.

3.2 Array antenna configuration

Let us consider a medium size slotted waveguide array. It has the gain around 35 dBi and 24 × 25 resonant slot elements. A single layer power divider is applied to this antenna as shown in Fig. 3.1. All the radiation waveguides are fed in phase and in the same amplitude by using π-junctions [3-14]. A broad wall of the radiation waveguide has resonant shunt slots which are parallel to the guide axis [3-15]. The slot offset in the x-direction from the center of the waveguide is the parameter controlling amplitude of slot excitation, while slot spacing in the z-direction determines its phase. A slot with larger offset couples more strongly with magnetic field of TE_{10} mode; slot offset is small near the feed point and increases toward the termination, which results in a uniform amplitude of antenna aperture. Staggered offset slots with longitudinal spacing of half guide wavelength are excited in phase and total radiation is in boresight direction. In order to avoid the growth of the reflections at the antenna input port, a few degrees beam tilting in the *H*-plane is adopted by controlling slot spacing, as is usual the case with general nonresonant-waveguide resonant-slot arrays [3-16]. A matching slot

consisting of a large slot with large offset and a short terminal is installed at the waveguide end in order to radiate all the residual power in the waveguide and quasi-traveling wave operation is realized.

We assume that the array length in the z-direction is long to some extent and that the desired aperture illumination is uniform or at least slowly varying. In this case, the slot offset as well as the slot length is changing slowly along the waveguide. Consequently, this array is a quasi-periodic one with two slots in one period as is indicated in Fig. 3.1.

3.3 Antenna design procedure

A one-dimensional array composed of N slots is considered first. The flow chart of the slot design is shown in Fig. 3.2. It consists of two steps, that is array synthesis and slot analysis. The former is well known procedure [3-17] and is briefly explained first. Once antenna gain is specified, aperture size and number of slots are derived first. The beam direction is determined so that a null point of an array factor may fall on the boresight direction. The slot spacings are determined in order to realize uniform phase illumination on the aperture in the desired beam direction θ_t. Transmission coefficient S_{21} for a resonant slot is real and the guide wave length is not perturbed in principle; actual slot spacing is obtained in the appendix A. The offset of the n-th slot from the center of the broad wall is d_n and the transversal position in staggered arrangement is given by $x = (-1)^n d_n$, where $(-1)^n$ assures the co-phase excitation of slots with half wavelength longitudinal spacing. A resonant shunt slot can be represented by an equivalent conductance g_n in a transmission line model shown in Fig. 3.3 [3-16], where internal mutual coupling via waveguide dominant mode is taken into account. The conductance g_n ($n = 1, 2, \cdots, N$) of each slot is assigned for uniform amplitude illumination by means of Ref. [3-17]. A matching slot is installed at the termination, whose admittance y_g equals to characteristic impedance of the waveguide. For uniform aperture illumination, radiation from the matching slot is set to be equal to the inner slots and the radiation power assigned for each slots as well as the matching slot is $1/N$.

As another step of the design, the relationship between the conductance g_n and slot parameters is obtained by a slot analysis taking mutual coupling into account as

discussed in detail in Sec. 3.4. This is conducted by method of moments by using periodic boundary condition.

The above two steps provide us the initial design for the inner slots except the matching ones. Termination slots are then designed using full wave analysis for infinite in E-plane and finite in H-plane model [3-4] which is depicted in Fig. 3.4 where $K = \infty$ is assumed (Appendix B). In the event of extremely high efficiency requirement, a few iterations are conducted to compensate the end-effects as well as the amplitude taper caused by neglect of slot offset variation in the periodic model; the inner slots designed before are also perturbed to enhance the aperture uniformity. In this optimization, the uniform slot spacings in z-direction are refined so that the boresight direction accurately coincides with the desired null of the radiation pattern. Two or three iterations are sufficient to achieve uniform illumination with ripples smaller than 2 dB. The resonance condition between the slot offset and the length is assumed be unchanged throughout the iterations. In our design of 36 dBi gain antenna, the iteration improves the gain by about 0.5 ~ 0.9 dB. After completion of the design of N slots, M identical waveguides designed above are arrayed to realize a two-dimensional array.

3.4 Slot conductance analysis in an array

3.4.1 Green's functions for simulating mutual coupling

In order to obtain the accurate relationship between the conductance and slot parameters in the two-dimensional array environment, a full wave analysis of a slot by Galerkin's method of moments [3-18] is conducted which simulates the external mutual couplings from adjacent slots. Periodic boundary walls containing two slots in staggered arrangement are introduced in the half free-space above the waveguide, so that the number of unknowns may not increase with the array size. For the comparison, we also analyze the isolated slot model which neglects the external mutual couplings. The Green's functions for the external regions in the two analyses are compared in this section.

Model A : Periodic boundary condition

Only the uniform excitation of slots are considered, where the effects of beam

tilting as well as the gradual change in slot offset along z-axis are all neglected. The analysis model for evaluation of S_{11} of one slot in an array which simulates the external mutual couplings is shown in Fig. 3.5. Total space is separated by two apertures S_1 and S_2 into three regions which are designated by waveguide internal region (region 1), slot internal region (region 2) and waveguide external region (region 3). Wall thickness t of the region 2 is taken into account in the analysis for high accuracy. The broad and narrow wall width of the waveguide is a_g and b_g, respectively and guide wave length of TE_{10} dominant mode is λ_g. The periodic boundary walls account for the mutual effects from adjacent slots via half free space. Two resonant slots (slot length: $2l$, width: $2w$) are contained within the walls since they are one period in an array arrangement. These slots on the broad wall of the waveguide are parallel to the guide axis and are placed at $(x, z) = (d, b_r/4)$ and $(-d, s + b_r/4)$, respectively. The region 3 is a virtual waveguide composed of periodic boundary walls with the size of $a_r (= a_g + h) \times b_r (= 2s)$ where h is the wall thickness between the waveguides and s is the longitudinal slot spacing, respectively. According to the field equivalence principle, each aperture can be replaced by unknown equivalent magnetic current backed with perfect conducting wall. Two unknown magnetic currents $\boldsymbol{M}_1$, $\boldsymbol{M}_2$ and $\boldsymbol{M}_3$ ($= \boldsymbol{M}_2$) are assumed on the apertures S_1, S_2 and S_3. Integral equations are derived by imposing continuity condition of tangential component of magnetic fields on two slot apertures S_1 and S_2;

On S_1,

$$\left\{ \boldsymbol{H}_{in} + \iint_{S_1} \boldsymbol{G}_1 \cdot \boldsymbol{M}_1 dS \right\} \times \hat{y}$$

$$= \left\{ -\iint_{S_1} \boldsymbol{G}_2 \cdot \boldsymbol{M}_1 dS + \iint_{S_2} \boldsymbol{G}_2 \cdot \boldsymbol{M}_2 dS \right\} \times \hat{y} \qquad (3.1)$$

On S_2,

$$\left\{ -\iint_{S_1} \boldsymbol{G}_2 \cdot \boldsymbol{M}_1 dS + \iint_{S_2} \boldsymbol{G}_2 \cdot \boldsymbol{M}_2 dS \right\} \times \hat{y}$$

$$= \left\{ -\iint_{S_2} \boldsymbol{G}_3 \cdot \boldsymbol{M}_2 dS - \iint_{S_3} \boldsymbol{G}_3 \cdot \boldsymbol{M}_2 dS \right\} \times \hat{y} \qquad (3.2)$$

where $\boldsymbol{G}_j$ ($j = 1, 2, 3$) are dyadic Green's functions for the magnetic field produced by a unit magnetic current in the region j [3-13] [3-18]. $\boldsymbol{H}_{in}$ is an incidence magnetic field (TE_{10} mode) propagating in the $+z$-direction. The Green's function $\boldsymbol{G}_3$ is expressed by normal mode functions of the wave propagating in the $-y$-direction since the four

periodic boundary walls surrounding the region 3 form a waveguide and slot plate provides a short termination. So G_3 is given by the following expression;

$$G_3(r|r_0) = \frac{1}{2}\sum_{\mu} H_{\mu}^{(-)}(r)[H_{\mu}^{(+)}(r_0) - H_{\mu}^{(-)}(r_0)] \tag{3.3}$$

$H_{\mu}^{(\pm)}$ is a normal mode function which satisfies the periodic boundary condition of Floquet's theorem [3-19, Chap. 9]. The advantage of this analysis is clear that mutual coupling effects of a two-dimensional array are simulated without increasing the number of unknown functions with the array size. The number of unknown functions is only two (M_1 and M_2). The combination of periodic boundary wall, piece-wise sinusoidal functions for the slot aperture fields expansion and the concept of virtual cavity [3-13] as applied to the Green's functions in the waveguide leads us to the slot voltages (M_1 and M_2) in the explicit form in terms of parameters such as, waveguide dimensions, wall thickness, slot length and offset etc., as is shown in Appendix C.

Model *B* : Model neglecting the mutual couplings

For the analysis neglecting the mutual coupling, almost the same model as Fig. 3.5 is used, provided the periodic walls as well as the paired slot M_3 is omitted from it. The integral equation is analogous to (1) and (2) but second term of right hand side of (2) vanishes. Principal difference is the Green's function G_3 for the external region 3 of half free space which is expressed by;

$$\begin{aligned} G_3(r|r_0) &= -j\omega A + \frac{A}{j\omega\varepsilon_0\mu_0}\nabla\nabla \\ A &= \frac{\varepsilon_0}{2\pi}\frac{\exp(-jk_0|r-r_0|)}{|r-r_0|} \end{aligned} \tag{3.4}$$

where k_0 ($= 2\pi / \lambda_0$), ε_0 and μ_0 is wave number, permittivity and permeability, respectively.

3.4.2 Slot admittance

Once excitation of the slot apertures (M_1 and M_2) are determined by the analysis, transmission and reflection coefficients, S_{11} and S_{21} in the scattering matrix for a slot is derived straightforwardly. Normalized equivalent slot admittances are obtained by the following expression [3-19, Sec. 5.7];

$$y = \frac{-2S_{11}}{1+S_{11}} \tag{3.5}$$

Resonant slot length $2l$ for given offset d is obtained by imposing that imaginary part of the equivalent slot admittance is equal to zero. Both the resonant slot length $2l$ and the offset d are expressed as functions of the equivalent slot conductance g (= Re [y]) as is shown in Fig. 3.5. The conductance g corresponds to g_n in Fig. 3.3. The design parameters are shown in Table 3.1 for the analysis.

3.4.3 Numerical results

Slot conductance in terms of length and offset derived here is utilized to synthesize the desired slot excitation and is reflected upon the aperture illumination in the final design of array. In order to show the effects of the mutual coupling in the model (A) with periodic boundary walls, two kinds of array parameters are compared. The relationship of normalized conductance and slot length or offset are presented for both design models (A) and (B) in Fig. 3.6. For given parameters of slot, normalized conductance evaluated in (A) is significantly larger than that in (B), which explains that the mutual couplings intensify the excitation [3-3].

3.5 Array design

In the final steps of the array design, all the slot parameters are determined by using the conductance assigned in Sec. 3.3 and the slot parameters given in Fig. 3.6. The design procedure in Fig. 3.2 is conducted for the array in Fig. 3.1. Important parameters of slot length and offset over the aperture in two designs (A) and (B) are shown in Fig. 3.7. The slot length by design (A) including mutual couplings is about 3% shorter than the one by (B) neglecting mutual coupling. Furthermore, large difference no less than 7 % of half the broad guide width is observed between the slot offset for (A) and (B). These miss-evaluation causes slot excitation error. The predicted difference of slot coupled power for the desired normalized conductance of 0.077 between design (A) [d = 0.51 mm, $2l$ = 6.22 mm] and design (B) [d = 0.86 mm (60 % error), $2l$ = 6.44 mm (3 % error)] is about 4 dB and that of phase is about 46 degrees; considerable amplitude decay and phase delay toward the termination would occur if mutual coupling was neglected.

3.6 Measurements

The superiority of design (A) to design (B) and the validity of "infinite in E-plane and finite in H-plane" model used in iteration is confirmed for various size (M) of the array by experiments. The mutual couplings from the slots on other waveguides are dominant factor in all the mutual effects, since element pattern of a slot is maximum in x-direction and null in z-direction; the number of waveguide M in transverse direction may affect the superiority. Three sizes ($M = 1$, 4 and 24) of arrays are fabricated by two design. Design (A) adopts periodic model as well as the associate iteration for $N = 25$ in Sec. 3.3 while Design (B) neglects mutual couplings. One-dimensional array ($M1$), 4-waveguides array ($M4$) and 24 waveguides array ($M24$) designed by (A) and (B) are denoted by array ($M1$-A), ($M1$-B), ($M4$-A), ($M4$-B), ($M24$-A) and ($M24$-B). Measured aperture illuminations of the arrays for $N = 25$, which are all subject to practical mutual coupling, are shown in Fig. 3.8. A probe scans along z-direction of the center of the antenna aperture and receives near field of the antenna. The distance between the probe and the test antenna is 30 mm (2.2 wavelength in free space). The levels of the amplitude and the phase are relative one since the reflection characteristics of the antennas are different. The dotted lines indicate the predicted illuminations using aperture illumination estimating model in Fig. 3.4 where K is set to be 0, 2, and 8 for $M1$, $M4$ and $M24$ arrays, respectively. The predicted illumination reasonably explains the measured one.

It is trivial that the array ($M1$-B) is more uniform than array ($M1$-A), since quite small mutual couplings exist in one-dimensional array. The effectiveness of our design (A) is well illustrated for array ($M24$). The mutual couplings degrade aperture illumination uniformity in the array ($M24$-B). In the array ($M24$-A) on the other hand, the mutual couplings in the two-dimensional array are effectively reflected in the design and uniform illumination is obtained over the aperture. Measurement of relatively small array ($M4$) shows similar superiority of design (A) over (B). So the design (A) assuming infinite E-plane is valid even for small arrays with no less than four waveguides. Hence the applicability of design model (A) for wide classes of two-dimensional arrays are suggested.

In the end of discussion, the illumination along the x-direction is presented in

Fig. 3.9 for 24-waveguides array which is measured above 13th slots at the center of the array in the z-direction. Uniformity is acceptable though small deviation due to the edge is observed [3-4]. The agreement between the measured curves and calculated ones for $M = 4$ and 24 in Fig. 3.8 partly supports the effectiveness of the analysis on the assumption of $M = \infty$.

3.7 Concluding remarks

An effective design of the slotted waveguide planar array is proposed in this chapter with taking mutual coupling into account using periodic boundary condition. The uniformity of measured aperture illumination of the planar array is confirmed by comparing with the array designed by neglecting mutual couplings. The applicability of this design is wide and is valid even for the array with as small as four waveguides.

References

[3-1] Elliott, R. S., Kurtz, L. A., " The design of small slot arrays," *IEEE Trans. on Antennas and Propagation*, vol. 26, no. 2, pp. 214-219, March 1978

[3-2] Elliott, R. S., " An improved design procedure for small arrays of shunt slots," *IEEE Trans. on Antennas and Propagation*, vol. 31, no. 1, pp. 48-53, January 1983

[3-3] Yee, H. Y., " Impedance of a narrow longitudinal shunt slot in a slotted waveguide array," *IEEE Trans. on Antennas and Propagation*, pp. 589-592, July 1974

[3-4] Scharstein, R. W., " Mutual coupling in a slotted phased array, infinite in E-plane and finite in H-plane," *IEEE Trans. on Antennas and Propagation*, vol. 38, no. 8, pp. 1186-1191, August 1990

[3-5] Edelberg, S. and Oliner, A. A., " Mutual coupling effects in large antenna arrays: part I - slot arrays," *IRE Trans. on Antennas and Propagation*, pp. 286-297, May 1960

[3-6] Lee, S. W. and Jones, W. R., " On the suppression of radiation nulls and broadband impedance matching of rectangular waveguide phased arrays," *IEEE Trans. on Antennas and Propagation*, vol. 19, no. 1, pp. 41-51, January 1971

[3-7] Wu, C. P. and Galindo, V., " Properties of a phased array of rectangular waveguides with thin walls," *IEEE Trans. on Antennas and Propagation*, vol. 14, no. 2, pp. 163-173, March 1966

[3-8] Farrell, Jr., G. F. and Kuhn, D. H., " Mutual coupling in infinite planar arrays of rectangular waveguide horns," *IEEE Trans. on Antennas and Propagation*, vol. 16, no. 4, pp. 405-414, July 1968

[3-9] Galindo, V. and Wu, C. P., " Numerical solutions for an infinite phased array of rectangular waveguides with thick walls," *IEEE Trans. on Antennas and Propagation*, vol. 14, no. 2, pp. 149-158, March 1966

[3-10] Pozar, D. M. and Schaubert, D. H., " Analysis of an infinite array of rectangular microstrip patches with idealized probe feeds," *IEEE Trans. on Antennas and Propagation*, Vol. 32, No. 10, October 1984

[3-11] Pozar, D. M. and Schaubert, D. H., " Scan blindness in infinite phased arrays of printed dipoles," *IEEE Trans. on Antennas and Propagation*, Vol. 32, No. 6, June 1984

[3-12] Konishi, Y., Mizutamari, H., Sato, S., Mano, S. and Katagi, T, " Analysis and design methods of planar array antennas with slotted waveguides taking into account mutual coupling," IEICE Technical report, vol. J71-B, no. 11, pp. 1325-1331, November 1988

[3-13] Seki, H., " An alternative representation of electromagnetic fields in a rectangular waveguide with an aperture in its wall," *IECE Natl. Conv. Rec.*, vol. 1, no. 16, Sep. 1984

[3-14] Hirokawa, J., Ando, M. and Goto, N., " A single-layer multiple-way power divider for a planar slotted waveguide array," *IEICE Trans. Commun.*, Vol. E75-B, No. 8, pp. 781-787, August 1992

[3-15] Johnson, R. C. and Jasik, H., *Antenna Engineering Handbook*, New York McGraw-Hill, Chap. 9, 1984

[3-16] Collin, R. E. and Zucker, F. J., *Antenna theory*, Sec. 14.8, McGraw-Hill, 1969

[3-17] Tsunoda, Y. and Goto, N., " Nonuniformly spaced slot array antenna with low sidelobe pattern," *IEE Proc.*, Vol. 133, Pt. H, No. 2, April 1986

[3-18] Hirokawa, J., Sakurai, K., Ando, M. and Goto, N., " Matching slot pair for a circularly-polarized slotted waveguide array," *IEE Proc.*, Vol. 137, Pt. H, No. 6, pp. 367-371, December 1990

[3-19] Collin, R. E., *Field Theory of Guided Waves*, IEEE PRESS

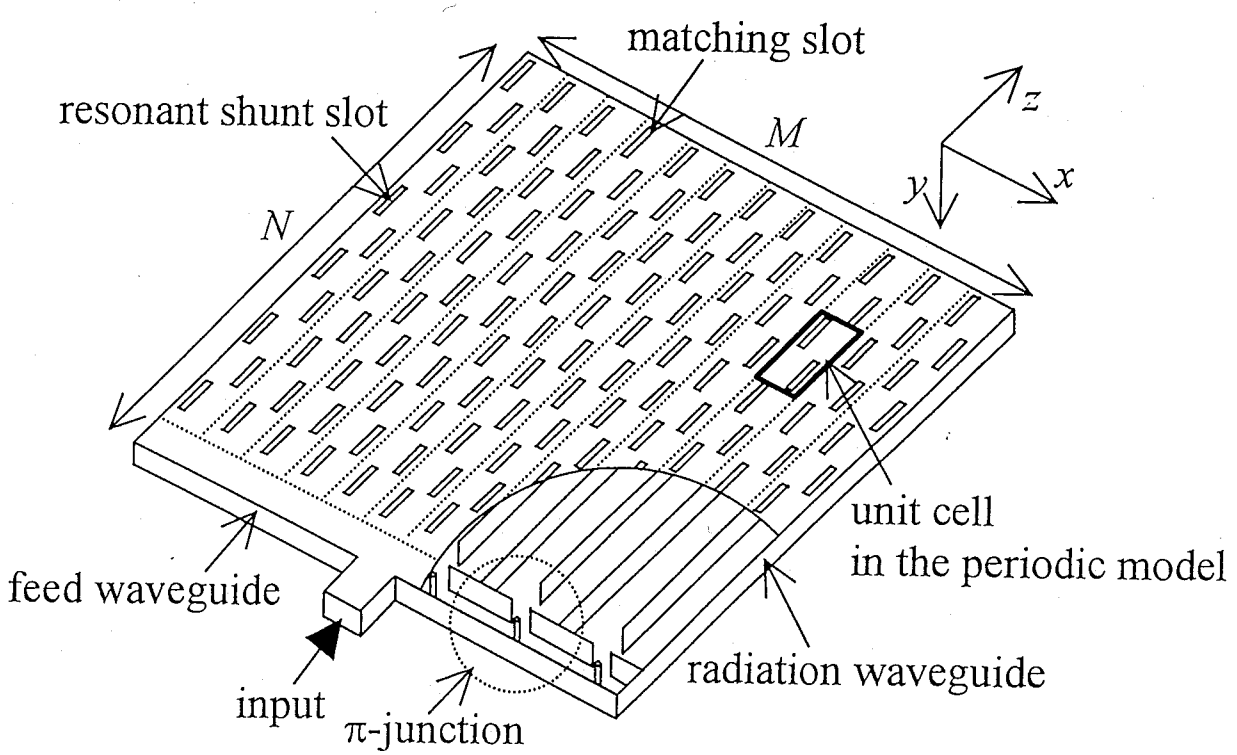

Fig. 3.1 Array antenna configuration

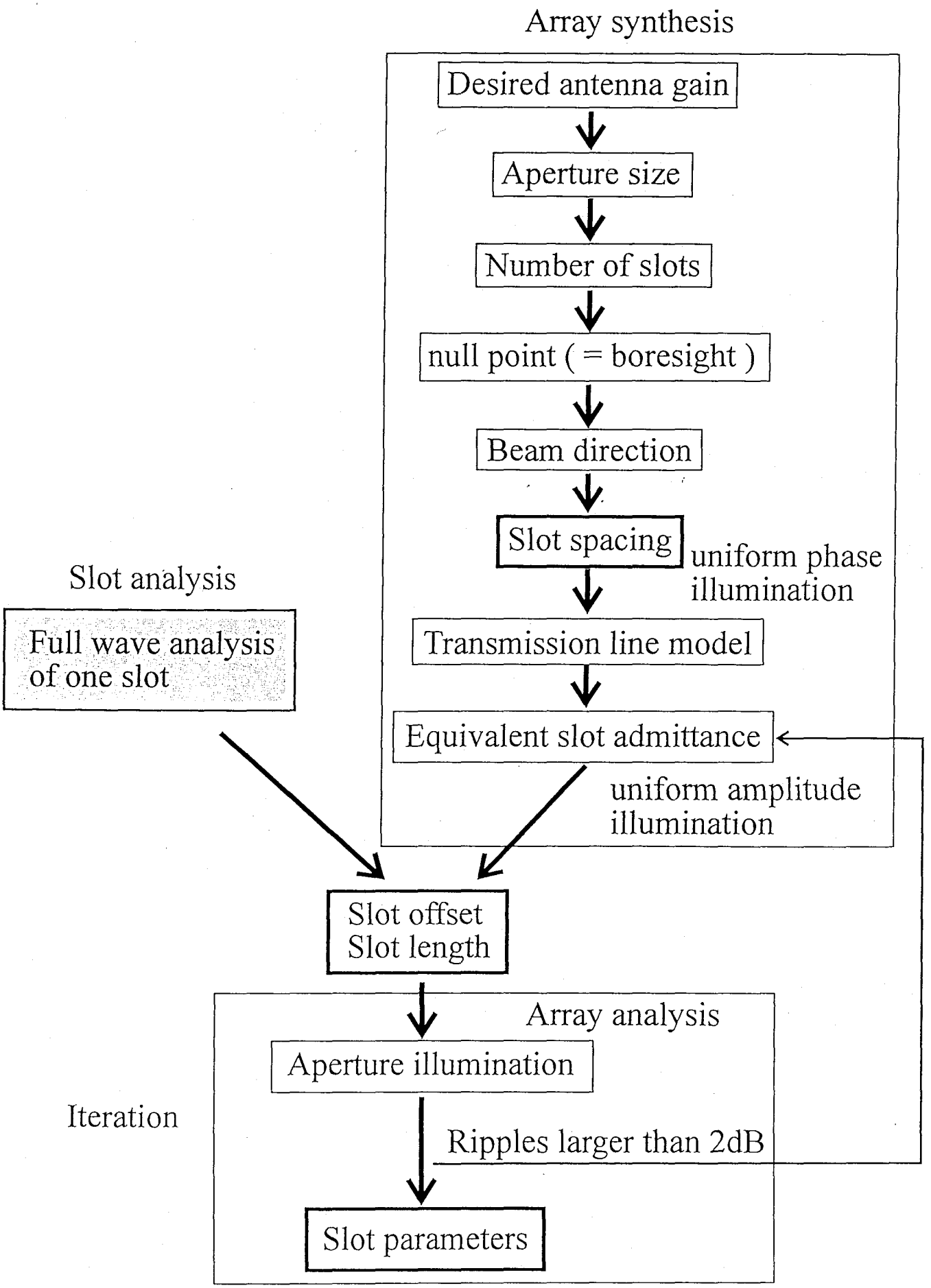

Fig. 3.2 Flow chart of the slot design

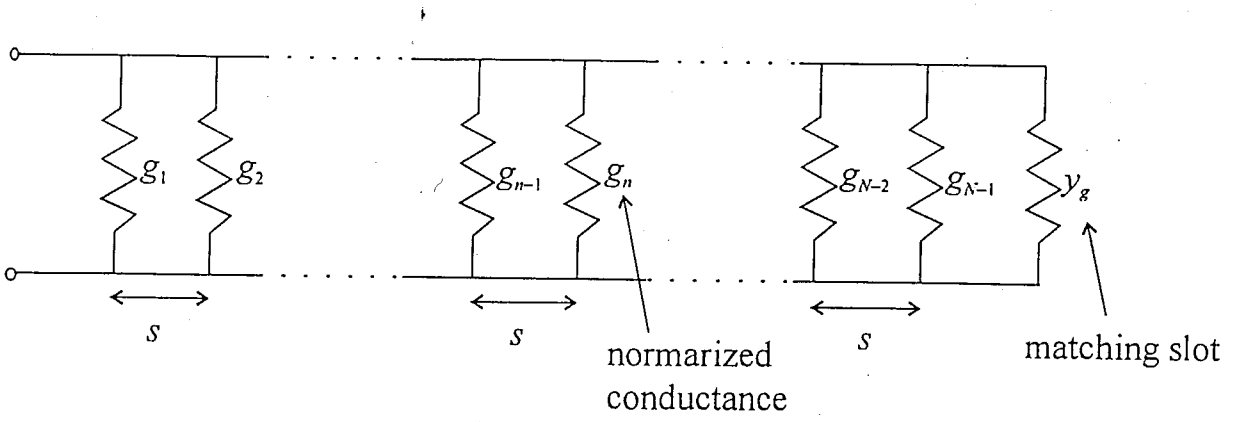

Fig. 3.3 Equivalent transmission line model of one-dimensional array

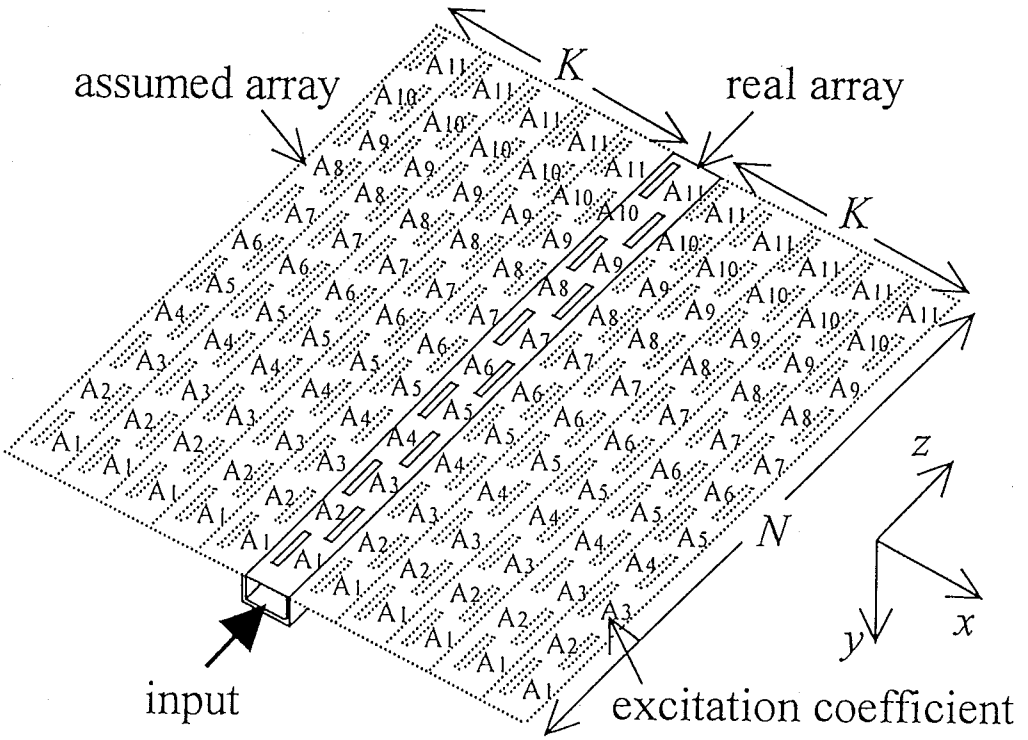

Fig. 3.4 Aperture illumination estimating model
of a two-dimensional array

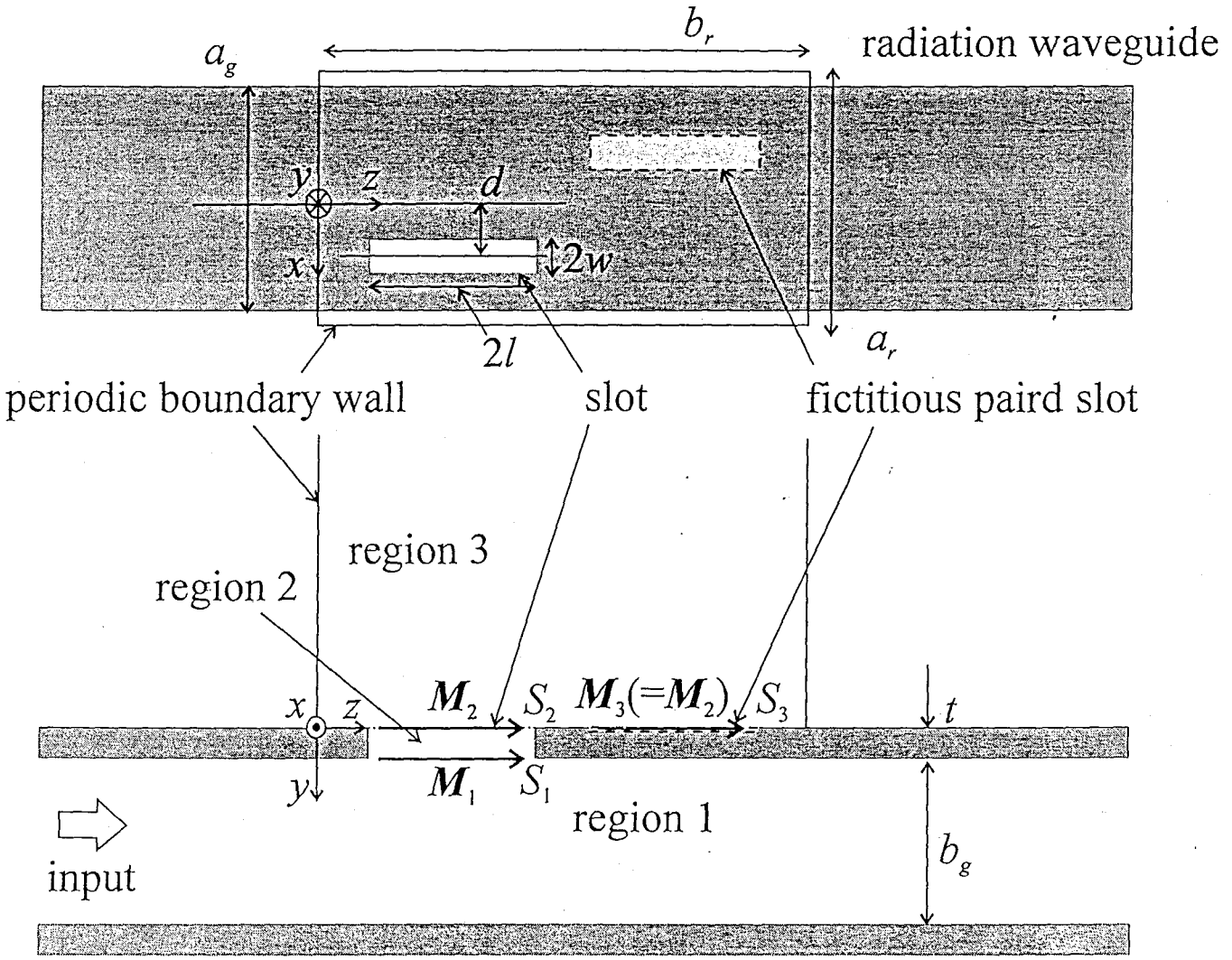

Fig. 3.5 Analysis model of one slot with periodic boundary walls in the external region

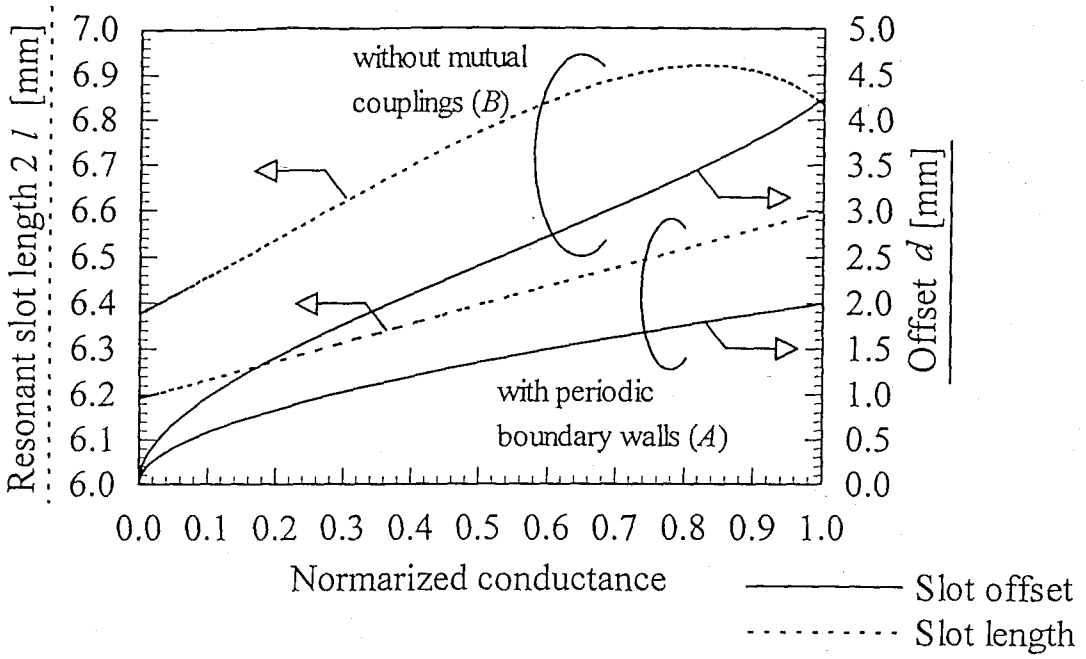

Fig.3.6 Slot parameters related to normarized conductance

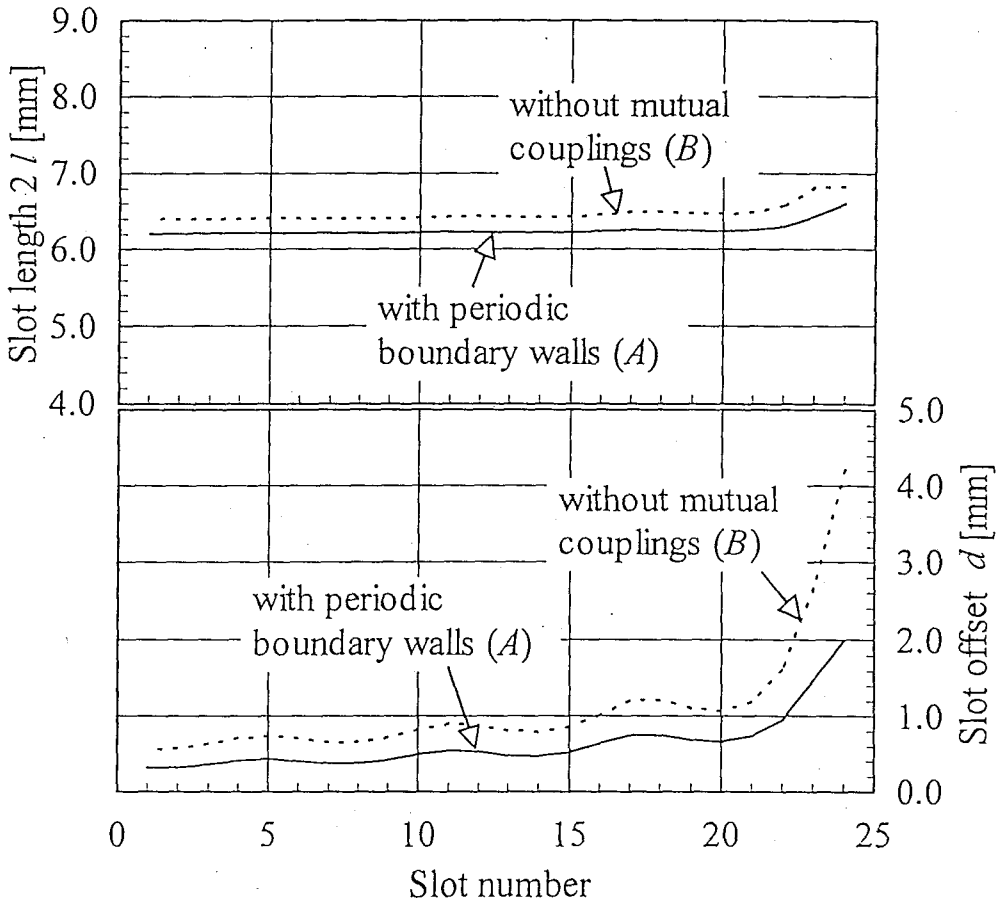

Fig. 3.7 Array parameters designed
by the model (*A*): with periodic boundary walls
and by the model (*B*): without mutual couplings.

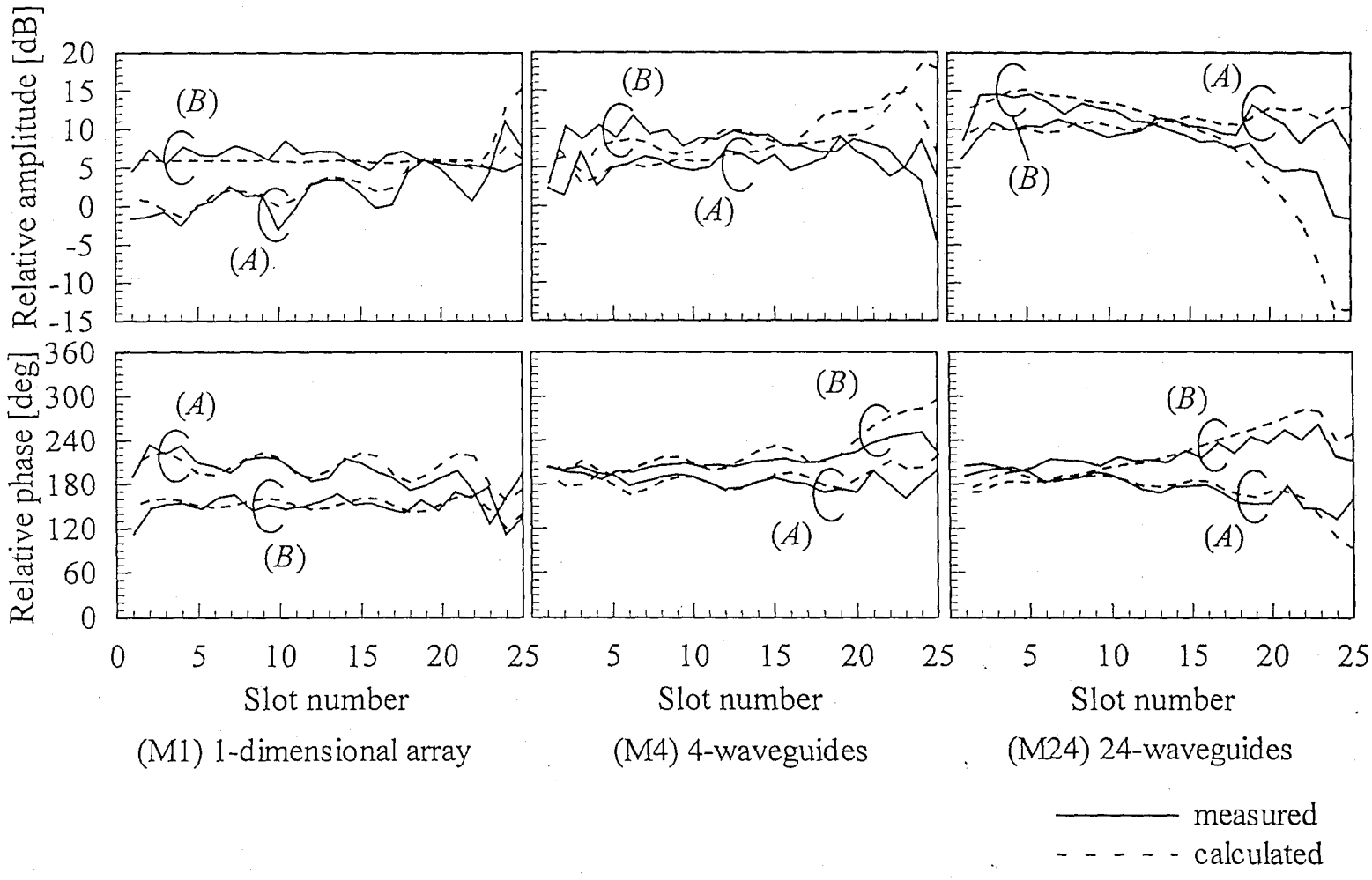

Fig. 3.8 Aperture distributions designed
by the model (*A*): with periodic boundary walls
and by the model (*B*): without mutual couplings.

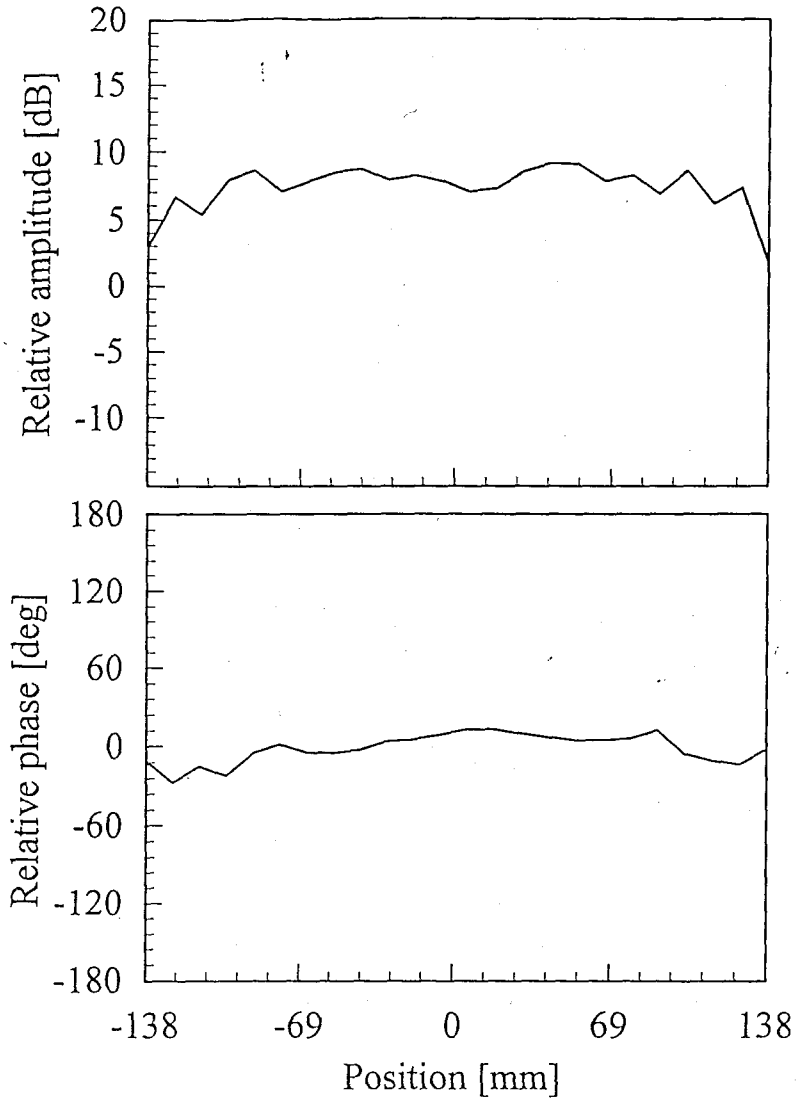

Fig. 3.9 Measured aperture distributions
in the x-direction (22.2GHz)

Table 3.1 Design parameters

design frequency f	22.2 GHz
broad guide width a_g	10 mm
narrow guide width b_g	4 mm
wall thickness between the waveguides h	2 mm
slot spacing in z-direction s	10.62 mm
periodic spacing a_r ($= a_g + h$)	12 mm
periodic spacing b_r ($= 2s$)	21.24 mm
slot plate thickness t	1 mm
beam tilting angle θ_t	5.8 deg

Chapter 4. Linearly-polarized shunt slot array

4.1 Introductory remarks

High gain planar antennas in milli-meter wave are the key device in collision avidance radar and high-speed wireless LAN etc. Typical reqirements are high gain of more than 35 dBi in 60 to 80 GHz band. Many works have been reported to this end, using microstrip and triplate line patch antennas [4-1]-[4-6]. However, the conducting loss becomes notable in this gain and frequency range; only the antennas with lower gain (20 - 30 dBi) or lower efficiency (20 - 60 %) have been reported. Waveguide antennas are free from conductor loss in principle and is an atractive candidate of high efficiency planar antenna. However, the complicated three-dimensional feed structure have been preventing the use for commercial application [4-7]. Drastic reduction of manufacturing cost to the level of microstrip and triplate ones is necessary.

Authors have developed low-profile single layer slotted waveguide arrays [4-8] [4-9]. This paper demonstrates the potential of this type of antennas for high gain and high frequency application [4-10]. Figure 4.1 shows the structure of a single-layer slotted waveguide array. A feed waveguide is placed perpendicularly in the same layer of the radiation waveguides. The antenna consists of only two parts and can be fabricated by placing the slotted plate on the groove structure. The slotted plate can be made by printing technology while the groove structure can be made by die casting; it is suitable for mass production and cost reduction. The feed waveguide is a cascade of π-junctions with an inductive walls [4-11] [4-12]. One window of the π-junction couples to two radiation waveguides and all the waveguides are excited in phase since the guide wavelength in the feed waveguide is set to be twice the width of the radiation waveguide including the wall thickness. They are excited in equal amplitude as well by controlling the widths of the windows in the π-junctions.

The peak efficiency of 75.6 % and the gain of 35.9 dBi are obtained at 22.15 GHz by the brazing-contacted test antenna sized 300 mm. It is quite high in comparison

with conventional planar antennas in this range of gain and frequency.

For the commercial application of this unique antenna to higher frequency, one key technology is the realization of mass produceable means for electric contact between the slotted plate and the base with the groove structure. Cost effective approaches such as laser welding and bonding are also under study [4-13].

4.2 Design of radiation waveguides

A radiation waveguide is an array of resonant shunt slots. The slots parallel to the guide axis are cut on the broad wall [4-13]. The slot offset from the center of the waveguide controls the amplitude of the slot excitation in order to realize a uniform distribution on the aperture, while the slot spacing determines the phase. In order to suppress reflections at the feed point, a few degrees beam tilting is adopted. A matching slot composed of a wide slot with large offset and a shorted circuit is placed at the waveguide terminal in order to radiate all the residual power and to realize quasi-traveling wave operation [4-14].

Design of the antenan have been basically explained in Chap. 3. In order to design it systematically, the radiation waveguide is replaced with a transmission model. A resonant shunt slot can be represented by an equivalent conductance in it [4-15] [4-16]. The conductance of each slot is assigned for uniform amplitude distribution on the aperture. The relationship between the conductance and the slot parameters such as the length and the offset is calculated by the method of moments [4-14] [4-17]. The periodic boundary condition is imposed in the half space in order to simulate external mutual couplings without incereasing the number of unknowns [4-18]-[4-20]. In order to enhance the uniformity of the aperture distribution determined above, several iterations based upon the full wave analysis is conducted in the final stage of the design to eliminate the end-effects of the finite array.

4.3 Experimental results of the test antenna in 22 GHz band

A two-dimensional slot array is fabricated for experiments in 22 GHz band.

The design parameters are listed in Table 4.1. Figure 4.2 shows the frequency dependence of the gain. The peak gain of 35.9 dBi is obtained and the antenna efficiency is 75.6 % at 22.2GHz. The reflection is smaller than −16 dB in the required 600 MHz bandwidth as is shown in Fig. 4.3. It is not enough but acceptable.

Figure 4.4 shows the aperture distributions at the center frequency (22.2 GHz) and at the edge of the 600 MHz bandwidth (21.9 GHz and 22.5 GHz). In the phase distribution along the radiation waveguides, tapers corresponding to the beam tilting are subtracted. The antenna is designed to realize the uniform illumination at 22.3 GHz. However, the aperture phase is actually uniform at 22.15 GHz. The frequency shift is mainly due to the thermal expansion of the waveguide in the brazing. In Fig. 4.2, the black dots indicate the predicted gain based upon the measured phase taper along the feed waveguide. Its tendency agrees with the measured ones.

Figure 4.5 shows the radiation patterns at 22.2 GHz. The H-plane pattern reflects the illumination along the radiation waveguide. The measured radiation pattern reasonably agrees with the predicted one. Furthermore, the symmetrical radiation pattern is obtained in the E-plane, which reflects the uniform power dividing by the feed circuit.

4.4 Application in higher frequency

Car collision avoidance radars are developed in some other laboratories and organizations. They are expected for improvement of car safety. Since the beam width of the radar antenna has to be narrow in order to keep angular resolution, the gain of the antenna is quite high. The radar antennas should perform high-gain and high-efficiency even in 60 GHz band and should be low-profile in order to install at the front of cars. The single layer slotted waveguide array realizes the efficiency of 75.6 % and the gain of 35.9 dBi in 22 GHz band mentioned in Sec. 4.2. It is promising for high performance radar antenna.

Based on the test antenna in 22 GHz band, a 60 GHz scale model is designed. The design parameters are shown in Table 4.2. The size of the aperture is the same with the 22 GHz antenna normarized by the wavelength. Slot spacing determines the beam direction. In order to suppress the reflections at the feed point, the second null from the peak should be chosen as the beam tilting angle. The equation (A.1) in appendix A explains that slot spacing is large for large beam tilting angle. The grating lobe appears

due to the large slot spacing. The beam tilting angle is chosen at the first null from the peak in order to suppress the grating lobe. The reflection is lower than −13 dB in 1 GHz bandwidth as is shown in Fig. 4.6 which is not enough due to small beam tilting angle. Provided that the slot spacing is smaller than half guide wavelength, the main beam inclines to opposite direction $-\theta_t$. In order to suppress the grating lobe and the reflections, negative second null would be chosen for the beam tilting angle in the next design.

Figure 4.7 shows aperture distribution along the radiation waveguide at the frequencies of 59.75, 60 and 60.25 GHz. Ripples are observed in the amplitude distributions. They are in 4 dB at the center frequency and in 7 dB at the edge of the bandwidth. The phase distributions are slightly tapered at the band edge due to the long line effect.

Figure 4.8 shows radiation pattern at 60 GHz. The slot spacing is 4.3 mm or 0.86 λ_0 which couses −25 dB grating lobes observed in −60 degrees direction. Radar antenna requires low side lobe characteristics. However, the side lobe level of this antenna is −10 dB. Pattern sinthsis is inevitable for the actual radar antenna. The beam width at half power points is 2.3 degrees. In order to resolve a 3.5 m lane of traffic at a distance of 100 m, the beam width of 2 degrees are required. The size of the antenna should be large. The side lobe level is low in the diagonal-plane of the antenna because the diagonal length of the antenna is longer than the side of the square. In order to avoid the interferance with the car in the opposite lane, 45 degrees inclined linearly-polarization is considered to be used. Such a square antenna may be effective in terms of the low side lobe in holizontal and perpendicular planes.

Figure 4.9 shows frequency dependence of the gain. The gain is higher than 36.3 dBi in 500 MHz bandwidth and the peak aperture efficiency is 90 %. However, several losses are predicted in such a high frequency band. Provided that the antenna efficiency is 60 %, the gain is higher than 34.4 dBi in 500 GHz bandwidth which is 1.9 dB lower than calculation.

In the measurement of the 60 GHz test antenna, the peak gain of 35.1 dB and the antenna efficiency of 58.8 % are realized at 60.2 GHz. It is extremely high in comparison with the results of any other planar antennas. The reflection characteristic is poor and the level is about −5 dB at 59.8 GHz. The gain would increase, if the reflection

characteristics is improved.

4.5 Concluding remarks

A high-efficiency and high gain planar slotted waveguide array is fablicated in 22 GHz band. The single-layer feed circuit composed of a cascade of π-junctions is adopted. A drastically simple structure is realized, which is suitable for mass-production. The test antenna is fabricated by placing the slot plate on the grooves. The peak antenna efficiency of 75.6 % is obtained when the gain is 35.9 dBi at 22.15 GHz, which is quite high in comparison with any other planar antennas in this frequency and gain range. These results explain the high potential for applications to higher frequency. The scale model antenna is designed for car collision avoidance radar in 60 GHz. These results would be the first step in order to apply the slotted waveguide antennas of this type for such higher frequency and high gain uses. Reduction of the loss without degrading the mass produceability is inevitable in the future study to fully demonstrate the superiority of a single-layer waveguide slot antenna mentioned in Chap. 2 [4-21] [4-22].

References

[4-1] Weiss, M. A., " Microstrip antennas for millimeter waves," *IEEE Trans. on A.P.*, vol. AP-29, No. 1, pp. 171-174, Jan. 1981

[4-2] Huang, J., " A Ka-band circularly polarized high-gain microstrip array antenna," *IEEE Trans. on A.P.*, pp. 113-116, Jan., 1995

[4-3] Kado, S., Ohta, M., Hirao, M., Wakushima, S., Nozue, Y. and Haneishi, M., " Radiation properties of 22 GHz band triplate feed type patch antennas with parasitic elements," *IEICE Natl. Conv. Rec.*, B-53, March 1994

[4-4] Ohta, M., Ishizaka, H., Wakushima, S., Uesato, Y. and Haneishi, M., " Radiation properties of triplate-feed-type patch antennas at 60 GHz band," *IEICE Natl. Conv. Rec.*, B-114, Sep. 1993

[4-5] Ohta, M., Ishizaka, H., Kose, R., Saito, T., Okubo, N. and Haneishi, M., " Radiation properties of circularly polarized triplate-feed-type patch antennas at 60 GHz band," *IEICE Natl. Conv. Rec.*, B-115, Sep. 1994

[4-6] Kitao, S., Yamato, M., Ohmine, H., Aoki, H. and Haruyama, T., " Radiation

properties of triplate line fed microstrip array antenna with polarization grid in the 60 GHz band," *IEICE Natl. Conv. Rec.*, B-60, Sep. 1995

[4-7] Collin, R. E., *Antennas and Radiowave Propagation*, New York McGraw-Hill, Chap. 1, pp. 6-7, 1985

[4-8] Sakakibara, K., Hirokawa, J., Ando, M. and Goto, N., " A slotted waveguide planar array antenna for entrance radio systems in mobile communication," *4th IEEE Int. Conf. on Universal Personal Commun.*, pp. 373-376, Tokyo, Nov. 1995

[4-9] Sakakibara, K., Hirokawa, J., Ando, M. and Goto, N., " A linearly polarized slotted waveguide planar array using single layer feed circuit for 22 GHz band radio system," *IEICE APMC Proc.*, pp. 307-310, Tokyo, Dec. 1994

[4-10] *R.C.R. news*, No. 403, Research & Development Center for Radio Systems, May. 4, 1993

[4-11] Hirokawa, J., Ando, M. and Goto, N., " A single-layer multiple-way power divider for a planar slotted waveguide array," *IEICE Trans. Commun.*, Vol. E75-B, No. 8, pp. 781-787, August 1992

[4-12] Takahashi, T., Hirokawa, J., Ando, M. and Goto, N., " The suppression of the reflection by an inductive wall of a power divider for a slotted waveguide array," *Tech. Rep. of IEICE*, AP-94-7, April 1994

[4-13] Johnson, R. C. and Jasik, H., *Antenna Engineering Handbook*, New York McGraw-Hill, Chap. 9, 1984

[4-14] Hirokawa, J., Sakurai, K., Ando, M. and Goto, N., " Matching slot pair for a circularly-polarized slotted waveguide array," *IEE Proc.*, Vol. 137, Pt. H, No. 6, pp. 367-371, December 1990

[4-15] Tsunoda, Y. and Goto, N., " Nonuniformly spaced slot array antenna with low sidelobe pattern," *IEE Proceedings*, Vol.133, Pt. H, No.2, April 1986

[4-16] Tsunoda, Y. and Goto, N., " A design of ununiformly spaced slot array antenna," *Technical report of IEICE*, AP 82-101, November 1982

[4-17] Seki, H., " An alternative representation of electromagnetic fields in a rectangular waveguide with an aperture in its wall," *IECE Natl. Conv. Rec.*, vol. 1, no. 16, Sep. 1984

[4-18] Collin, R. E., *Field Theory of Guided Waves*, *IEEE PRESS*, Chap. 9, pp. 605-608

[4-19] Edelberg, S. and Oliner, A. A., " Mutual coupling effects in large antenna arrays:

part I – slot arrays," *IRE Trans. on Antennas and Propagation*, pp. 286-297, May 1960

[4-20] Sakakibara, K., Hirokawa, J., Ando, M., and Goto, N., " Simple evaluation of mutual slot couplings in a slotted waveguide planar array antenna," *IEEE AP-S*, Newport Beach, pp. 1838-1841, June, 1995

[4-21] Goto, N., " A waveguide-fed printed antenna," *Technical Report of IEICE*, AP 89-3, pp. 17-21, April, 1989

[4-22] Hirose, R., Ando, M. and Goto, N., " A design of a multiple-way power divider for a single layered slotted waveguide array," *Technical Report of IEICE*, AP 90-130, pp. 29-34, Feb. 1991

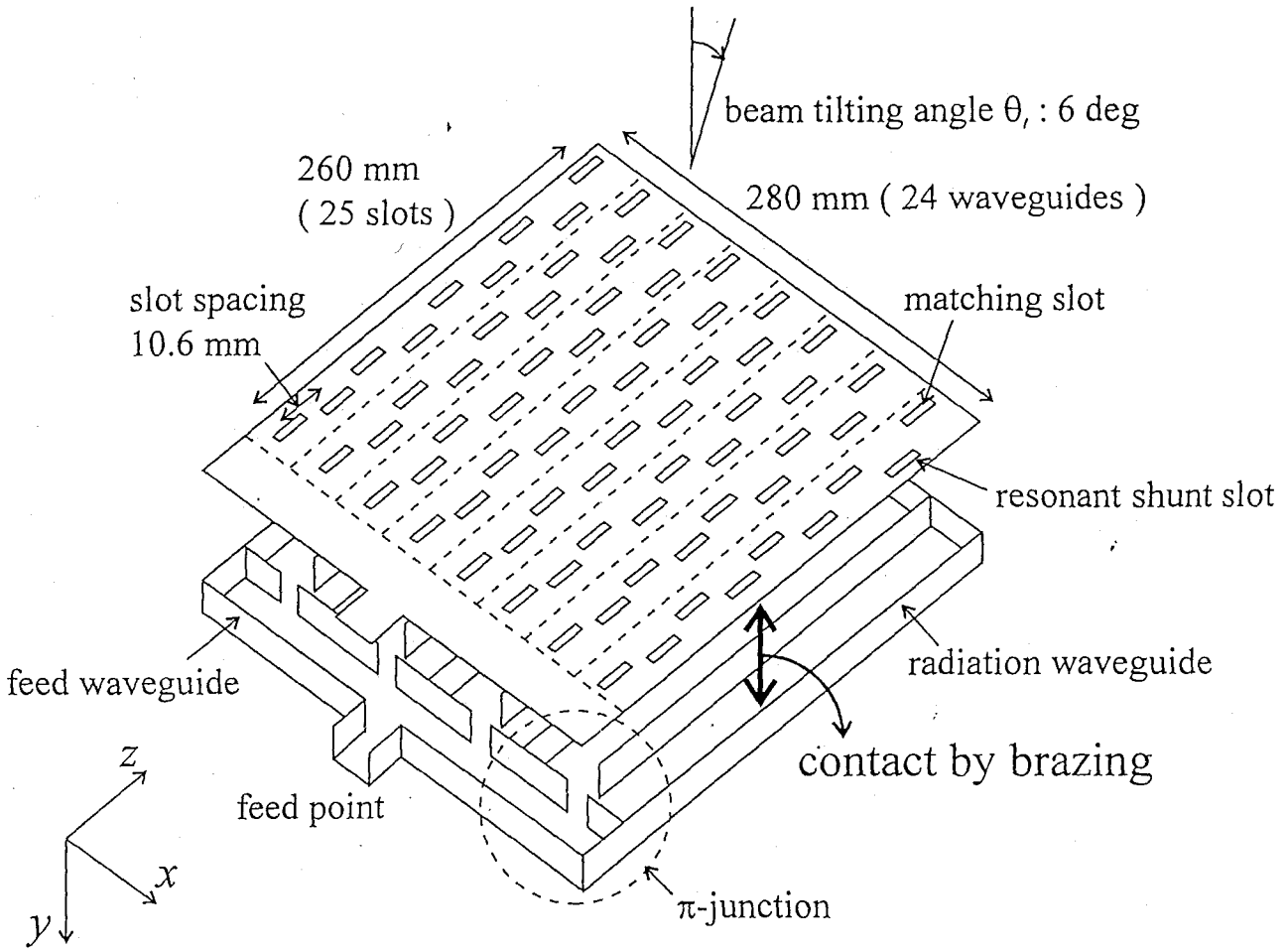

Fig. 4.1 Configuration of test antenna

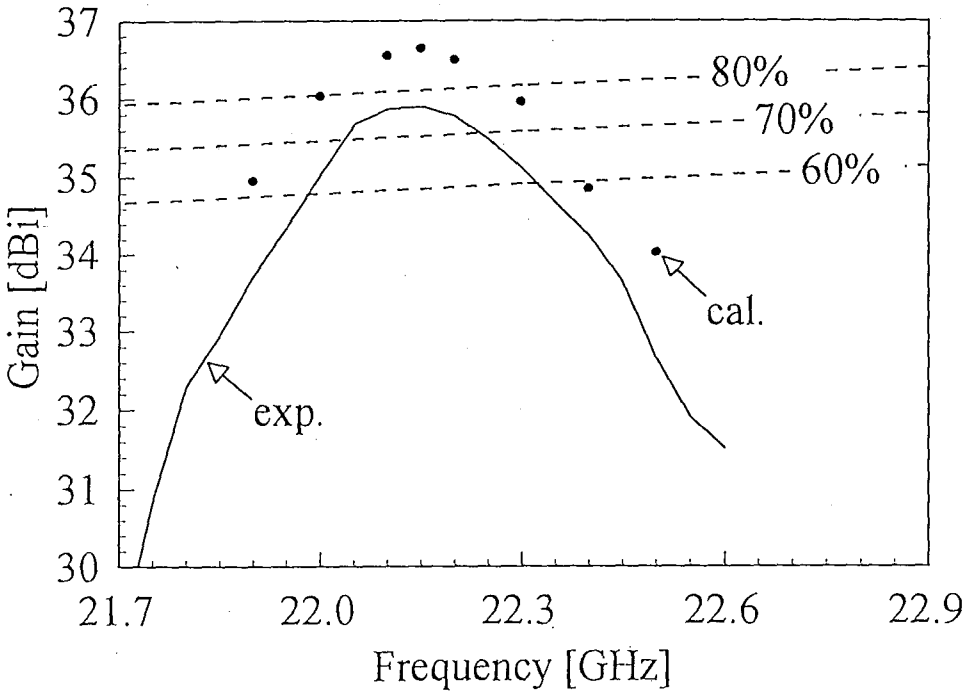

——— : experiment

. : calculation including measured phase taper along feed waveguide

Fig. 4.2 Gain and antenna efficiency

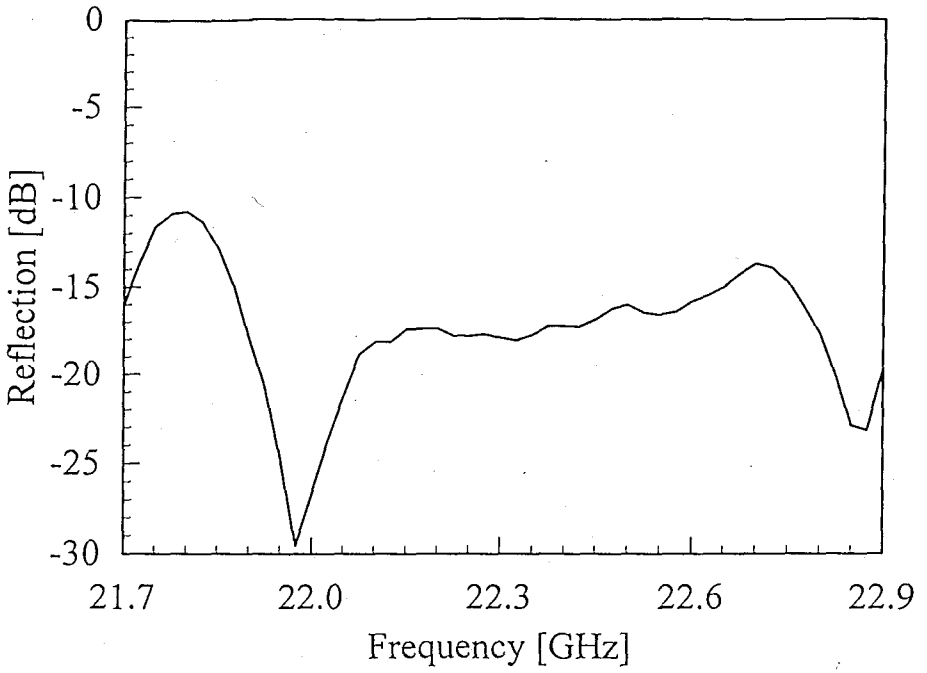

Fig.4.3 Reflection characteristics

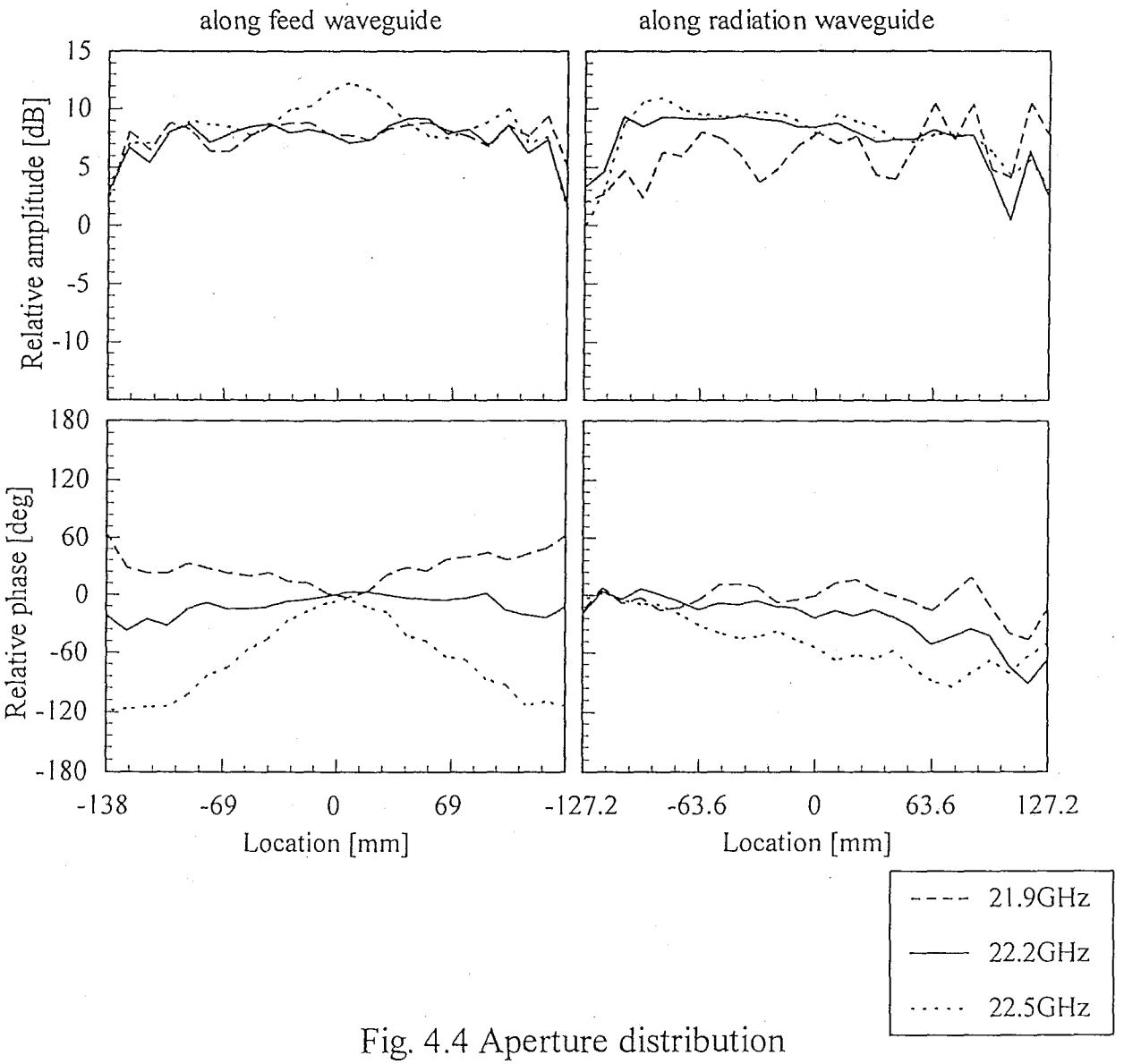

Fig. 4.4 Aperture distribution

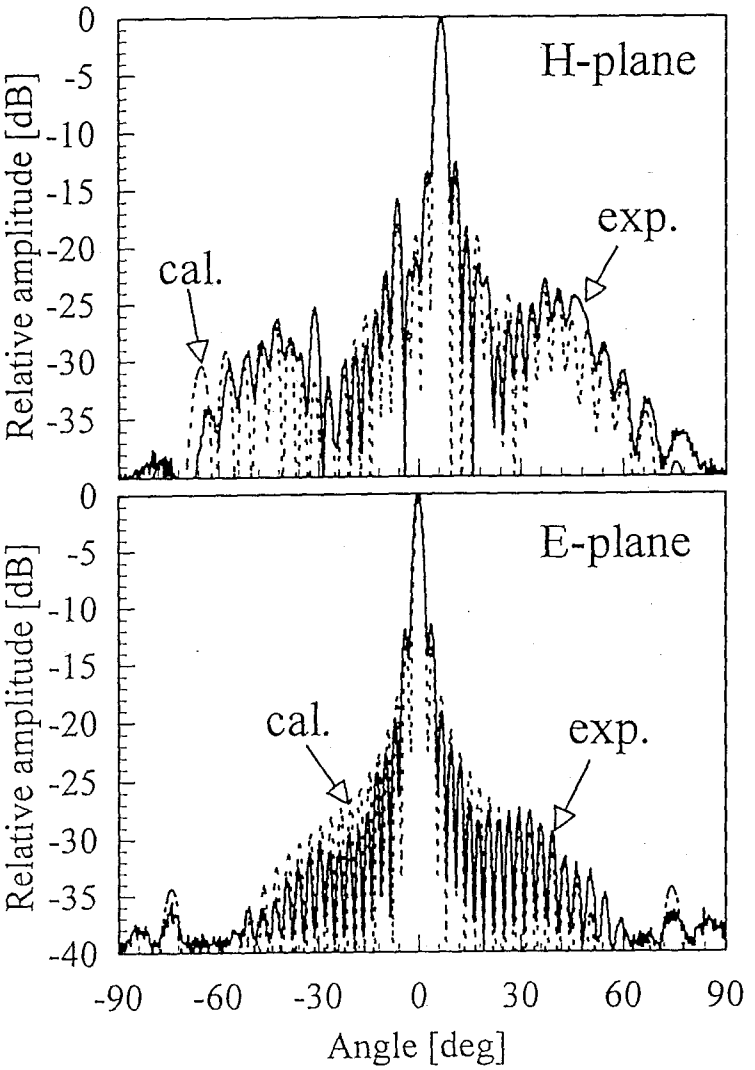

Fig. 4.5 Radiation pattern (22.2 GHz)

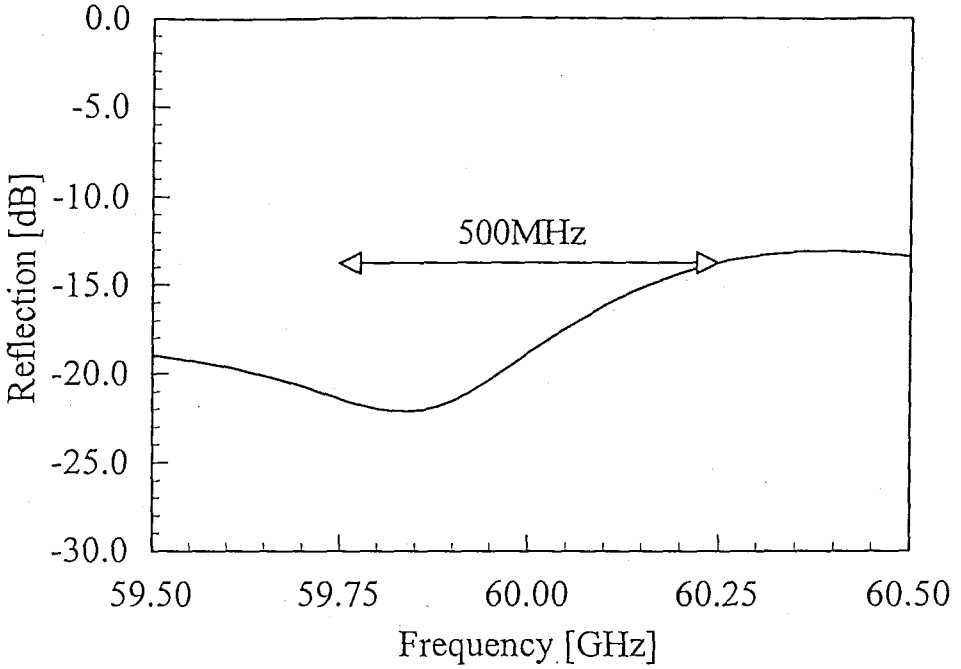

Fig. 4.6 Numerical reflection characteristics

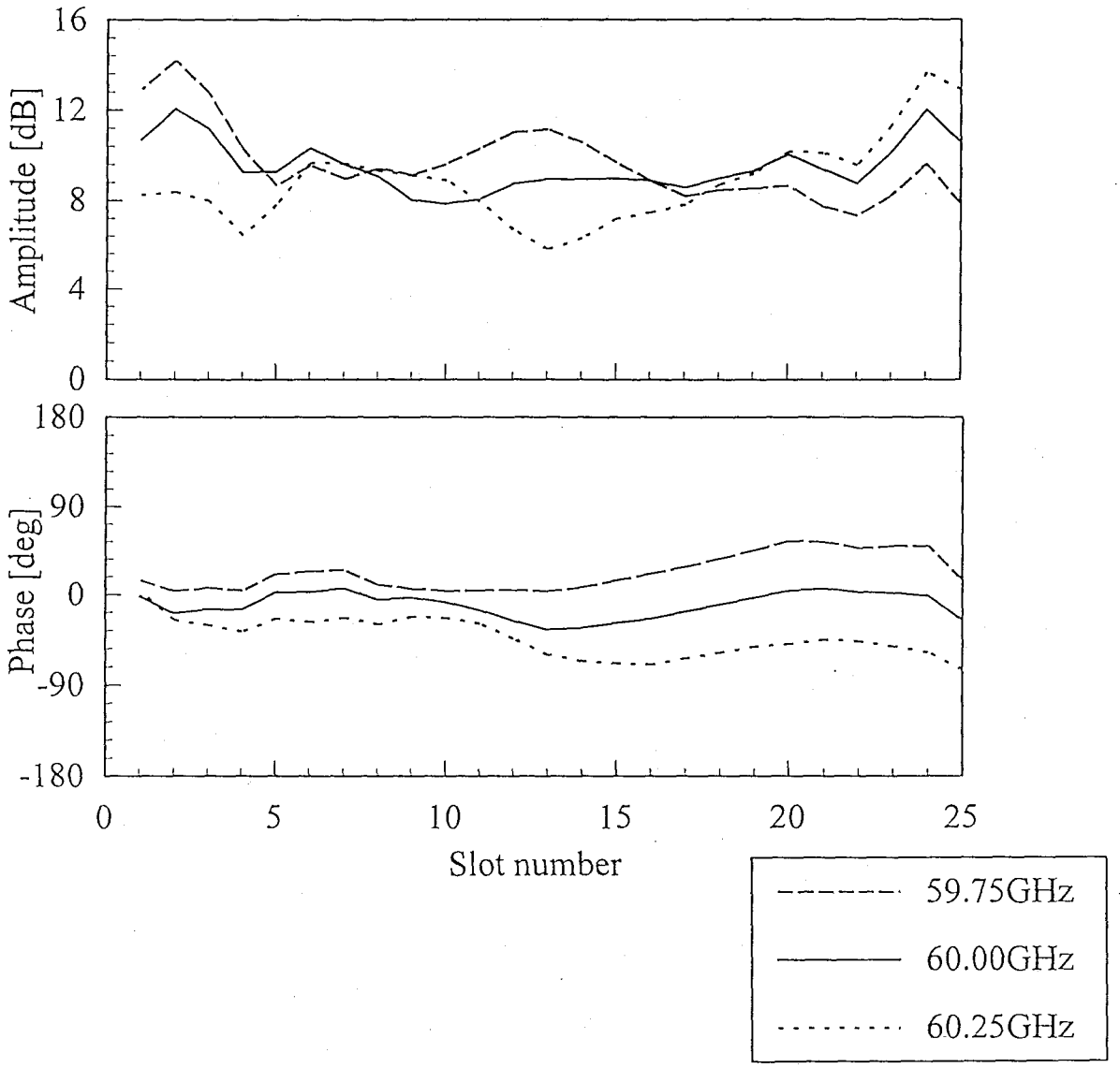

Fig. 4.7 Aperture distribution along the z-direction

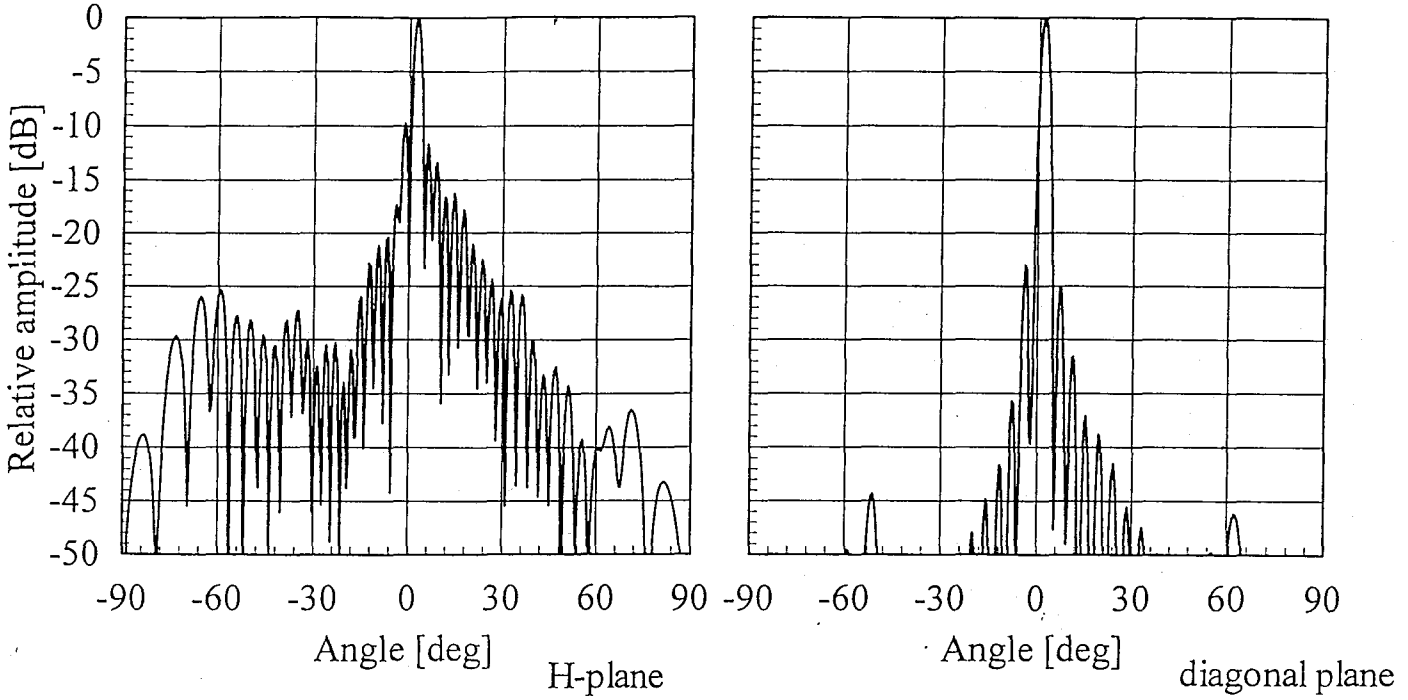

Fig. 4.8 Radiation pattern

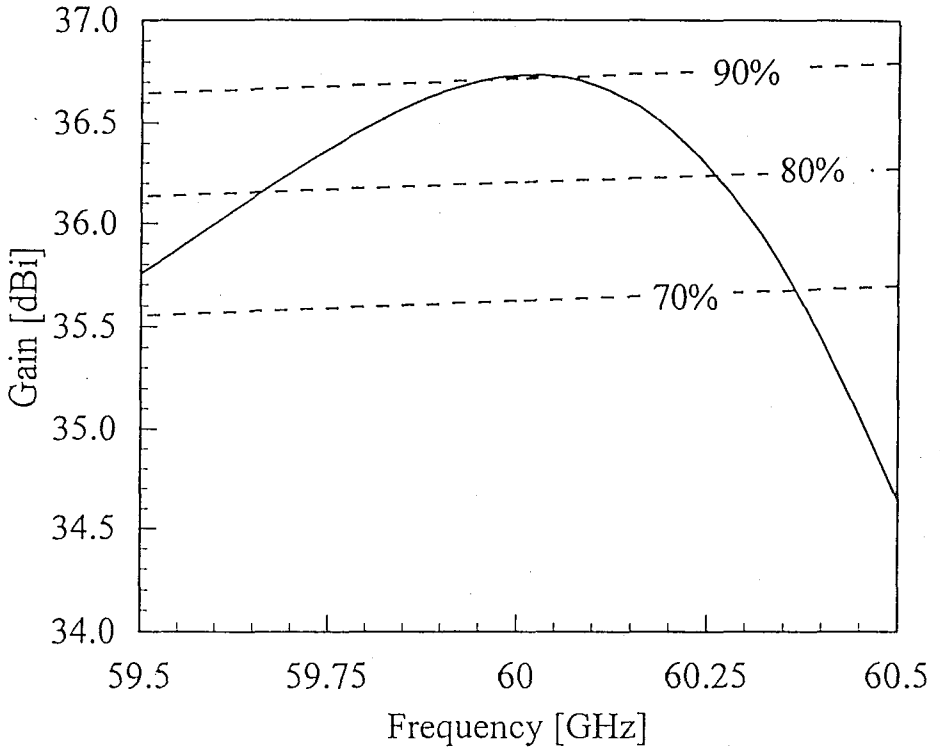

Fig. 4.9 Gain and antenna efficiency

Table 4.1 Design parameters (22 GHz antenna)

Design frequency	22.2 GHz
Number of radiation waveguides	24
Number of slots (per waveguide)	25
Number of slots (all)	600
Array length (z)	260 mm
Array length (x)	280 mm
Broad guide width of feed waveguide a_f	8.1 mm
Broad guide width of radiation waveguide a_r	10.0 mm
Narrow guide width b	4.0 mm
Slot spacing (z)	10.6 mm
Beam-tilt angle	6 deg

Table 4.2 Design parameters (60 GHz antenna)

Design frequency	60 GHz
Number of radiating waveguides	24
Number of slots (per waveguide)	25
Number of slots (all)	600
Array length (z)	120 mm
Array length (x)	105 mm
Broad guide width of feed waveguide a_f	3.10 mm
Broad guide width of radiating waveguide a_r	3.22 mm
Narrow guide width b	1.88 mm
Slot spacing (z)	4.30 mm
Beam-tilt angle	2.4 deg

Chapter 5. A two-beam slotted leaky waveguide array for mobile reception of dual polarization DBS

5.1 Introductory remarks

Mobile reception of direct broadcast from satellite (DBS) has been popular; the number of vehicles with DBS receiving systems is also increasing in Japan [5-1]-[5-4]. Low-profile, mass-produceable, beam-tilting and high-efficiency receiving antennas had been desired to this end. A single-layer slotted leaky waveguide array antenna has been developed in our laboratory for the single-polarized DBS in Japan [5-5] [5-6] which satisfies all these requirements. Novel single layer feed structure is applied to the antenna, which consists of cascades of π-junctions [5-7] [5-8] and the radiation waveguides as is shown in Fig. 5.1. The feed waveguide couples to two radiation waveguides through each window in phase since the guide wavelength of the feed waveguide is set to be twice the width of the radiation waveguide. The width of the window is controlled to divide input power into all the radiation waveguide equally. Inductive pins for matching in a conventional antenna are all replaced by inductive walls, which contribute to mass-produceability. The cross slots are densely arranged on the broad wall of the radiation waveguides. The leaky wave radiates a circular polarized beam in a large tilting angle of about 45 degrees from the zenith. It is advantageous for mobile DBS reception since the antenna can be installed horizontally on the roof of the vehicles. A mechanical system steers the antenna to tracks the satellite only in the azimuthal plane. Tracking is not necessary in the elevation plane, since the beam width of the antenna with short radiation waveguide is broad. In order to maximize the gain, uniform aperture distribution is synthesized by varying slot length.

Dual-circular polarization DBS service with more than 175 channels has started in the U.S. [5-9] [5-10]. The concept of above antenna is extended for receiving dual-polarization DBS. A two-beam antenna is proposed where polarization is altered by

switching the beam mechanically shown in Fig. 5.1. Two feed waveguides are attached at both ends of the leaky waveguides. By changing the direction of propagation of the leaky waves, either of two circularly-polarized waves can be received in opposite beam directions. The tracking system rotates the antenna by 180 degrees for switching the beam or the polarization. Input power fed from port #1 radiates from the slots on all the radiation waveguides and some residual power at the radiation waveguide joins at port #2 through another feed waveguide. The principle to radiate dual circular polarization from a cross slot is explained in Fig. 5.2. Slot #2 is excited by TE_{10} mode propagating into $+z$ direction with 90 degrees time progress to slot #1, which radiates right-hand circular polarization. Due to the leaky wave excitation the main beam is directed to $+\theta_t$. On the other hand, if the cross slot is excited by the mode propagating to $-z$ direction, left-hand polarization radiates into $-\theta_t$ direction. Consequently, port #1 and #2 correspond the right- and left-hand circular polarization in $+\theta_t$ and $-\theta_t$, respectively. These two beams are switched by mechanical azimuthal rotation of 180 degrees.

For the balanced performance between two polarizations, the antenna structure including slot design should be symmetrical with respect to $z = 0$. The aperture field distribution is optimized to maximize the efficiency by using the calculus of variations [5-11] [5-12] [5-13] under the condition of the symmetry with $z = 0$. As a result of the analysis, the efficiency with optimum distribution and non-uniform slots is almost the same with that for the antenna with the constant coupling factor and uniform but optimized slots. A model antenna with uniform slots is fabricated. The antenna efficiency of 71 % for the right-hand circular polarization and 64 % for the left-hand one are obtained by measurements.

5.2 Optimization of aperture distribution

Continuous source distribution on the aperture is assumed in order to derive optimum in an analytical form. The size of the aperture is L (waveguide length) $\times$ a (width). It should be noted that the slot design or the slot coupling distribution is symmetrical with respect to $z = 0$ since the quality of two beams fed from the two ports should be the same. Termination loss t is the residual power which joins together at the π-junctions and results in the coupling into the other port #2; $1-t$ is the radiation power. The antenna efficiency is a function of the distribution of the slot coupling.

The radiation from the source causes the attenuation of the field inside the waveguide. The energy conservation gives

$$abP(z) - abP(z+\Delta z) = a\Delta z P(z)\{2b\alpha(z)\} \tag{5.1}$$

where $\alpha(z)$ is defined as the coupling factor, which corresponds to the inner field attenuation per unit length and is determined by the slot length. $P(z)$ is the inner power flow at z while a and b are the broad and narrow wall width, respectively. Taking the limit of $\Delta z \to 0$, we have the following differential equation;

$$\frac{d}{dz}P(z) = -2\alpha(z)P(z) \tag{5.2}.$$

Solving it for $P(z)$ by including the following normalization of incidence power;

$$P(-L/2) = 1 \tag{5.3},$$

the aperture field density is proportional to

$$\begin{aligned} E(z) &= \sqrt{\alpha(z)P(z)} \\ &= \sqrt{\alpha(z)}\exp\left(-\int_{-L/2}^{z}\alpha(y)dy\right) \end{aligned} \tag{5.4}.$$

The overall gain for the in-phase radiation will be further degraded by the termination loss t :

$$\begin{aligned} G &= \frac{4\pi}{\lambda_0^2}\frac{\left|\int E(z)dS\right|^2}{\int|E(z)|^2 dS}(1-t) \\ &= \frac{4\pi}{\lambda_0^2}2a\left\{\int_{-L/2}^{L/2}E(z)dz\right\}^2 \end{aligned} \tag{5.5}$$

where dS equals to adz and

$$\begin{aligned} \int|E(z)|^2 dS &= a\int_{-L/2}^{L/2}|E(z)|^2 dz \\ &= -\frac{a}{2}\int_{-L/2}^{L/2}\frac{d}{dz}P(z)dz \\ &= \frac{a}{2}(1-t) \end{aligned} \tag{5.6}.$$

The aperture efficiency η is obtained by substituting eq. (5.4) into eq. (5.5) and imposing symmetrical distribution $\alpha(-z) = \alpha(z)$ as

$$\eta = \frac{G}{\frac{4\pi}{\lambda_0^2} aL}$$
$$= \frac{2}{L}\left\{\int_{-L/2}^{L/2} E(z)dz\right\}^2$$
$$= \frac{8}{L} e^{-2u(L/2)}\left[\int_0^{L/2} \sqrt{u'(z)}\cosh\{u(z)\}dz\right]^2 \qquad (5.7)$$

where

$$u(z) = \int_0^z \alpha(y)dy \qquad (5.8).$$

Now, we maximize the efficiency η in the following two approaches. One is to optimize the termination loss t under the condition of uniform coupling ($\alpha(z)$ = const.) or the uniform slots (A) [5-14] while another one is to synthesize or optimize the distribution of the slot coupling $\alpha(z)$ by calculus of variations (B) [5-12] [5-13].

5.2.1 Uniform slot coupling (A)

We assume all the slots have identical length and $\alpha(z)$ is constant ($= \alpha_0$), so

$$u(z) = \alpha_0 z \qquad (5.9).$$

By replacing $u(z)$ in eq. (5.7) with eq. (5.9), the antenna efficiency η is simplified as the function of t.

$$\eta = \frac{8}{L} e^{-\alpha_0 L}\left[\int_0^{L/2} \sqrt{\alpha_0}\cosh(\alpha_0 z)dz\right]^2$$
$$= -\frac{4(1-\sqrt{t})^2}{\log t} \qquad (5.10)$$

where t is the termination loss and equals to $P(L/2)$ or $\exp(-2\alpha_0 L)$. By differentiating the equation (5.10), we arrive at

$$\frac{d\eta}{dt} = \frac{4}{t(\log t)^2}(1-\sqrt{t})(\sqrt{t}\log t + 1 - \sqrt{t}) \equiv 0 \qquad (5.11)$$

The η takes its maximum of 81.45 % for $t \equiv t_{opt}^{(A)} = 0.081$ which is independent with the aperture length L. For this value, the coupling factor α_0 is given by

$$\alpha_0 = -\frac{1}{2L}\log_e t_{opt}^{(A)} \qquad (5.12)$$

which depends upon the length of waveguides. The aperture distribution is obtained by eq. (5.4) as;

$$E(z) = \sqrt{\alpha_0}\exp\left\{-\alpha_0\left(\frac{L}{2}+z\right)\right\} \tag{5.13}.$$

5.2.2 Optimum distribution of slot coupling (*B*)

The problem obtaining $\alpha(z)$ to maximize the efficiency expressed by eq. (5.7) is replaced with that for maximizing the following integral

$$J(u) = \int_0^{L/2} \sqrt{u'(z)}\cosh\{u(z)\}dz \tag{5.14}$$

which can be solved by calculus of variations in appendix D. The Euler equation [5-11], which is the condition to furnish the extremum of the functional $J(u)$ or to give the first variation zero, is expressed as follows;

$$u'' = -2u'^2\tanh(u) \tag{5.15}.$$

With the boundary condition;

$$u(0) = 0 \tag{5.16}$$

and

$$\begin{aligned} u(L/2) &= \int_0^{L/2}\alpha(y)dy \\ &= \frac{1}{2}\int_{-L/2}^{L/2}\alpha(y)dy \\ &= -\frac{1}{4}\log_e P(L/2) \\ &= -\frac{1}{4}\log_e t \end{aligned} \tag{5.17},$$

the differential equation (5.15) is solved as;

$$2u + \sinh(2u) = pz \tag{5.18}$$

where

$$p = \frac{1}{L\sqrt{t}}\left(1 - t - \sqrt{t}\log_e t\right) \tag{5.19}.$$

Differentiating both sides of eq. (5.18) with respect to z, we can express α by

$$u' = \alpha = \frac{p}{2(1+\cosh 2u)} = \frac{p}{4\cosh^2 u} \tag{5.20}.$$

Elimination of u from eqs. (18) and (20) results in the following relation between α and z;

$$z = \pm\left\{\frac{\sqrt{p-4\alpha}}{2\alpha\sqrt{p}} + \frac{1}{p}\log\left(\frac{\sqrt{p}+\sqrt{p-4\alpha}}{\sqrt{p}-\sqrt{p-4\alpha}}\right)\right\} \tag{5.21}$$

From eqs. (5.17) and (5.20), the antenna efficiency (5.7) can be expressed as a function of t as

$$\eta = \frac{1}{2}(1 - t - \sqrt{t}\log_e t) \tag{5.22}.$$

The aperture distribution is derived by using eqs. (5.4), (5.8), (5.17) and (5.20) as a function of u;

$$E(z) = \sqrt{\frac{p}{2(1-\cosh 2u)}}\exp\left(\frac{1}{4}\log_e t - u\right) \tag{5.23},$$

which is a function of u or z by means of eq. (5.18).

5.2.3 Optimum aperture distribution

Figure 5.3 compares the antenna efficiency for the design (A) and (B) as a function of the termination loss t. The two different designs result in substantially identical efficiency for all the values of t. The maximum efficiency for the uniform coupling model (A) is 81.45 % and the termination loss $t_{opt}^{(A)}$ equals to 8.10 %, which is almost equal to that of 81.72 % for the optimum distribution with t equals to 7.75 %. In order to extract the efficiency of distribution, the aperture efficiency is calculated by following equation;

$$\eta_a = \frac{\eta}{1-t} \tag{5.24}.$$

The aperture efficiency of the uniform coupling model (A) is 88.63 % which is higher than that of 88.59 % for the optimum distribution (B). The slot coupling distribution $\alpha(z)$ is presented in Fig. 5.4 for an aperture length L of 230 mm. The highest coupling of 0.0065 /mm is adopted for the non-uniform design (B) and the termination loss $t_{opt}^{(B)}$ is 0.35 % smaller than $t_{opt}^{(A)}$. The electric field distribution on the aperture is shown in Fig. 5.5. Distribution is tapered down at the both ends of the aperture by about 10 dB. All these results shows that both design have indistinguishable potential. Theoretical efficiency of more than 80 % is reasonable while the termination loss degrading the isolation is around 8 %.

5.3 Design and experimental results

With the equal potential of two designs in mind, the uniform coupling model (A) is fabricated because the slot design is much simpler and parameter study for compensating slot manufacturing error would be straightforward. The slots of the same geometry are arrayed. The design parameters for the Japanese and the USA DBS antennas are listed in Table 5.1. The slot length l is controlled to realize the slot coupling optimized in eq. (5.12) for the maximum antenna efficiency in Chap. 2. Axial ratio of the circular polarization depends on the slot cross angle and the slot offset from the center of the waveguide. These slot parameters are obtained by referring the parameters of Japanese DBS and COMETS antennas [5-5] [5-6] as appendix E. Since adjacent slots are quite close along the z direction, the mutual couplings between the slots are strong. The full wave analysis simulating the effect accurately should be used for the design of the antenna such as an analysis of Method of Moments [5-15].

The design parameters are shown in Table 1. The size of the antenna is determined to cover 500 MHz bandwidth for the DBS in the U.S. with the required gain. The beam width in the elevation angle has to be broad in order to compensate the vehicle inclination during motion, which is achieved by limiting the number of slots on a radiation waveguide.

Figure 5.6 shows the reflection and the isolation of the test antenna. As for the reflection, S_{11} and S_{22} of port #1 and #2 are lower than −13.7 dB and −14.4 dB in the required frequency bandwidth, respectively. It is not sufficient but is acceptable. As for the isolation, S_{12} is −11.53 dB (7.03 %) and S_{21} is −11.91 dB (6.44 %). Each level is close to the predicted one and basic operation is confirmed.

The two-dimensional aperture distribution is measured at the distance of 10 mm above the aperture. Figure 5.7 shows the data after backward transformation onto the slot aperture by means of Fourier transform [5-16] [5-17]. The phase taper corresponding to beam tilting ($k_0 z \sin\theta_t$) is omitted. The phase distribution is flat for the beam direction of 42 degrees. The actual beam direction slightly shifts from the desired one of 45 degrees, which is due to the estimation error of the phase progress of the cross slot in the waveguide. In the amplitude distribution, predicted tapers are observed in the z direction. The gradients of the tapers are almost equal between that of

port 1 and 2. That of port 1 is slightly small and the uniformity is better. Difference of the both top and bottom levels are around 10 dB which is almost equal to the calculated aperture distribution shown in Fig. 5.5. Though all the waveguides have identical slots, about 3 dB ripples exist in the x direction which may be due to the effect of finite size array.

The spin-linear radiation patterns in the different polarization operations are shown in Fig. 5.8. Upper ones are those in the yz-plane and lower ones are those in its perpendicular plane including the main lobe. The axial ratios in operation #1 and #2 are relatively large and are 2.3 dB and 3.0 dB, respectively. It would be possible to improve the axial ratios by adjusting the cross angle θ_c in a cross slot.

The frequency dependence of the gain is shown in Fig. 5.9. The measured peak gain of port #1 is 29.3 dBi (antenna efficiency: 71 %) and that of antenna #2 is 28.9 dBi (antenna efficiency: 64 %). The difference in the efficiency mainly comes from that of the axial ratios and the termination loss. The single polarization antenna reported in Ref. [5-5] [5-6] has the antenna efficiency of about 75 %. Considering these, we can conclude that the measured efficiency of 71 and 64 % for dual polarization is considerably high in this beam-tilting angle and under the symmetry condition of the slots which leads to the tapered amplitude distribution on the aperture. The difference between these efficiencies is mainly due to the difference of the aperture distributions as shown in Fig. 5.7. The frequency dependent beam shifting reduces the gain in fixed beam angle at the frequency band edge, which is common disadvantages of the leaky wave antennas.

5.4 Concluding remarks

A two-beam slotted leaky waveguide array is proposed for mobile reception of dual polarization DBS. Uniform slots are adopted with their coupling optimized in terms of antenna efficiency. The efficiency for this design is quite close to that of the optimum distribution with non-uniform slots under the condition of symmetrical array for dual polarization. The amplitude distribution is tapered by about 10 dB. Large axial ratios of 2.3 dB for port #1 and 3.0 dB for port #2 should be improved in near future. Antenna efficiency of the test antennas is evaluated as 71 % for the right-hand circular polarization and 64 % for the left-hand one in the measured gain. These results are a bit

inferior to those for the single polarized antenna developed for Japanese use, but is providing attractive candidates for dual polarization antennas.

References

[5-1] K. Omaru, "A mobile satellite broadcasting receiver," *Broadcast. Eng.*, vol. 43, no. 9, pp. 119-123, Sept. 1990.

[5-2] A. Kuramoto, N. Endo, A. Kawaguchi, R. Shimizu, Y. Furukawa, S. Oyaizu, K. Maehara, and Y. Suzuki, "Mobile DBS receiving antenna system," in *IEICE Nat. conv. Rec.*, vol. B-59, Mar. 1991.

[5-3] K. Takano, T. Murata, M. Fujita, and D. Kato, "Compact mobile receiver for direct satellite broadcasting," in *IEICE Nat. Conv. Rec.*, vol. B-46, Mar. 1993.

[5-4] M. Shigihara, Y. Ohtaki, and T. Kumagai, "Mobile DBS receiving antenna system -antenna unit-," in *IEICE Nat. Conv. Rec.*, vol. B-118, Sept. 1994

[5-5] J. Hirokawa, M. Ando, N. Goto, N. Takahashi, T. Ojima, and M. Uematsu, "A low-profile mobile DBS receiving system using a single-layer slotted leaky waveguide array," in *IEEE AP-S*, Seattle, June 1994

[5-6] J. Hirokawa, M. Ando, N. Goto, N. Takahashi, T. Ojima, and M. Uematsu, "A single-layer slotted leaky waveguide array antenna for mobile reception of direct broadcast from satellite," *IEEE Trans. on Vehicular Tech.*, vol. 44, No. 3, Aug. 1995

[5-7] J. Hirokawa, M. Ando, and N. Goto, "A single-layer multiple-way power divider for a planar slotted waveguide array," *IEICE Trans. Commun.*, vol. E75-B, No. 8, pp.781-787, Aug. 1992

[5-8] T. Takahashi, J. Hirokawa, M. Ando, and N. Goto, "A single-layer power divider planar slotted waveguide array using p-junctions with an inductive wall," *IEICE Trans. Commun.*, to be published

[5-9] B. Frank, *Miniature Satellite Dishes*, Aug. 1994

[5-10] *Popular science*, vol. 246, No.1, pp-60, B & W T Co., Jan. 1995

[5-11] R. Courant and D. Hilbert, *Methods of mathematical physics*, vol. 1, Chap. 4, pp. 164, Wiley, 1989

[5-12] M. Takahashi, J. Takada, M. Ando, and N. Goto, "A slot design for uniform aperture field distribution in single-layer radial line slot antennas," *IEEE Trans. on Antennas and Propagation*, vol. 39, No. 7, July 1991

[5-13] M. Takahashi, "A study of single-layered radial line slot antennas," Ph.D. dissertation, Tokyo Inst. of Tech., pp. 37, 1993

[5-14] N. Goto, "A single-layered slotted waveguide antenna for dual circular-polarization," in *IEICE Nat. Conv. Rec.*, vol. B-87, Mar. 1995

[5-15] J. Hirokawa, K. Sakurai, M. Ando, and N. Goto, "Matching slot pair for a circularly-polarized slotted waveguide array," *IEE Proc.*, vol. 137, Pt. H, No. 6, pp. 367-371, Dec. 1990

[5-16] T. P. Demetius, L. Jr. Marchall, and B. J. Edward, "Basic theory of probe-compensated near-field measurements," *IEEE Trans. on Antennas and Propagation*, AP-26, No.3, pp.373-379, 1978

[5-17] Y. Iijima, M. Ando, and N. Goto, "Evaluation of excitation coefficients of elements in slotted waveguide arrays by near-field measurements," *Tech. Rep. of IEICE*, A·P 95-66, Oct. 1995

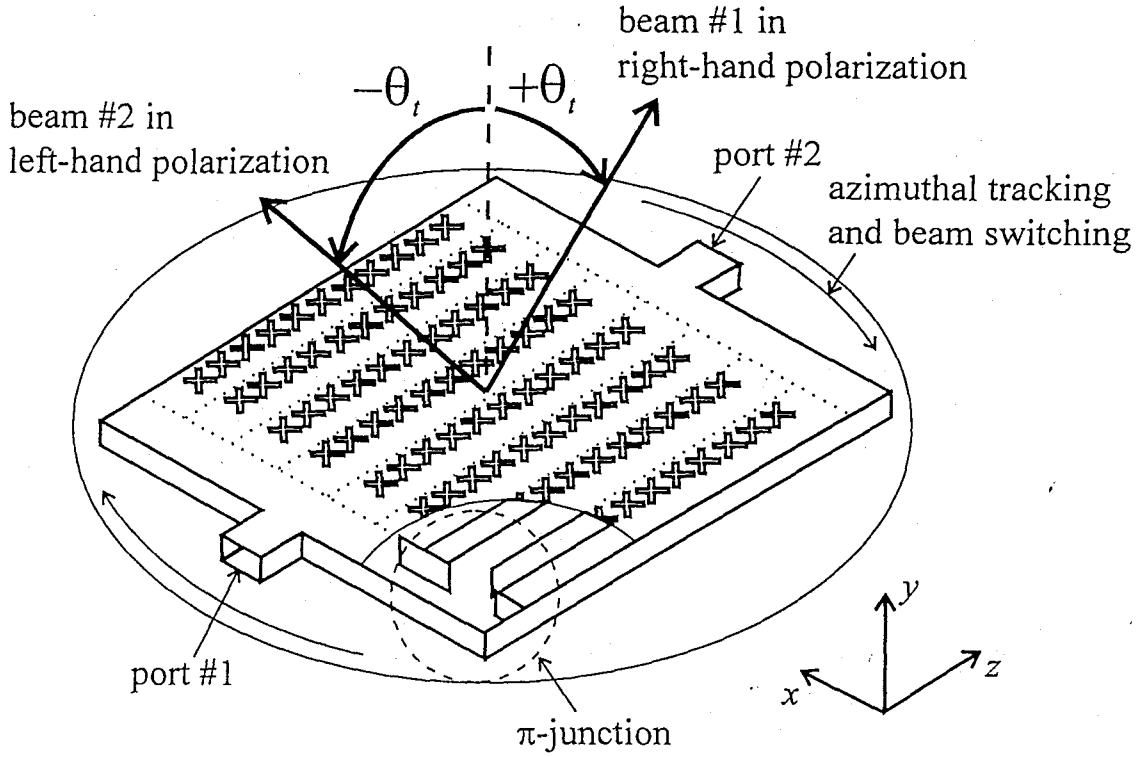

Fig. 5.1 Antenna structure (θ_t : beam tilting angle)

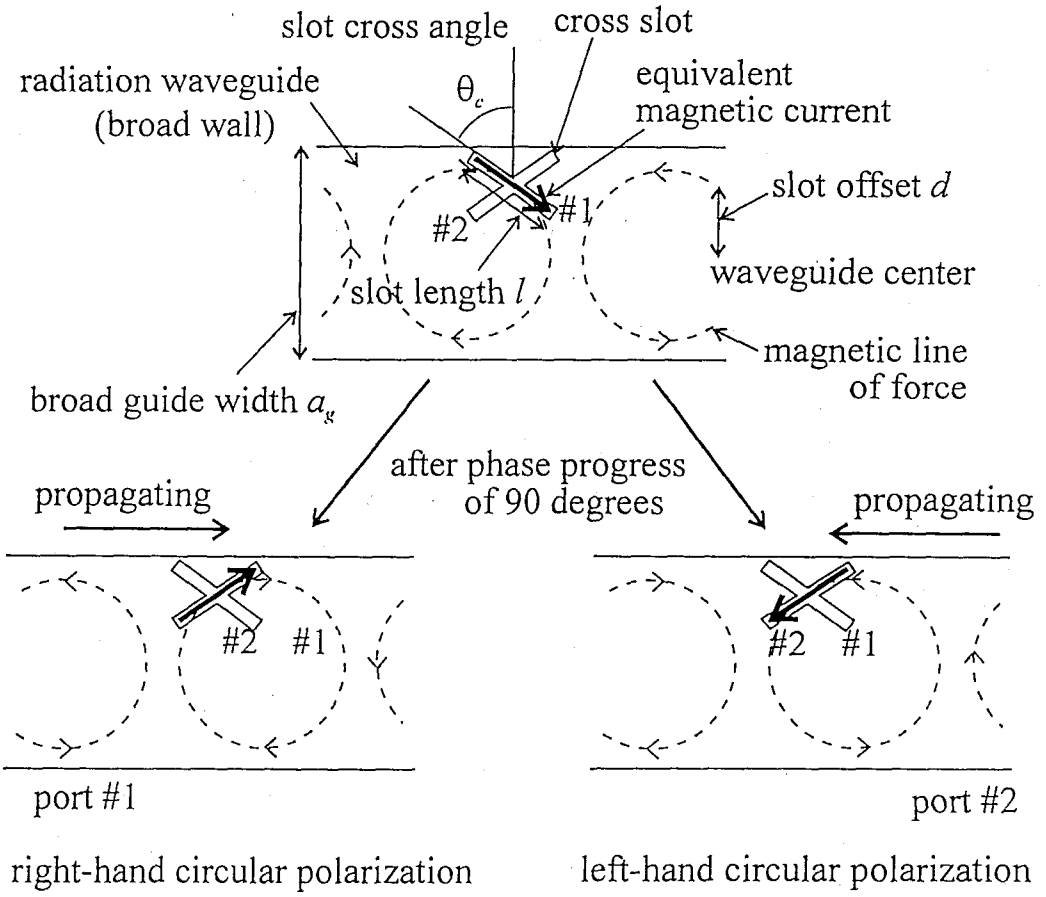

Fig. 5.2 Dual-circular polarization radiating principle of a cross slot

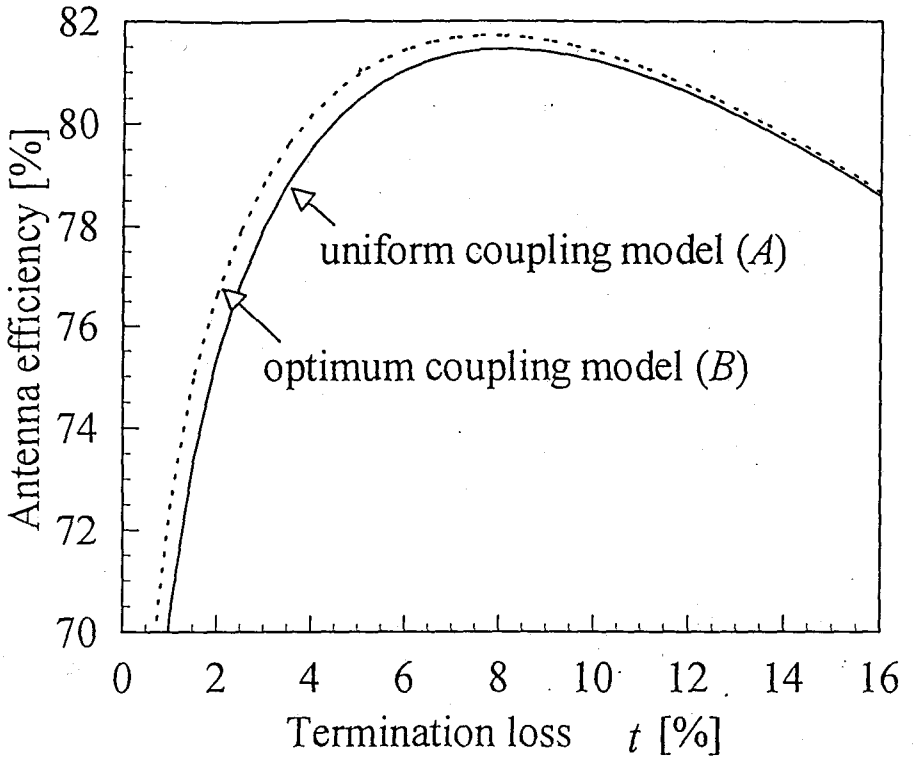

Fig. 5.3 Antenna efficiency related to termination loss for uniform distribution of slot coupling : model (*A*) and for optimum distribution of slot coupling : model (*B*)

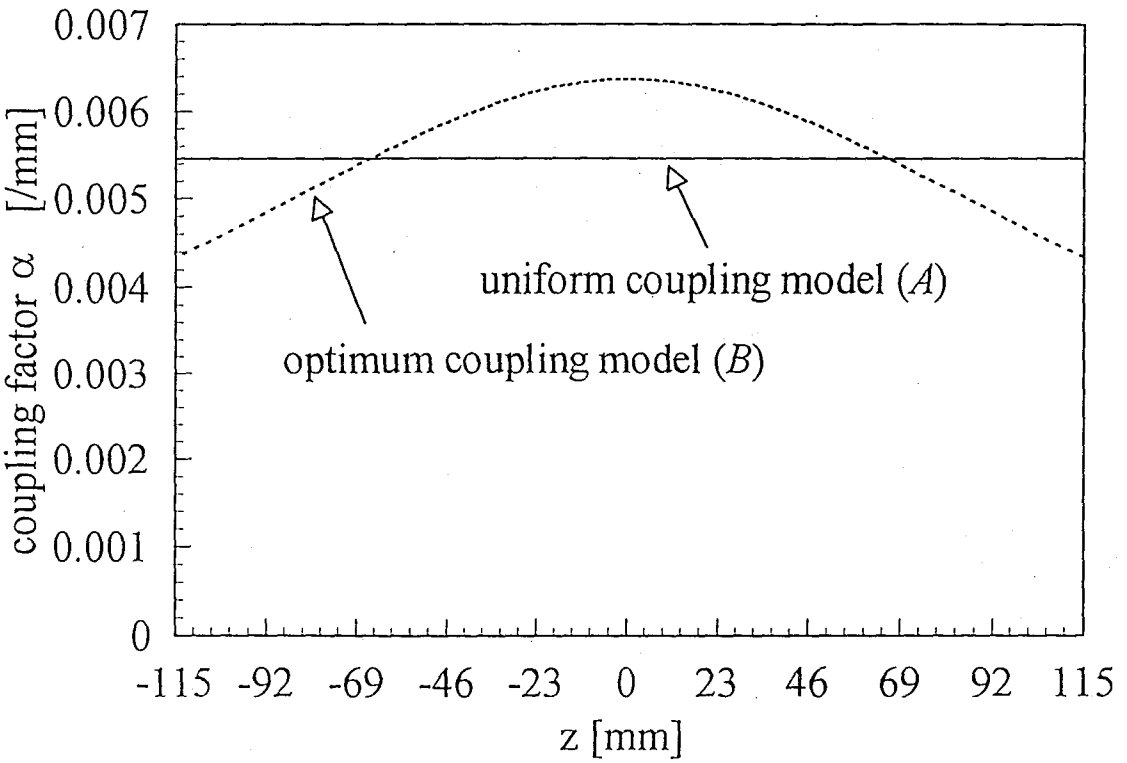

Fig. 5.4 Coupling factor distribution of model (*A*) and (*B*)

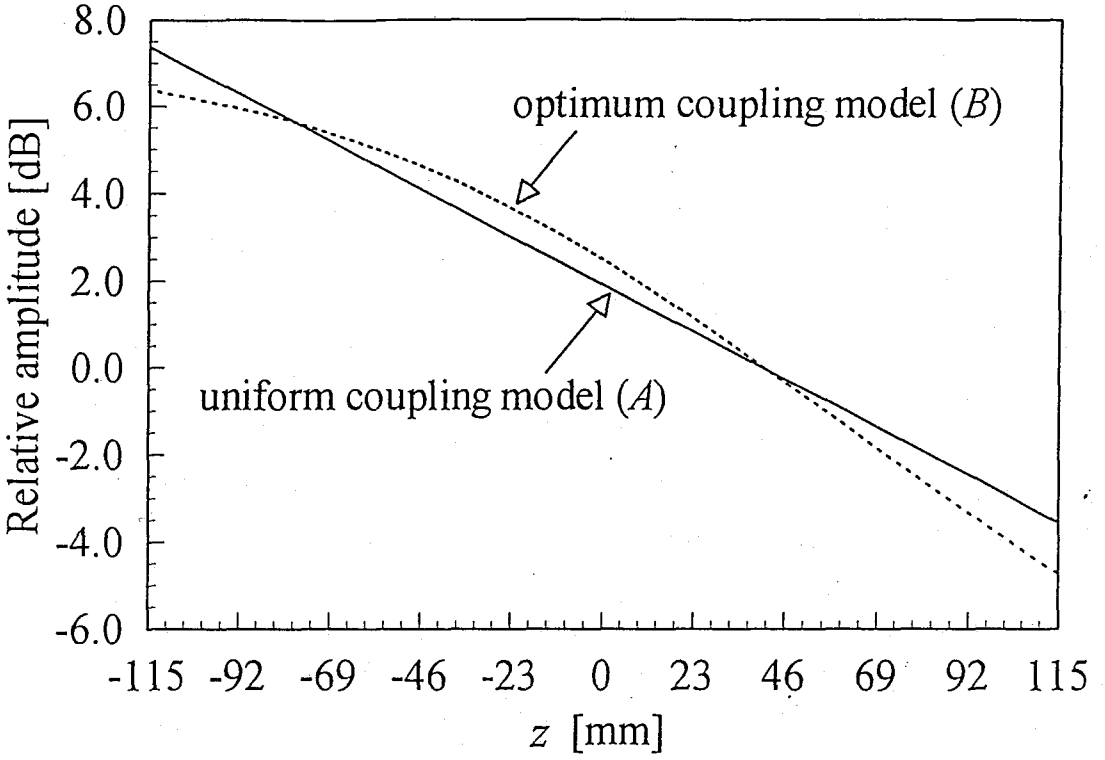

Fig. 5.5 Numerical aperture field distributions

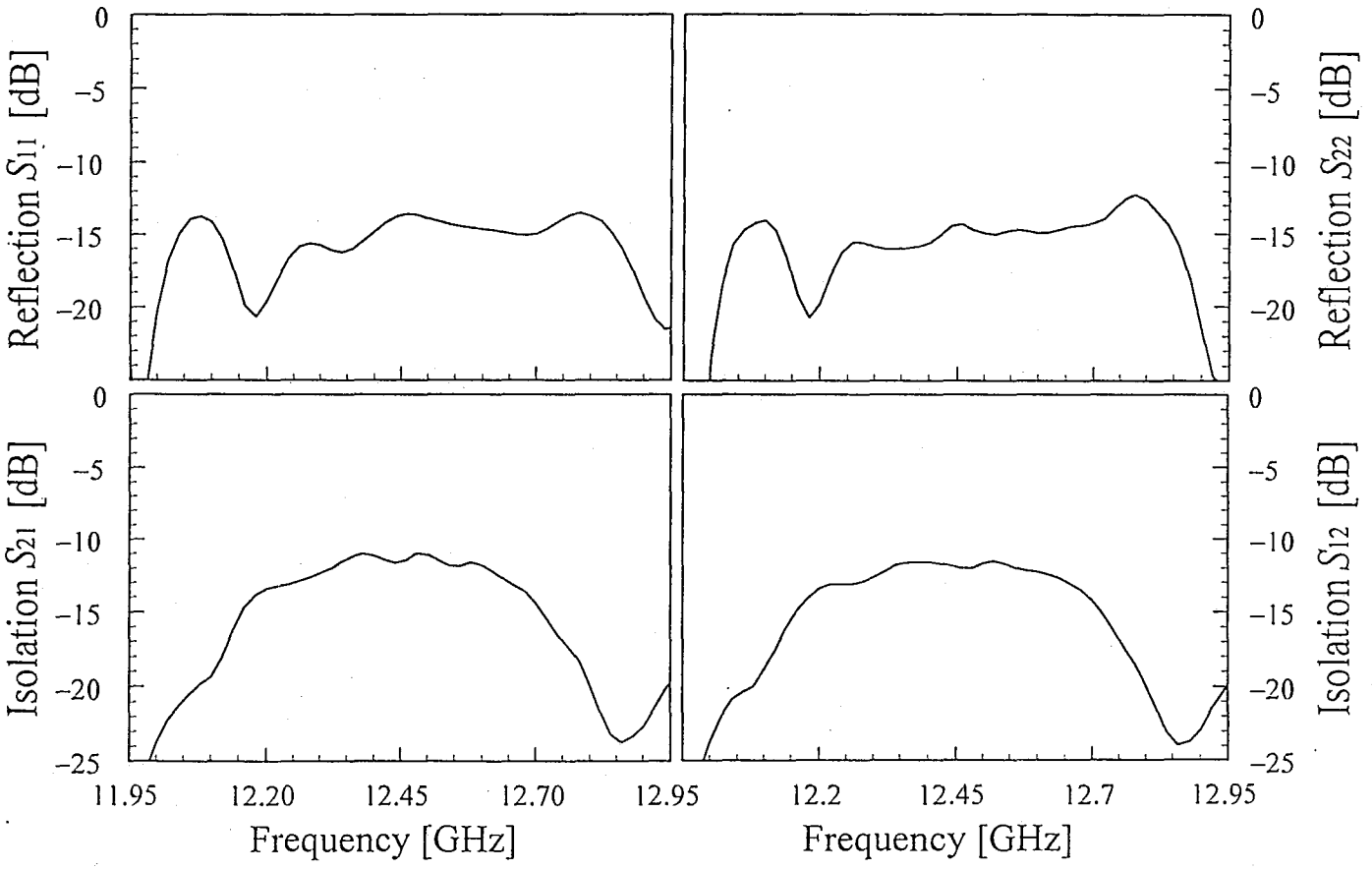

Fig. 5.6 Reflection and isolation characteristics of port #1 and #2

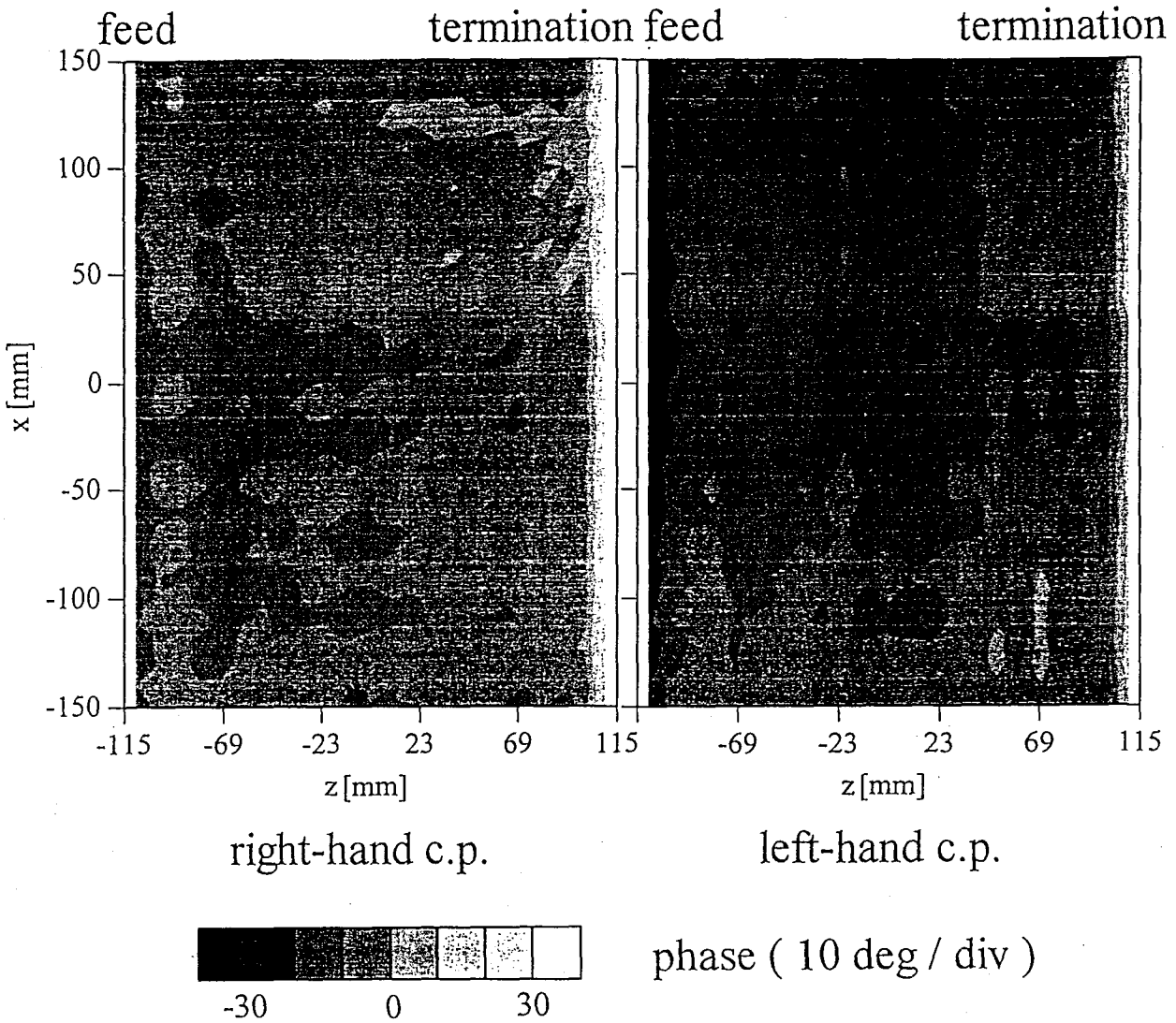

Fig. 5.7 (a) Phase distribution on the aperture

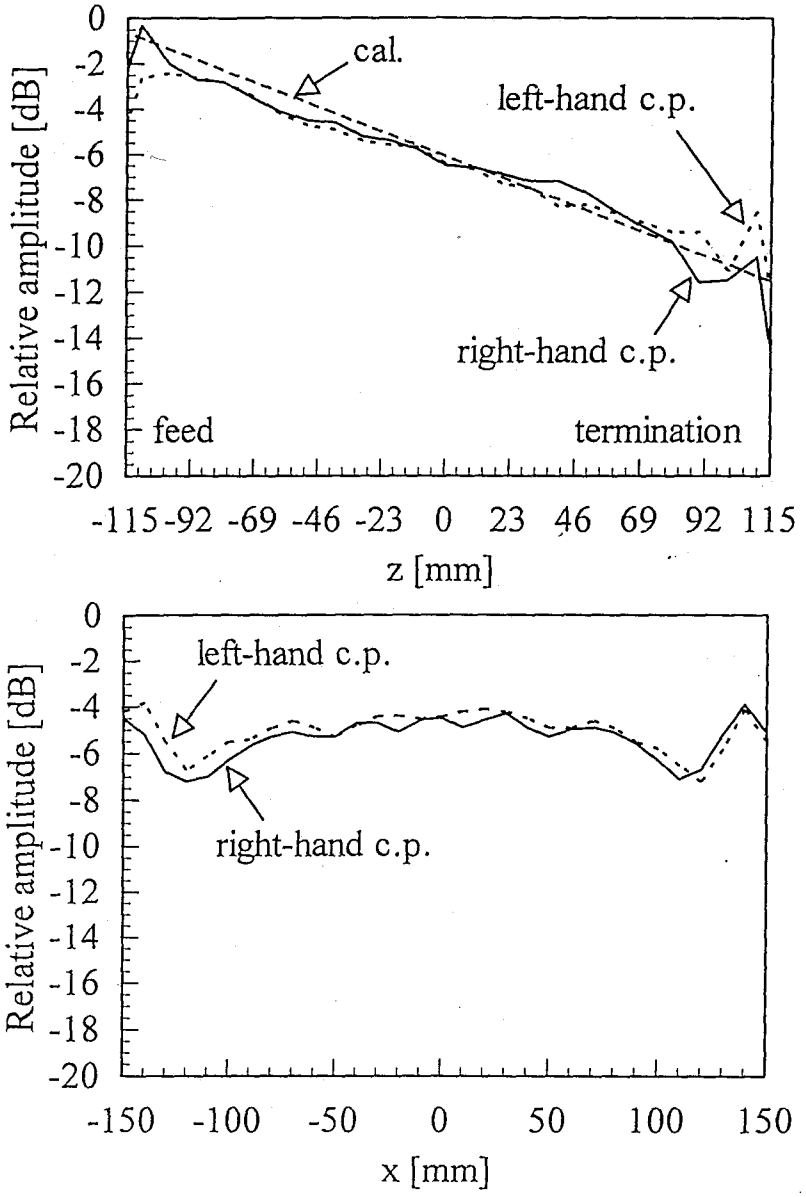

Fig. 5.7 (b) Amplitude distribution on the aperture

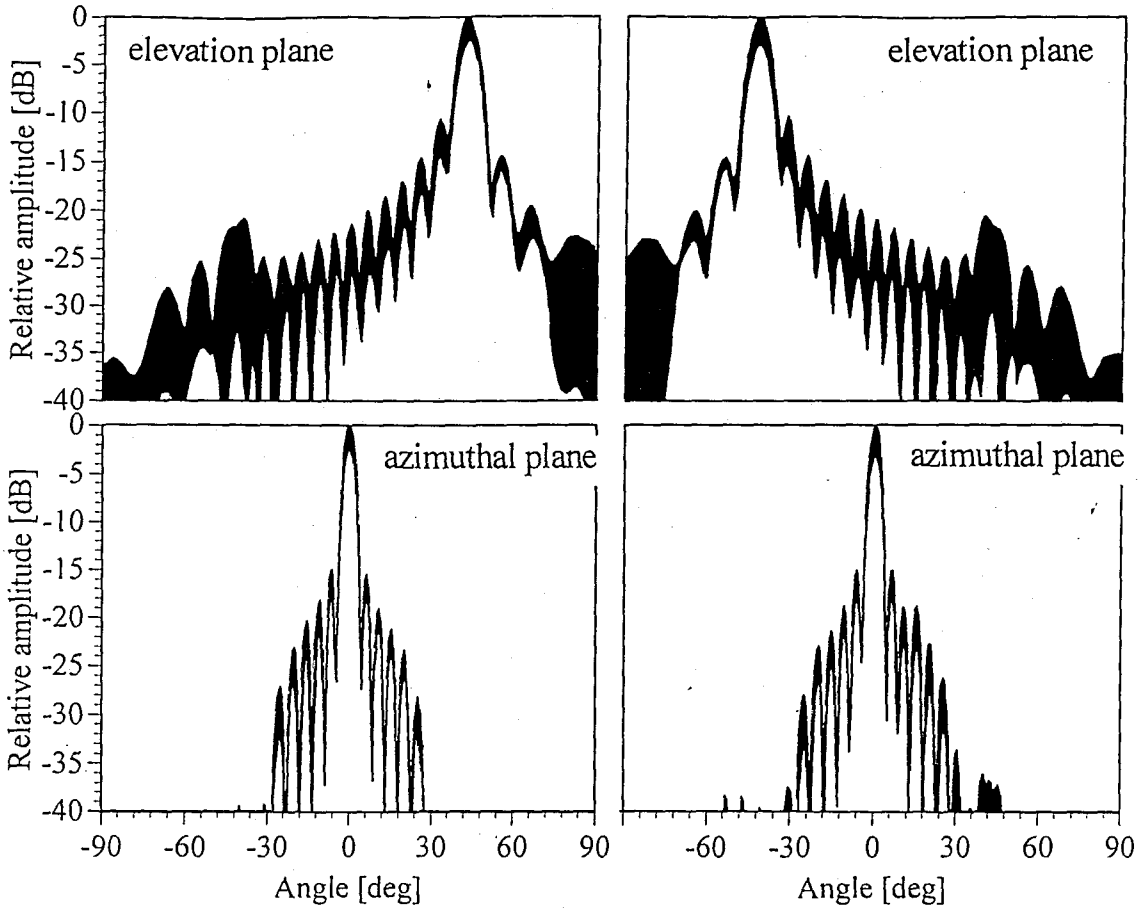

Port #1 (right-hand polarization) Port #2 (left-hand polarization)

Fig. 5.8 Radiation pattern

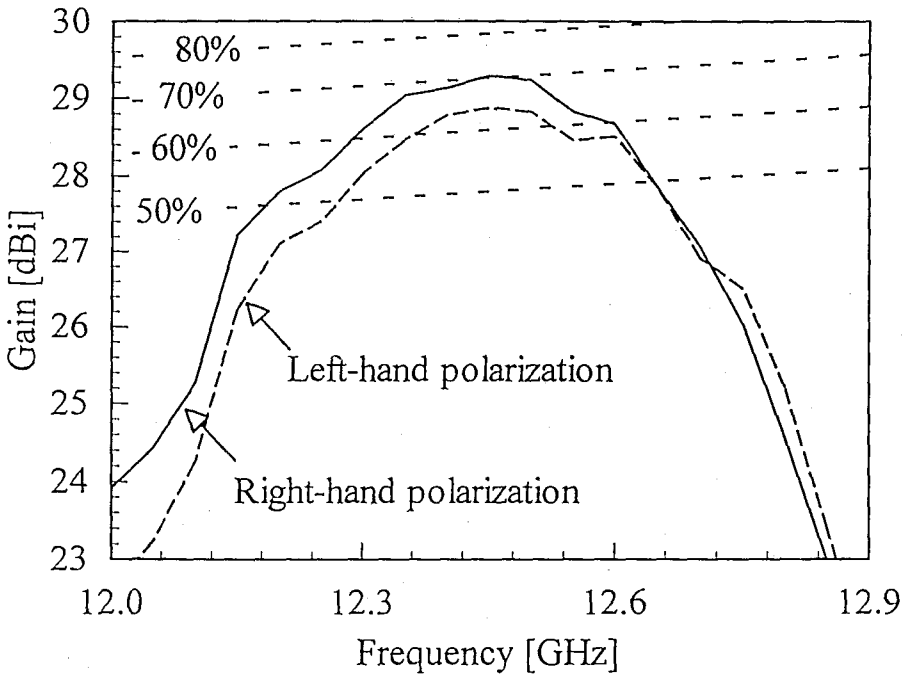

Fig. 5.9 Gain and antenna efficiency

Table 5.1 Design parameters

Frequency bandwidth	12.2 ~ 12.7 GHz
Design frequency	12.45 GHz
Number of waveguides	20
Number of slots	26
Length of aperture along radiation waveguide L	230 mm
Length of aperture along feed waveguide	320 mm
Beam direction θ_t (from zenith)	45 degrees
Broad guide width of radiation waveguide a_g	14.3 mm
Broad guide width of feed waveguide a_f	17.9 mm
Wall thichness between the waveguides	2.0 mm
Slot cross angle θ_c	55 deg.
Slot offset d	2.3 mm
Slot length l	9.67 mm

Chapter 6. Reflection-cancelling slot pair array

6.1 Introductory remarks

Resonant slots are widely used for conventional slotted waveguide array. Reflection from each slot causes a standing wave in the waveguide and beam tilting technique is essential to suppress the reflection at the antenna input port. But the slot reflection narrows the overall frequency bandwidth and the design taking it into account is complicated. This paper proposes a reflection cancelling slot pair as an array element, which consists of two slots spaced by $1/4\lambda_g$. Round trip path-length difference between them is $1/2\lambda_g$ and reflection waves from a pair disappear and traveling-wave excitation in the waveguide is realized.

The full wave analysis reveals that mutual coupling between paired slots is large and seriously reduces the radiation from a pair. Offset arrangement of slots in a pair is recommended to decrease the mutual coupling and to realize strong coupling. In practical array design, the mutual couplings from other pairs were simulated by imposing periodic boundary conditions above the aperture.

To clarify the advantages of the slot pair over a conventional resonant slot, the predicted characteristics are compared. Reflection characteristics of the array using the slot pair is excellent and a boresite beam array can be realized. In addition, a slot pair can realize stronger coupling than the conventional resonant slot, while the bandwidth of the former in terms of the aperture field phase illumination is narrower than that of the latter. These suggests that the slot pair array is much more suitable for a small array than conventional one. Finally, the predicted characteristics are confirmed by experiments.

6.2 Reflection-cancelling slot pair

The conventional slotted waveguide array consists of resonant slots which are spaced by $1/2\lambda_g$ (λ_g : guide wavelength) [6-1]. In order to cancel the reflections from all the slots at the feed point, a few degree beam tilting has been adopted in general which results in the following disadvantages.

(i) A standing wave in the waveguide results in a narrow frequency bandwidth of the antenna.

(ii) The tilt angle of the main beam can not be arbitrarily chosen and may degrade the design flexibility.

(iii) Slot coupling is controlled by offsetting a shunt slot but the maximum coupling is limited.

(iv) The mutual coupling and reflections from slots make the design complicated. Experimental optimization and time consuming iterative method have been adopted for the design [6-2].

In the design of a small array where slots couple strongly, the effects of (iii) and (iv) become serious.

In this paper, the authors propose a novel slotted array antenna using "reflection-cancelling slot pairs" which can radiate a boresite beam. This concept is a general one applicable for realizing slot antennas operating in traveling wave mode [6-3]. The design, analysis and experimental results of the reflection-cancelling slot pair array are presented.

Figure 6.1 shows a linearly polarized slotted waveguide array using reflection-cancelling slot pairs. The pairs are spaced by a guide wave length: λ_g and the adjacent waveguides are excited in opposite phase; the pairs are interleaved to suppress the grating lobes from the array.

The "reflection-cancelling" principle is shown in Fig. 6.2. A pair consists of two slots which are cut on the waveguide broad-wall with a spacing of about $1/4\lambda_g$. The reflections from the two slots are cancelled out with each other due to the round trip path-length difference of about $1/2\lambda_g$. Reflections from a pair do not exist and traveling-wave excitation is realized.

The following advantages are expected for the array using the reflection-cancelling slot pairs;

(i) Reflection is small and the beam-tilting technique is not required.

(ii) The array design is simple and straightforward since the pair coupling can be determined in sequence from the termination to the feed point without any iterations.

(iii) Wide frequency bandwidth in terms of gain and reflection is expected in association with traveling-wave excitation.

On the other hand, some disadvantages are also foreseen. The main radiation of a pair is not in boresite direction but in endfire direction as is shown in Fig. 6.2 since the two slots are excited in 90 degrees out of phase. This gives rise to grating lobes in one-dimensional array with the element spacing of λ_g. In the design of two-dimensional array, an alternative phase feed system [6-4] in Fig. 6.1 is indispensable to suppress these grating lobes in the endfire direction. Furthermore the dielectric filling in the waveguide is required to suppress them in the diagonal plane.

6.3 Analysis

6.3.1 Analysis model

Figure 6.3 shows the analysis model of a slot pair. The parameter a, b and h indicate the waveguide broad-wall and the narrow-wall widths and the wall thickness, respectively. Slots #1 and #2 are cut on the broad-wall at y=0. Both slots are parallel to the x-axis. They are centered at (x, z) = ($-p$, $-q$) and (p, q), respectively. The lengths of slot #1 and #2 are $2l_1$, $2l_2$ and the widths are $2w_1$, $2w_2$. An infinite conductor plate containing the slots is assumed at $y = -h$. A reflection-cancelling slot pair is designed first based upon the full wave analysis. As applied to the two dimensional array, mutual coupling between the pairs along the z-axis via the outer space is large though that via the inner space in the waveguide is small. Hence one-dimensional uniform array shown in Fig. 6.4 is used to include the mutual coupling into the design of a pair. In this model, the field outside the waveguide is expressed as the sum of contributions from the array of pairs spaced by s and excited equally.

6.3.2 Integral equations

As is shown in Fig. 6.3(b), the analysis model is divided into the following four regions by taking the wall thickness into account [6-5]: the waveguide (region 1), slot

#1 (region 2), slot #2 (region 3) and the half free space bounded by periodic boundaries (region 4). S_1 and S_2 are the slot #1 and #2 apertures facing to the waveguide. Those facing to the half space are S_3 and S_4, respectively. According to the field equivalence theorem, the upper and the lower slot apertures facing to the waveguide and the half space, respectively, are replaced by unknown equivalent magnetic current sheets backed with perfectly conducting walls. On the apertures S_i (i = 1 ~ 4) unknown magnetic current sheets $\boldsymbol{M}_i$ are assumed, where $\boldsymbol{M}_i$ are related to the unknown aperture electric fields $\boldsymbol{E}_i$ by

$$\boldsymbol{M}_i = \boldsymbol{E}_i \times \hat{y} \tag{6.1}$$

where $\hat{y}$ is a unit vector in the y axis. The continuity conditions of the tangential magnetic fields on S_i require the integral equations for $\boldsymbol{M}_i$:

On S_1,

$$\boldsymbol{H}_{in} + \iint_{S_1} \boldsymbol{G}_1 \cdot \boldsymbol{M}_1 dS + \iint_{S_2} \boldsymbol{G}_1 \cdot \boldsymbol{M}_2 dS = -\iint_{S_1} \boldsymbol{G}_2 \cdot \boldsymbol{M}_1 dS + \iint_{S_3} \boldsymbol{G}_2 \cdot \boldsymbol{M}_3 dS \tag{6.2}$$

On S_2,

$$\boldsymbol{H}_{in} + \iint_{S_1} \boldsymbol{G}_1 \cdot \boldsymbol{M}_1 dS + \iint_{S_2} \boldsymbol{G}_1 \cdot \boldsymbol{M}_2 dS = -\iint_{S_2} \boldsymbol{G}_3 \cdot \boldsymbol{M}_2 dS + \iint_{S_4} \boldsymbol{G}_3 \cdot \boldsymbol{M}_4 dS \tag{6.3}$$

On S_3,

$$-\iint_{S_1} \boldsymbol{G}_2 \cdot \boldsymbol{M}_1 dS + \iint_{S_3} \boldsymbol{G}_2 \cdot \boldsymbol{M}_3 dS = -\iint_{S_3} \boldsymbol{G}_4 \cdot \boldsymbol{M}_3 dS - \iint_{S_4} \boldsymbol{G}_4 \cdot \boldsymbol{M}_4 dS \tag{6.4}$$

On S_4,

$$-\iint_{S_2} \boldsymbol{G}_3 \cdot \boldsymbol{M}_2 dS + \iint_{S_4} \boldsymbol{G}_3 \cdot \boldsymbol{M}_4 dS = -\iint_{S_3} \boldsymbol{G}_4 \cdot \boldsymbol{M}_3 dS - \iint_{S_4} \boldsymbol{G}_4 \cdot \boldsymbol{M}_4 dS \tag{6.5}$$

where $\boldsymbol{G}_l$'s (l = 1 ~ 4) are the dyadic Green's functions for the magnetic field produced by a unit magnetic current in the region l. $\mathbf{G}_4$ reflects the contribution from infinite pairs in Fig. 6.4. $\boldsymbol{H}_{in}$ is the tangential component of the incident magnetic field (TE_{10} mode) transmitting in the $+z$ direction.

6.3.3 Dyadic green's function

The dyadic Green's function $\boldsymbol{G}_1$ for region 1 is determined first by the following procedure. For later use in the integration over the xz-plane, expansion in terms of modes propagating in the $\pm y$-direction is advantageous. The concept of virtual cavity composed of virtual conducting walls located at $z = -c$ and $z = c$ is adopted [6-6] [6-7] to this end where c is arbitrary provided $c>q$ and is set to be $0.375\lambda_g$. The Green's

function G_y for this cavity is expanded in terms of a complete set of normal mode functions propagating in the $\pm y$ direction.

$$G_y(r|r_0)=\frac{1}{4}\sum_{\mu}\frac{1}{\sinh(\gamma_{y\mu}b)}[H_{y\mu}^{(+)}(r)\exp(+\gamma_{y\mu}b)-H_{y\mu}^{(-)}(r)\exp(-\gamma_{y\mu}b)]$$
$$[H_{y\mu}^{(-)}(r_0)-H_{y\mu}^{(+)}(r_0)] \qquad (6.6)$$

Then the Green's function $\mathbf{G}_1$ is given as

$$G_1(r|r_0)=G_y(r|r_0)+\frac{1}{4}\sum_{\mu}\frac{\exp(-\gamma_{z\mu}c)}{\sinh(\gamma_{z\mu}2c)}[H_{z\mu}^{(+)}(r)\exp(+\gamma_{z\mu}c)-H_{z\mu}^{(-)}(r)\exp(-\gamma_{z\mu}c)]H_{z\mu}^{(+)}(r_0)$$
$$+\frac{1}{4}\sum_{\mu}\frac{\exp(-\gamma_{z\mu}c)}{\sinh(\gamma_{z\mu}2c)}[H_{z\mu}^{(-)}(r)\exp(+\gamma_{z\mu}c)-H_{z\mu}^{(+)}(r)\exp(-\gamma_{z\mu}c)]H_{z\mu}^{(-)}(r_0) \qquad (6.7)$$

where $H_{z\mu}^{(\pm)}$ is a normal mode function for the magnetic field propagating in $\pm z$-direction, r is an observation point vector, r_0 is a source point vector and $\gamma_{z\mu}$ is the propagating constant of the μ-th mode.

The dyadic Green's functions for rectangular waveguide regions 2 and 3 are easily expanded in terms of a complete set in the $\pm y$-direction as follows;

$$G_2, G_3(r|r_0)=\begin{cases}\frac{1}{4}\sum_{\mu}\frac{1}{\sinh(\gamma_{\mu}h)}\left[H_{\mu}^{(-)}(r)\exp(\gamma_{\mu}h)-H_{\mu}^{(+)}(r)\exp(-\gamma_{\mu}h)\right] & \\ \qquad\left[H_{\mu}^{(+)}(r_0)-H_{\mu}^{(-)}(r_0)\right] & (0\le y<y_0) \\ \frac{1}{4}\sum_{\mu}\frac{1}{\sinh(\gamma_{\mu}h)}\left[H_{\mu}^{(+)}(r)-H_{\mu}^{(-)}(r)\right] & \\ \qquad\left[H_{\mu}^{(-)}(r_0)\exp(\gamma_{\mu}h)-H_{\mu}^{(+)}(r_0)\exp(-\gamma_{\mu}h)\right] & (y_0<y\le h)\end{cases} \qquad (6.8)$$

The upper expression corresponds to the case of the source on S_3 and S_4, while the lower one does to the source on S_1 and S_2 in Fig. 6.3. The different lengths and widths between slot 1 and slot 2 result propagation constant γ_μ and normal mode function $\mathbf{H}_\mu^{(\pm)}$ in different for respective slots.

The dyadic Green's function G_4 for region 4 expresses the effect of a uniform array. Many fictitious slot pairs, with the same parameters $2l_1$, $2l_2$, $2q$ and with the constant excitation coefficients E_3 and E_4 for slot1 and slot 2 respectively, are arrayed on both sides of the real pair with the spacing of s as is shown in Fig. 6.4. If the array is large to some extent, G_4 is given as the sum of the contribution from 2 (N_d + 1)

magnetic currents to the half free space above an infinite conducting plate, which is equivalent to that from 2 ($N_d + 1$) magnetic currents $2\boldsymbol{M}$ to free space as

$$\boldsymbol{G}_4(\boldsymbol{r}|\boldsymbol{r}_0) = \sum_{i=1}^{2(N_d+1)} [-j\omega A_i + \frac{\nabla\nabla A_i}{j\omega\mu_0\varepsilon_0}] \qquad (6.9)$$

$$A_i = \frac{\varepsilon_0}{2\pi} \frac{\exp(-jk_0|\boldsymbol{r} - \boldsymbol{r}_{0i}|)}{|\boldsymbol{r} - \boldsymbol{r}_{0i}|} \qquad (6.10)$$

where k_0 ($= 2\pi / \lambda_0$), m_0 and e_0 are the wave number, permeability and permittivity of free space, respectively. The number of fictitious pairs N_d is increased until the slots excitation coefficients E_3 and E_4 converge; 3 or 4 is sufficient, provided that the slot is not resonant.

6.3.4 Galerkin's method

Galerkin's method of moments is adopted to transform Eqs. (2) ~ (5) to a system of linear equations. An unknown electric field in every slot aperture $\boldsymbol{E}_j$ ($j = 1 \sim 4$) is assumed to have only a component along the slot width and is approximated as

$$\boldsymbol{E}_j = E_j f(x_j) g(z_j) \hat{z}_j = E_j \boldsymbol{e}_j \qquad (6.11)$$

where E_j is an unknown coefficient for the j-th aperture. The functions $f(x_j)$ and $g(z_j)$ are the longitudinal and transverse electromagnetic field distributions, respectively.

$$f(x_j) = \frac{\sin\{k_0(l_j - |x_j|)\}}{\sin(k_0 l_j)} \qquad (6.12)$$

$$g(z_j) = \frac{1}{\sqrt{w_j^2 - z_j^2}} \qquad (6.13)$$

The integral equations (6.2) ~ (6.5) with $\boldsymbol{E}_j$ ($j = 1 \sim 4$), substituted by (6.11), are multiplied by the basis functions $\boldsymbol{m}_i$ ($= \boldsymbol{e}_i \times \hat{y}$) ($i = 1 \sim 4$) and are integrated over the apertures S_i. A system of linear equations for four unknown coefficients E_j ($j = 1 \sim 4$) is written as

$$E_1(Y_{11}^1 + Y_{11}^2) + E_2 Y_{12}^1 - E_3 Y_{13}^2 = -T_1 \qquad (6.14)$$

$$E_1 Y_{21}^1 + E_2(Y_{22}^1 + Y_{22}^3) - E_4 Y_{24}^3 = -T_2 \qquad (6.15)$$

$$-E_1 Y_{31}^2 + E_3(Y_{33}^2 + Y_{33}^4) + E_4 Y_{34}^4 = 0 \qquad (6.16)$$

$$-E_2 Y_{42}^3 + E_3 Y_{43}^4 + E_4(Y_{44}^3 + Y_{44}^4) = 0 \qquad (6.17)$$

where Y_{ij}^l in region l and T_i are given as

$$Y_{ij}^{I} = \int_{S_i}\int_{S_j} \boldsymbol{m}_i \cdot \boldsymbol{G}_I \cdot \boldsymbol{m}_j dS_j dS_i \qquad (6.18)$$

$$T_i = \int_{S_i} \boldsymbol{m}_i \cdot \boldsymbol{H}_{in} dS_i \qquad (6.19)$$

Excitation coefficients E_j of the apertures are the solutions of Eqs. (6.14) ~ (6.17).

Once E_j is determined, the reflection and the transmission coefficients S_{11}, S_{21} are evaluated in a straightforward manner using the aperture magnetic currents $\boldsymbol{M}_1$ and $\boldsymbol{M}_2$ facing to the waveguide, while the radiation pattern is calculated using the aperture magnetic currents $\boldsymbol{M}_3$ and $\boldsymbol{M}_4$ facing to the half space. The phase of the transmission θ_t and the radiation θ_r are also derived for the later use in the array design.

6.4 Design

6.4.1 Slot pair design

For given slot length $2l_1$, the slot length $2l_2$ and the spacing between the two slots $2q$ are optimized for minimum reflection from a pair in the waveguide. In the practical procedure, l_2 and q is varied with the step of 0.01mm and the reflection is calculated. The procedure stops when the reflection is reduced below –50dB. This is repeated for various slot length $2l_1$ or various slot pair coupling. As the length l_1 approaches resonant one, the reflection less than –50dB is no longer realized. The coupling for this length l_1 is defined as the maximum coupling. Slot spacing $2q$ is smaller than $\lambda_g/4$ due to phase delay of nonresonant slot admittance. Mutual coupling between two slots in a pair is large and diminishes the radiation from a pair. When the waveguide is filled with dielectric in order to suppress the grating lobes, the slot spacing becomes smaller and these effects are notable. The offset p is an important parameter reducing it and enhancing the radiation.

Figure 6.5 shows the relation of $2l_1$, $2l_2$ and $2q$ for minimum reflection as functions of various slot pair coupling ($=1-|S_{21}|^2$). Figure 6.5 (a) shows parameters for the offset p = 3.2mm, while Fig. 6.5(b) shows those without the offset (p = 0). The design parameters are shown in Table 1. In the latter case, the optimum slot spacing $2q$ seriously deviates from $\lambda_g/4$ due to strong mutual coupling. As the slot coupling increases, the phase difference also increases and the optimum spacing $2q$ decreases further. Since the minimum slot spacing $2q$ is mechanically limited and is about 2 mm,

the slot pair coupling can not exceeds 35 %. On the other hand, the phase difference in the pair with offset p remains unchanged for wide range of slot coupling. Then the optimum spacing $2q$ is nearly equal to $\lambda_g/4$ and the slot pair coupling more than 70 % is realized. The offset p plays an important role in the design of slot pairs near the termination for which strongest pair coupling is required.

6.4.2 Array design

One dimensional array with uniform aperture illumination is designed. N slot pairs are arrayed and numbered from the feed point (pair number 1) to the termination (pair number N). By ignoring the reflections in the waveguide, the following procedure is adopted for the array design.

At first, the coupling of each pair is specified in sequence from the N-th to the 1-st pair. Once the maximum coupling power $C(N)$ for the last pair is given, uniform amplitude field illumination is realized by setting the coupling power of the n-th pair $C(n)$ according to the following equation:

$$C(n-1)=\frac{C(n)}{1+C(n)} \qquad (n=2,3,4,\cdots,N) \qquad (6.20)$$

For $C(n)$ thus defined, the slot lengths $2l_1(n)$, $2l_2(n)$ and slot spacing $2q(n)$ are derived by referring to Fig. 6.5.

Next, the pair spacing $s(n)$ are determined to realize uniform phase illumination. The following equation is imposed:

$$k_g \cdot s(n) = 2\pi + \theta_r(n-1) - \theta_t(n-1) - \theta_r(n) \qquad (n=2,3,4,\cdots,N) \qquad (6.21)$$

where k_g ($= 2\pi/\lambda_g$) is the wave number of the waveguide and the predicted phase delays of the transmission and the radiation are $\theta_t(n)$ and $\theta_r(n)$.

The above design procedure dispenses with iteration. However, excitation coefficients of slots located at the end of the array may deviate from prediction, since the unit pair analysis in Sec. 6.3.2 assumes fictitious slots on both side, while the slot exist only on one side of the end pair. If one requires highly uniform illumination, a short iterative procedure may be used to optimize parameters in the last few pairs.

6.5 Numerical results

6.5.1 Model antenna

To clarify the advantages of the slot pair over a single slot, a relatively small array is designed and predicted characteristics are compared to each other. A shunt slot array [6-8]-[6-10] is adopted as a conventional resonant-slot array. It has parallel slots and common advantage of excellent XPD over a series slot array with non-parallel slots.

The common design parameters are as follows. The design frequency is set at 12 GHz. The size of the waveguide cross section a, b is 17.5 mm × 4.5 mm and the wall thickness h is 0.5 mm. The waveguide narrow-wall width b is set smaller than that of the standard waveguide to make the slot coupling strong. The array length is 330 mm and the waveguide is terminated by a matched load. An array using 11 paired slots is designed as shown in Fig. 6.6 (a). Two kinds of design are tested and compared. The first one is the design developed in Sec. 6.4.2 which is based upon the unit design of a slot pair and dispenses with iteration. The second one adopts further iteration taking the end effects of the array into account. A conventional slot array which has 15 resonant-slots is also designed as is shown in Fig. 6.6 (b). The slots parallel to the guide axis are cut on the broad wall. The resonant length is found by the analysis as a function of slot offset. When the slot offset from the center of the waveguide increases, the slot coupling also increases. The couplings are determined so as to obtain uniform amplitude field illumination. Since the electromagnetic field distribution forms a standing wave in the waveguide, iterative design procedure is indispensable to arrive at the desired illumination [6-2]. Furthermore beam-tilting technique is adopted to the resonant-slot array in order to cancel reflections at the feed point: main beam is tilted by 9 degrees so that the second null coincides with boresite direction ($\theta = 0$). All the slot spacings are set to be equal to $\pi / (k_g - k_0 \sin\theta_e)$ (θ_e: tilt angle, s: slot spacing) as the initial value in the iteration for obtaining uniform phase distribution.

6.5.2 Calculated results of test antenna

Calculated results of reflection and termination loss in the waveguide are shown in Fig. 6.7. Reflection of the slot pair array without beam-tilting technique is

suppressed below –20 dB and has almost the same potential as the resonant-slot array with beam-tilting.

Aperture phase illuminations of both antennas at three frequencies are shown in Fig. 6.8. Contrary to what one expected, the array with slot pair is more narrow banded than the conventional one. Since array lengths and long line effects of both antennas are the same, it is due to the frequency dependence of the transmission θ_t and the radiation phase θ_r of non-resonant slots in the new antenna.

To demonstrate the effectiveness of simple design without iterations in the slot pair array, the results with iterations are also included in the figure; they are almost the same as those for the simple design.

6.6 Experimental results

A 16-element model antenna is manufactured at 12 GHz. The design parameters are indicated in Table 6.1. Permittivity of dielectric in the waveguide is 1.59. The slot offset p in a slot pair is 3.2 mm. The waveguide is terminated by a matched load.

Fig. 6.9 shows the aperture field illumination. The amplitude and phase is sufficiently uniform at 12.2 GHz, which is 200 MHz higher than the design one. This frequency shift may be due to error in permittivity of dielectric. New permittivity of 1.54, which explains the measurement better, is used instead of 1.59 in the calculations hereafter. The phase change in Fig. 6.9 (a) is due to both the long line effect and the slot coupling. The former is a general frequency dependence due to a path length difference of the array elements for traveling wave excitation; this is also presented in Fig. 6.9. The amplitude is a bit tapered but the illumination is uniform within 2 dB error.

Fig. 6.10 shows frequency characteristics of reflection and termination loss. Fine agreement between measurement and calculation was obtained. Reflection (S_{11}) is less than –17 dB and termination loss of the array (S_{21}) is less than –18 dB in 400 MHz bandwidth centered at 12.2 GHz.

Radiation pattern is shown in Fig. 6.11. Reasonable agreement between measured and calculated ones was obtained. Small differences in the radiation pattern are due to the amplitude taper in the aperture illumination. The side lobes are much higher in the termination direction ($\theta \fallingdotseq 90^\circ$). This phenomenon is due to an element

pair radiation pattern shown in Fig. 6.12. This lobe is suppressed in two dimensional array by applying the alternative phase feed system.

6.7 Concluding remarks

A novel slotted waveguide array using "reflection-cancelling slot pair" is proposed. The antenna design and analysis are presented. Reflection characteristic of the slot pair array is excellent and a boresite beam array can be realized. In addition, a slot pair can realize stronger coupling than the conventional resonant slot; termination power can be set small even for a small array. On the other hand, the analysis reveals that the bandwidth of the slot pair array in terms of the aperture field phase illumination is narrower than the conventional one. Consequently, the slot pair array is much more suitable for small arrays than conventional one.

References

[6-1] Johnson, R.C., and Jasik, H.: "Antenna engineering handbook," New York McGraw-Hill, Chap.9, 1984

[6-2] Hamadallah, M.: "Frequency limitations on broad-band performance of shunt slot arrays," *IEEE Trans. on A. P.*, Vol. 37, No. 7, July 1989

[6-3] Takada, J., Nii, K., Ando, M., and Goto, N.: "A reflection canceling slot set using parallel slot pairs for linearly-polarized radial line slot antennas," Proc. ISAP Japan, Vol.1, pp117-120, September 1992

[6-4] Goto, N.: "A waveguide-fed printed antenna", IEICE Japan, Tech. Rep., AP89-3, April 1989

[6-5] Seki, H., and Goto, N.: "On the effect of wall-thickness upon a waveguide slot antenna," IECE Japan, Tech. Rep., AP80-48, July 1980

[6-6] Seki, H.: "An alternative representation of electromagnetic fields in a rectangular waveguide with an aperture in its wall," in Conf. Rec., Nat. Conv., 1, (16), IECE Japan, September 1984

[6-7] Hirokawa, J., Sakurai, K., Ando, M., and Goto, N.: "Matching slot pair for a circularly-polarized slotted waveguide array," *IEE Proc.* H, 137, (6), pp. 367-371, 1990

[6-8] Oliner, A. A.: "The impedance properties of narrow radiating slots in the broad face of rectangular waveguide," *IRE Trans. on A.P.*, AP-5, 1, pp 4-20, Jan. 1957

[6-9] Yee, H. Y.: "Impedance of a narrow longitudinal shunt slot in a slotted waveguide array," *IEEE Trans. on A.P.*, AP-22, 7, pp. 589-592, July 1974

[6-10] Elliott, R. S.: "An improved design procedure for small arrays of shunt slots," *IEEE Trans. on A.P.*, AP-31, 1, Jan. 1983

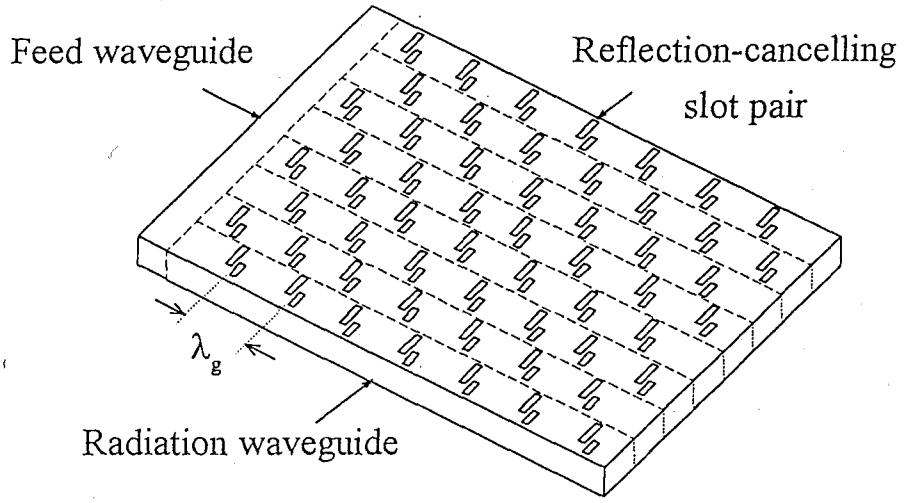

Fig. 6.1 Configuration of reflection-cancelling slot pair planar array

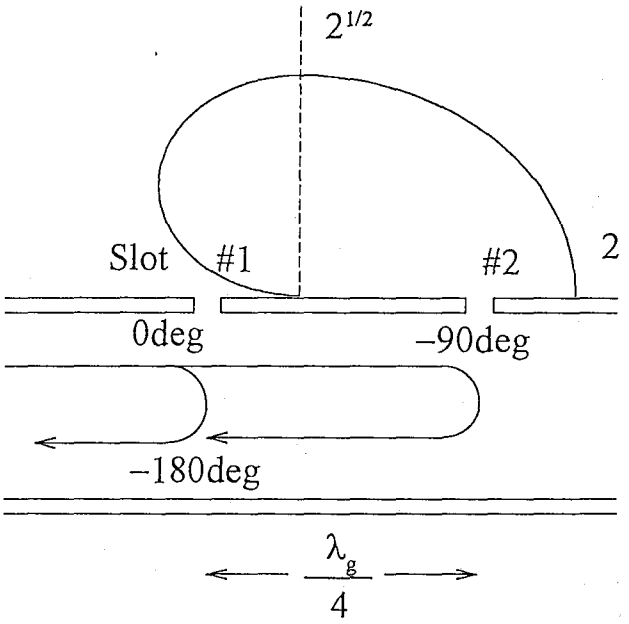

Fig. 6.2 Reflection-cancelling principle of a slot pair and its element pattern

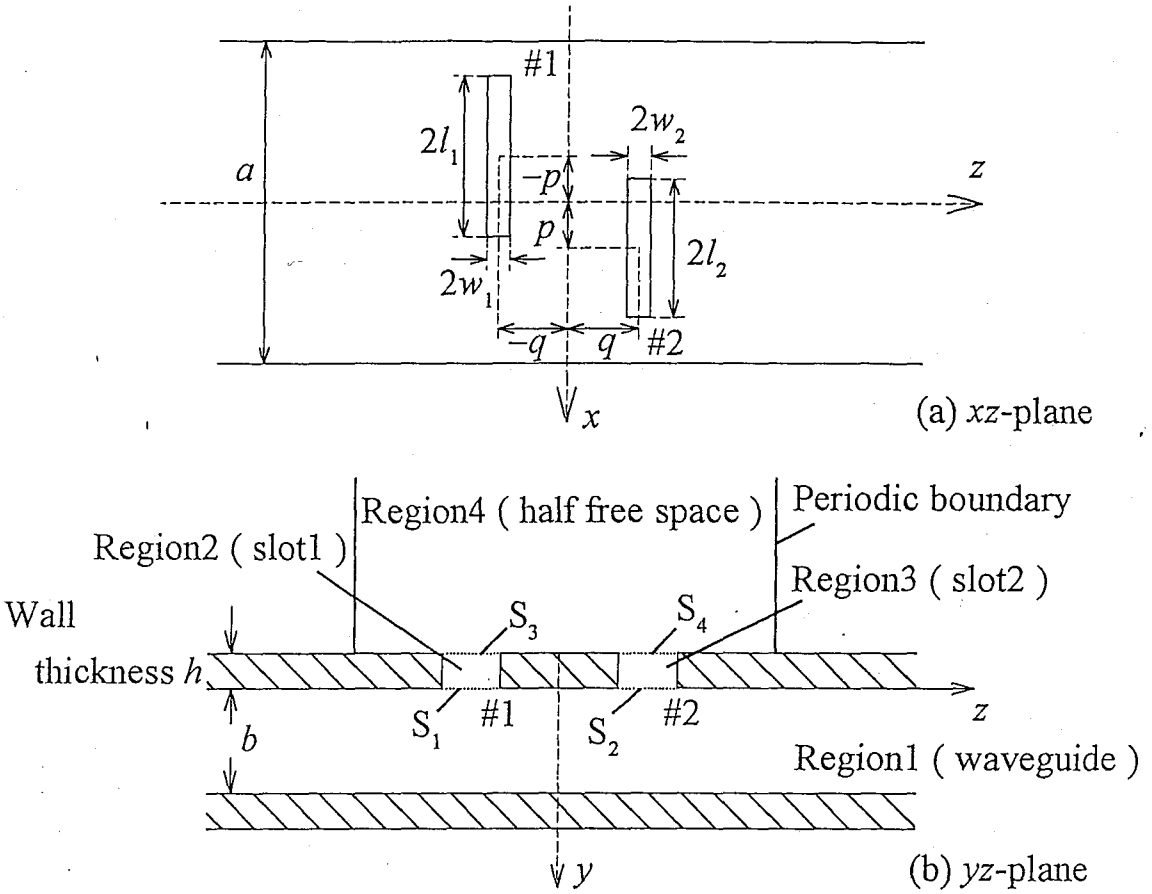

Fig. 6.3 Analysis model of reflection-cancelling slot pair

(a) xz-plane (b) yz-plane

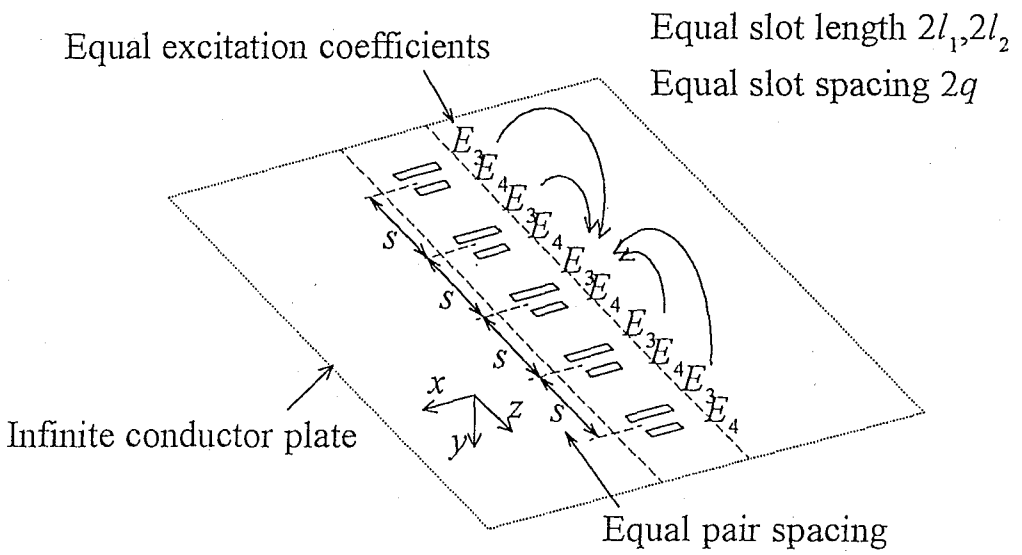

Fig. 6.4 Uniform array approximation
of periodic boundary condition for one-dimensional array

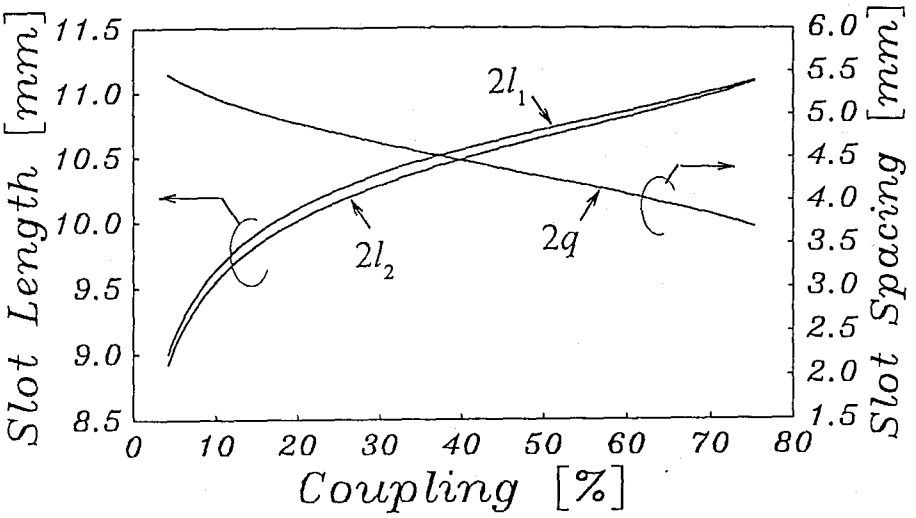

(a) with offset (p = 3.2 mm)

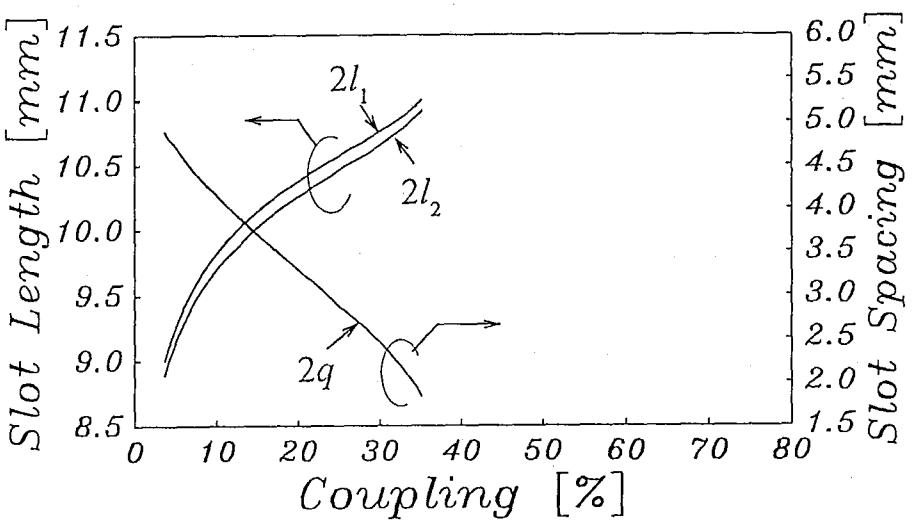

(b) without offset (p = 0)

Fig. 6.5 Slot pair parameters for reflection cancelling
(coupling = $1-|S_{21}|^2$)

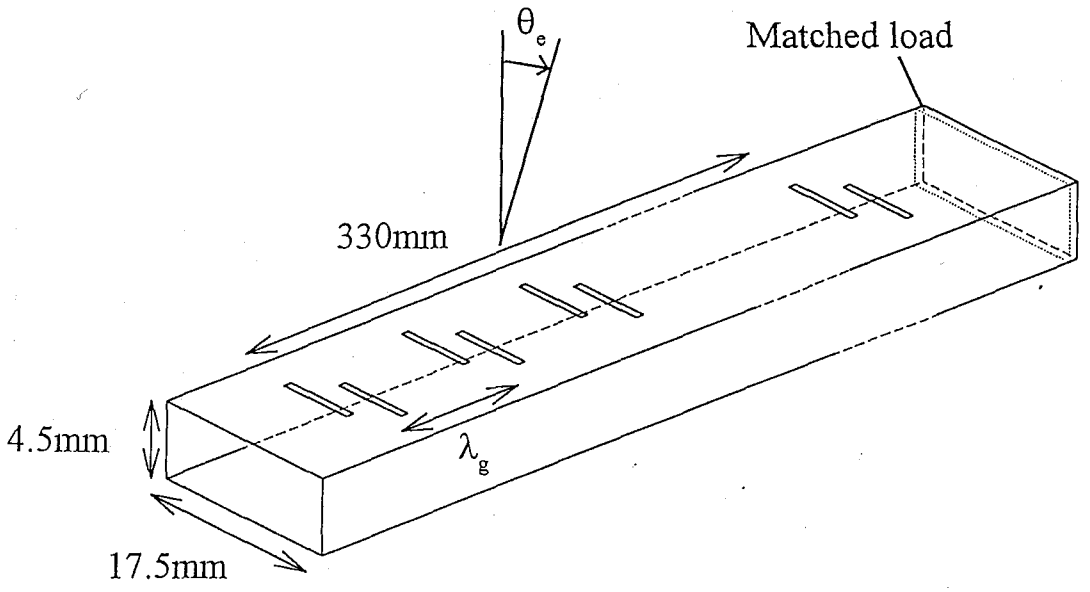

(a) Reflection-canceling slot pair array

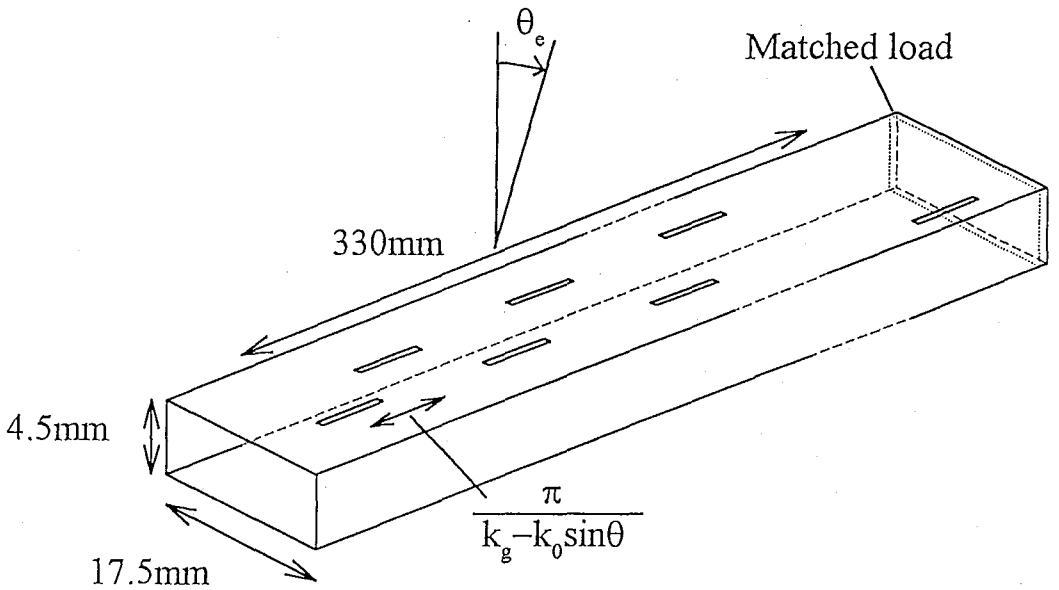

(b) Resonant slot array

Fig. 6.6 Design parameters of manufactured arrays

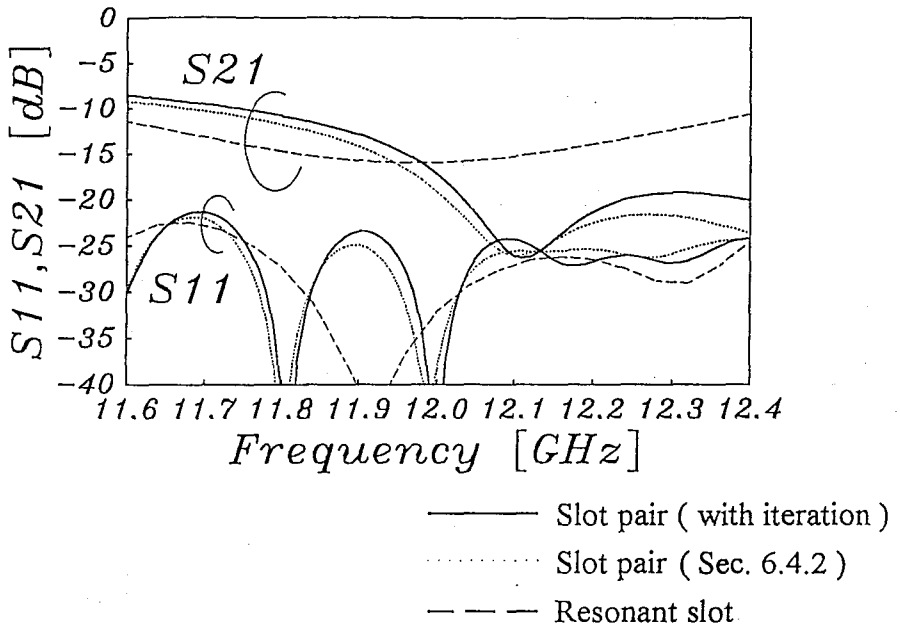

Fig. 6.7 Reflection and transmission
of the reflection-cancelling slot pair array and the resonant slot array

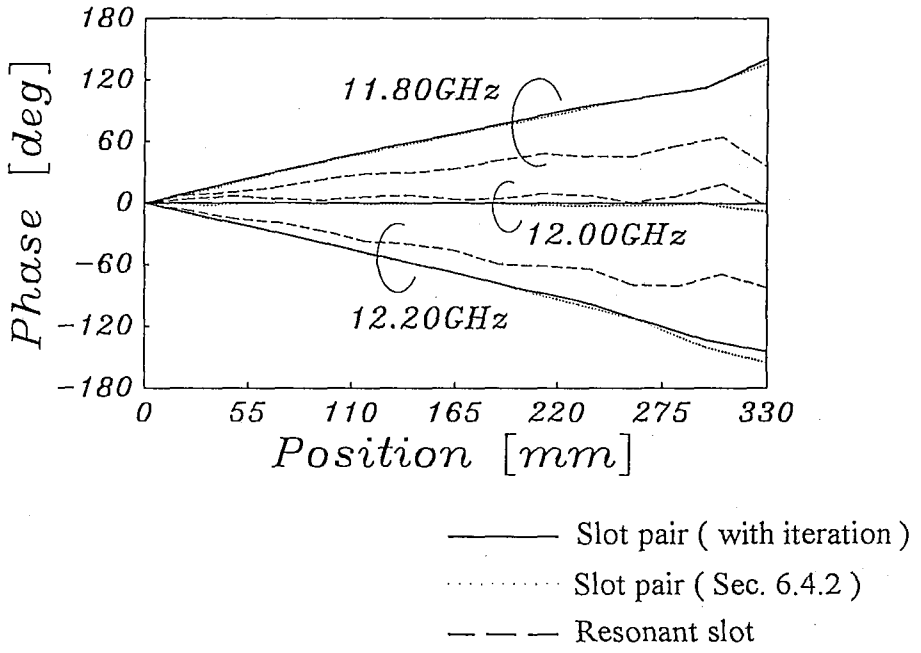

Fig. 6.8 Electromagnetic field illumination
of the reflection-cancelling slot pair array and the resonant slot array

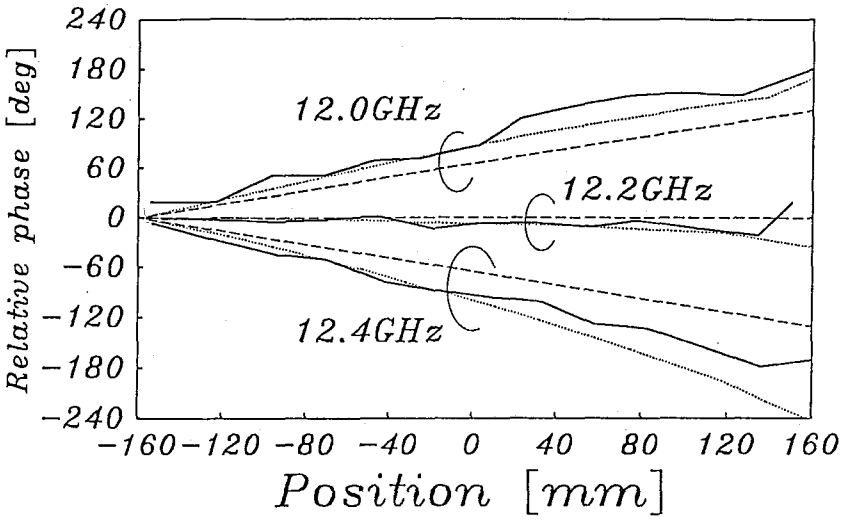

(a) phase

——— Experimental results

····· Calculated results

– – – – Long line effect

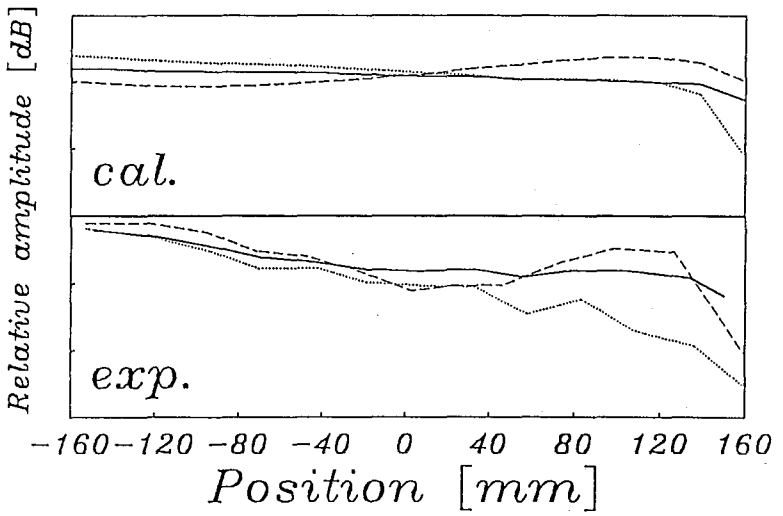

(b) amplitude (5dB/dvi)

– – – – 12.0GHz

——— 12.2GHz

····· 12.4GHz

Fig. 6.9 Aperture field illumination

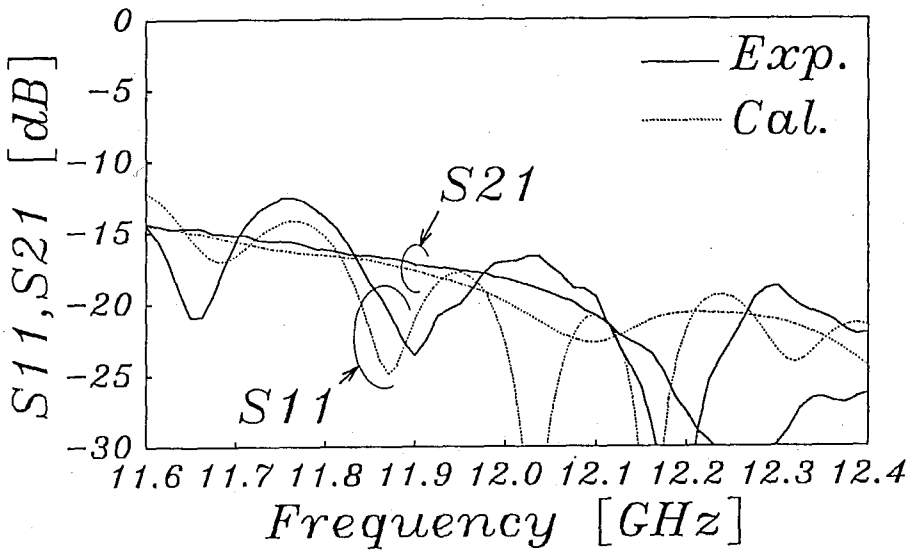

Fig. 6.10 Reflection and transmission
frequency characteristics

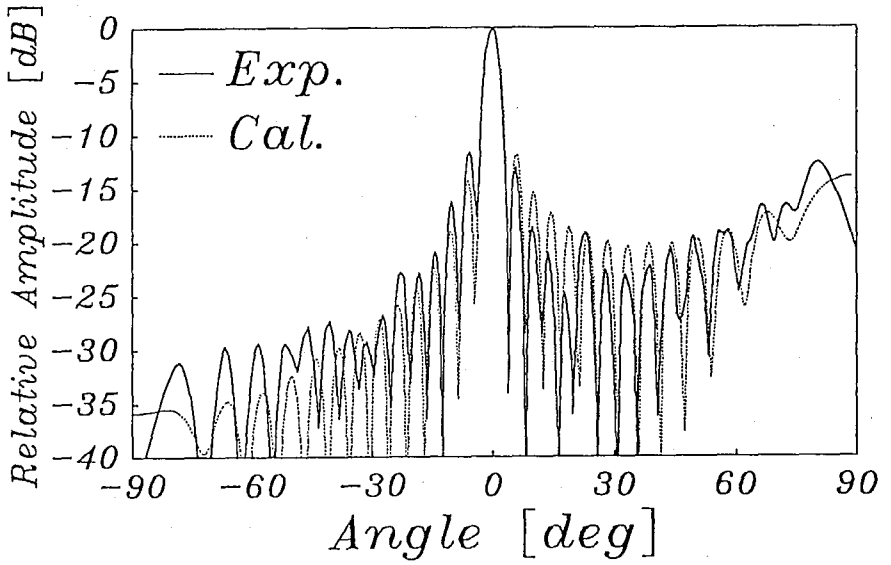

Fig. 6.11 Radiation pattern

Table 6.1 Design parameters

Design frequency	12 GHz
Relative dielectric constant in the waveguide	1.59
Slot offset	3.2 mm
Waveguide broad wall width	17.5 mm
Waveguide narrow wall width	4.0 mm
Slot plate thickness	0.5 mm
Array length	330 mm
Slot width	1.0 mm

Chapter 7. Conclusion

7.1 Summary of preceding chapters

Single layer slotted waveguide antennas are attractive in the respect of the simple structure. The antenna is fabricated by only putting a slot plate on a groove feed structure. Since both of the components are two-dimensional one, the slots are cut on the plate by press and the grooves are manufactured by die casting. Only TE_{10} mode transmits in the single mode waveguide. It is possible to analyze the two parts; the radiation and the feed waveguides, independently each other. It is easy to analyze the two-dimensional structure of the feed circuit.

Chapter 2 point out the problems in applying the single layer slotted waveguide array to the high frequency use. The high frequency use antenna can be designed by scaling down the lower frequency use antenna for its wavelength in principle. However, slot width, slot plate thickness and wall thickness are limited in fabrication. Furthermore, in higher frequency, the sizes of the components are reduced and high fabrication accuracy is required. We have to take care of the accuracy in setting the slot plate on the grooves. Test antennas are fabricated for experiment in 22 GHz band. Three types of contact are examined by measuring the antenna characteristics.

Bonding: The contact is electrically incomplete.

Laser welding: Grating lobes appear due to the slot plate shrinkage.

Brazing: Center frequency shifts due to the extension of both the slot plate and the base feed structure.

The alternating phase feed system is proposed in order to avoid the difficulty in fabrication. The basic operation is confirmed by experiments in 22 GHz band. The advantages of the feed system can not be confirmed by the bonding contact antenna. It is because the adhesive cuts the current between the two waveguides.

The mutual effect in the external region of the waveguide is quite complicated. It makes the slot array design difficult in general. The arrays designed in this study are relatively large and are 24 × 25 element one. Periodic boundary condition which is equivalent to the infinite slot arrangement is introduced to the analysis. The experiments

confirm the effectiveness of the analysis for the design of the array. Further investigation confirms that the analysis is effective for relatively small array such as 4 × 7 elements one. Since this concept is general one, it can be used for any other type array antenna.

In the first step toward the application of millimeter-wave array, high gain antenna of 36 dBi is realized in 22 GHz band explained in Chap. 4. The slot plate and the base feed grooves are in contact by brazing technique as is mentioned in Chap. 2. The frequency at the peak gain shifts in 150 MHz lower than the design one. The peak gain and the antenna efficiency result 35.9 dBi and 75.6 %, respectively. They are much higher than any other planar antennas. The single layer slotted waveguide antenna is expected to apply to millimeter-wave use. The antenna for 60 GHz band is designed and is confirmed to realize almost equal characteristics to the antenna for 22 GHz band.

A circular-polarized single layer slotted waveguide array is realized by using cross slots for the DBS service in the USA in Chap. 5. Both right and left-hand circular polarizations radiates toward different directions from the same cross slots. They are fed from the opposite ports of the leaky waveguide each other. In the design, the optimum aperture distribution is derived for the symmetrical structure by the calculus of variations. The array with all the same slots gives almost the same characteristics with the optimum one. As results of experiments, predicted taper of amplitude is obtained on the aperture. The antenna efficiency results 71 % and 64 % of right and left-hand polarization, respectively. In comparison with 75 % antenna efficiency of the Japanese DBS antenna whose aperture is uniform, the efficiency is sufficiently high.

Reflection canceling slot pair consists of two slots. The mutual coupling between the two slots in a pair reduces the radiation from the slot pair. It is suppressed by slot shifts toward the different direction each other. The features of the reflection canceling slot pair are clarified by comparison with resonant shunt slot array. As results of the experiments of one-dimensional array, we can confirm;

- Beam tilting technique is adopted to the resonant shunt slot array in order to suppress the reflection at the feed point. Arbitrary slot arrangement is possible for the reflection canceling slot pair array.
- The frequency dependence of the transmission phase change through the slot pair is large. The frequency bandwidth of gain would be slightly narrow.

7.2 Remarks for future studies

The remarks for further investigations are listed.

(1) Millimeter-wave applications are increasing recently. We have a plan to develop the antenna for the car collision avoidance radar in 60 GHz band and the COMETS (communications and broadcasting engineering test satellite) antenna in 40 GHz band.

(2) Alternating phase feed system is advantageous for high frequency use. The development of the system is highly required for the applications mentioned in (1).

Acknowledgments

I wish to express my gratitude to Professor Naohisa Goto for helpful suggestions and comments. I also wish to express my thanks to Professor Makoto Ando for his continuous guidance and encouragement.

I am indebted to Professor Yoshiyuki Naito, Professor Kazuhito Furuya, Professor Yasutaka Shimizu, Professor Kiyomichi Araki, Associate Professor Tetsuya Mizumoto, Associate Professor Jun-ichi Takada and the member of Microwave and Device Research Group for valuable comments and criticisms.

I wish to thank Mr. Kimio Sakurai for his experimental helps and Ms. Kumiko Kaneta for her support. I would like to thank Associate Professor Hiroyuki Arai in Yokohama National University and Dr. Masaharu Takahashi in Musashi Institute of Technology for valuable advice. I gratefully acknowledge helpful discussions with Dr. Jiro Hirokawa on several points of my work.

I would like to express my appreciation to Mr. Koji Miyata, Mr. Masahiro Uematsu, Mr. Takashi Ojima, Mr. Nobuharu Takahashi, Mr. Motonobu Moriya and Mr. Kazuhiro Muraishi of Nippon Steel Co., Mr. Hidenori Ishiwata, Mr. Kiyoshi Seshimo and Mr. Isamu Hirai of NHK Spring Co., Dr. Kunitoshi Nishikawa and Mr. Toshiaki Watanabe of Toyota Central R&D Labs. Inc., Mr. Hisao Ono, Mr. Toru Fukui and Mr. Michihiro Ue of Yupiteru Industries Co., Ltd., Mr. Masanori Suzuki of Toppan Printing Co. for their helps of antenna fabrications and experiments.

I would like to thank Mr. Seiji Hosono for encouragement and to acknowledge helpful discussions with him. My special thanks are due to Mr. Kyong-Sik Min, Mr. Tetsuya Yamamoto, Mr. Yoshihiro Iijima, Mr. Kenji Fukazawa, Mr. Akihiro Iriyama, Mr. Yuichi Kimura and any other members of Goto, Ando and Takada laboratories for valuable helps.

This work is partly supported by The Murata Science Foundation.

Finally, I express my respects to my parents for their support.

List of publications

Papers

1. Sakakibara, K., Hirokawa, J., Ando, M. and Goto, N., "A linearly-polarized slotted waveguide array using reflection cancelling slot pairs," *IEICE Trans. on Commun.*, Vol. E77-B, No. 4, pp.511-518, April 1994
2. Sakakibara, K., Hirokawa, J., Ando, M. and Goto, N., "A high-gain and high-efficiency single-layer slotted waveguide array for use in 22 GHz band," *IEE Electronics Letters*, Vol. 32, No. 4, pp. 283-284, Feb. 1996
3. Sakakibara, K., Hirokawa, J., Ando, M. and Goto, N., "Periodic boundary condition for evaluation of external mutual couplings in a slotted waveguide array," to be published in *IEICE Trans. Commun.*
4. Sakakibara, K., Kimura, Y., Hirokawa, J., Ando, M. and Goto, N., "A two-beam slotted leaky waveguide array for mobile reception of dual polarization DBS," submitted to *IEEE Trans. Vecular Technology*
5. Sakakibara, K., Hirokawa, J., Ando, M. and Goto, N., "Single-layer slotted waveguide array for millimeter wave applications," submitted to *IEICE Trans. Commun.*

International conferences

1. Sakakibara, K., Hirokawa, J., Ando, M. and Goto, N., "Design of a slotted waveguide array using reflection-cancelling slot pairs," *IEICE Proc. of ISAP '92*, Sapporo, Japan, pp. 121-124 Sep., 1992
2. Sakakibara, K., Hirokawa, J., Ando, M. and Goto, N., "A slotted waveguide array using reflection-cancelling slot pairs," *IEEE, AP-S Digest*, Michigan, pp. 1570-1573, June, 1993
3. Sakakibara, K., Hirokawa, J., Ando, M. and Goto, N., "A single layer slotted waveguide array for 22 GHz band radio system between mobile base stations," *IEEE, AP-S Digest*, Seattle, pp. 356-359, June, 1994
4. Sakakibara, K., Hirokawa, J., Ando, M. and Goto, N., "A linearly polarized slotted waveguide planar array using single layer feed circuit for 22 GHz band radio system," *'94 APMC Proc.*, Tokyo, pp. 307-310, Dec., 1994

5. Sakakibara, K., Hirokawa, J., Ando, M. and Goto, N., "Simple evaluation of mutual slot couplings in a slotted waveguide planar array antenna," *IEEE, AP-S Digest*, Newport beach, pp. 1838-1841, June, 1995
6. Sakakibara, K., Hirokawa, J., Ando, M. and Goto, N., "A slotted waveguide planar array antenna for entrance radio systems in mobile communication," *4th IEEE ICUPC*, Tokyo, pp. 373-376, Nov., 1995
7. Sakakibara, K., Hirokawa, J., Ando, M. and Goto, N., "A high-gain and high-efficiency single-layer slotted waveguide array for use in 22 GHz band for entrance radio relay system in mobile communications," submitted to *IEEE AP-S*, July, 1996
8. Hirokawa, J., Sakakibara, K., Ando, M. and Goto, N., "A two-beam slotted leaky waveguide array for mobile reception of dual polarization DBS," submitted to *IEEE AP-S*, July, 1996
9. Ando, M., Sakakibara, K., Hirokawa, J. and Goto, N., "A 60 GHz band single-layer planar waveguide arrays," submitted to *IEEE AP-S*, July, 1996
10. Ando, M., Sakakibara, K., Yamamoto, T., Hirokawa, J. and Goto, N., "Single layer planar waveguide array for millimeter wave applications," submitted to *URSI*, Aug., 1996
11. Sakakibara, K., Hirokawa, J., Ando, M. and Goto, N., "A high-gain and high-efficiency single-layer slotted waveguide arrays in millimeter-wave band," submitted to *IEICE Proc. of ISAP '96*, Makuhari, Japan
12. Hirokawa, J., Sakakibara, K., Kimura, Y., Ando, M. and Goto, N., "Single-layer slotted leaky waveguide arrays for applications to mobile satellite communications," submitted to *IEICE Proc. of ISAP '96*, Makuhari, Japan

Papers of technical group on antennas and propagation IEICE

1. Sakakibara, K., Hirokawa, J., Ando, M. and Goto, N., "A linearly-polarized slotted waveguide array using reflection-canceling slot pairs," AP91-121, NTT Yokosuka labs., Kanagawa, Feb. 1992
2. Sakakibara, K., Hirokawa, J., Ando, M. and Goto, N., "A slotted waveguide array for subscriber radio system in 22 GHz band," AP93-58, Makuhari Messe, Chiba, Aug. 1993

3. Sakakibara, K., Takahashi, T., Hirokawa, J., Ando, M. and Goto, N., "A single layer slotted waveguide array for 22 GHz band radio system between mobile base stations," AP93-145, Kikai Shinko Kaikan, Tokyo, Feb. 1994
4. Sakakibara, K., Kimura, Y., Hirokawa, J., Ando, M. and Goto, N., "A two-beam slotted leaky waveguide array for mobile reception of dual polarization DBS," AP95-86, Yumicho-club, Dec. 1995

National convention records of IEICE

1. Sakakibara, K., Hirokawa, J., Ando, M. and Goto, N., "A waveguide array using reflection canceling slot pairs," B-133, Science Univ. of Tokyo, March 1992
2. Sakakibara, K., Hirokawa, J., Ando, M. and Goto, N., "Design of a slotted planar array antenna for subscriber radio system at 22 GHz band," B-60, Nagoya Univ., March 1993
3. Sakakibara, K., Hirokawa, J., Ando, M. and Goto, N., "A feed circuit of a slotted waveguide array for subscriber radio system at 22 GHz band," B-61, Nagoya Univ., March 1993
4. Sakakibara, K., Hirokawa, J., Ando, M. and Goto, N., "Design of a slotted waveguide planar array antenna using resonant slots for subscriber radio system at 22 GHz band," B-69, Hokkaido Institute of Technology, Sep. 1993
5. Sakakibara, K., Hirokawa, J., Ando, M. and Goto, N., "A slotted waveguide planar array using single layer feed circuits for 22 GHz subscriber radio system," B-55, Keio Univ., March 1994
6. Sakakibara, K., Hirokawa, J., Ando, M. and Goto, N., "Characteristics of a 22 GHz band linearly polarized waveguide planar array," B-113, Tohoku Univ., Sep. 1994
7. Sakakibara, K., Hirokawa, J., Ando, M. and Goto, N., "Simple evaluation of mutual couplings in a slotted waveguide planar array," B-82, Fukuoka Institute of Technology, March 1995
8. Sakakibara, K., Hirokawa, J., Ando, M. and Goto, N., "A slotted waveguide array for car-collision avoidance radar in 60 GHz band," B-103, Chuo Univ., Sep. 1995
9. Sakakibara, K., Iriyama, A., Hirokawa, J., Ando, M. and Goto, N., "A high-frequency and high-efficiency single-layer slotted waveguide array," B-102, Tokyo Institute of Technology, March 1996

Appendix A : Determination of slot spacing

Slot spacings are constant and are given by following expression;

$$s = \frac{1}{\frac{2}{\lambda_g} - \frac{2}{\lambda_0}\sin\theta_t} \tag{A.1}$$

where λ_0 and λ_g are wave lengths in the free space and that in the radiation waveguide respectively and θ_t is beam tilting angle from the zenith. θ_t is chosen so that m-th null point of an array factor may fall on the boresight direction in order to suppress the reflection at the feed point. Therefore, $k_0 s \cdot \sin\theta_t$ can be substituted by $\frac{2\pi}{N}m$, so following expression of the slot spacing is obtained;

$$s = \frac{\lambda_g}{2} + m\frac{\lambda_g}{N} \tag{A.2}$$

The spacing is a little larger than a half guide wave length. However, the null number m is chosen so that grating lobes do not appear in the radiation pattern.

Appendix B: Aperture illumination estimating model

Aperture illumination estimating model as is shown in Fig. 3.4 is introduced. Neglecting the edge deviation in the transversal direction of x, K identical one-dimensional arrays are arranged in both sides of the real one. The method of moments analysis is conducted for deriving slot excitation coefficients A_n ($n = 1, \cdots N$), where A_n is the unknown coefficients of magnetic current M_n. The number of unknown functions is N and remain the same as that in one dimensional array.

Appendix C: Analytical expression of aperture field on the slot

Aperture field on the slot is derived in simple expression analytically which includes mutual effect from all the surrounding slots approximately. The field distribution along the z-direction is assumed by piece-wise sinusoidal function and that along the x-direction is by Maxwell's function in the method of moments. The excitation coefficients E_1 and E_2 are unknown and the magnetic currents M_1 and M_2 are expressed as

$$M_u = E_u \frac{\sin k_0(l-|z-\frac{s}{4}|)}{\sin k_0 l} \frac{1}{\sqrt{w^2-(x-d)^2}} \qquad (u=1,2) \qquad \text{(C.1)}$$

All the integrals in the green's functions in Sec. 3.4.1 are derived analytically. As a result, the excitation coefficients E_1 and E_2 are simply expressed by following formula;

$$\begin{bmatrix} E_1 \\ E_2 \end{bmatrix} = \frac{I_1}{AD-BC}\begin{bmatrix} D \\ -C \end{bmatrix} \qquad \text{(C.2)}$$

$$I_1 = \frac{\pi k_{cP10}}{\gamma_{P10}}\sqrt{Y_{hP10}}\sqrt{\frac{2}{a_g b_g}}J_0\left(\frac{\pi}{a_g}w\right)\frac{2k_0}{k_0^2+\gamma_{P10}^2} \cos\left\{\frac{\pi}{a_g}\left(\frac{a_g}{2}-d\right)\right\}\{\cosh(\gamma_{P10}l)-\cos(k_0 l)\} \qquad \text{(C.3)}$$

$$A=Y_{WS}+Y_V+Y_P \qquad \text{(C.4)}$$

$$B=Y_{WM} \qquad \text{(C.5)}$$

$$C=Y_{WM} \qquad \text{(C.6)}$$

$$D=Y_H+Y_{WS} \qquad \text{(C.7)}$$

$$Y_{WS} = -\sum_{m'n'}\coth(\gamma_{Wmn}t)\frac{1}{k_{cWmn}^2}\frac{\varepsilon_{mn}}{4lw}\frac{4\pi^2k_0^2}{\left\{\frac{(2m'+1)\pi}{2l}-k_0^2\right\}^2} \cot^2 k_0 l\{J_0(n'\pi)\}^2\left\{Y_{hWmn}\left(\frac{m\pi}{2l}\right)^2+Y_{eWmn}\left(\frac{n\pi}{2w}\right)^2\right\} \qquad (m=2m'+1,\ n=2n') \qquad \text{(C.8)}$$

$$Y_{WM} = -\sum_{m'n'} \frac{1}{\sinh(\gamma_{Wmn} t)} \frac{1}{k_{cWmn}^2} \frac{\varepsilon_{mn}}{4lw} \frac{4\pi^2 k_0^2}{\left\{\frac{(2m'+1)\pi}{2l} - k_0^2\right\}^2}$$

$$\cot^2 k_0 l \left\{J_0(n'\pi)\right\}^2 \left\{Y_{hWmn}\left(\frac{m\pi}{2l}\right)^2 + Y_{eWmn}\left(\frac{n\pi}{2w}\right)^2\right\}$$

$$(m = 2m'+1,\ n = 2n') \qquad \text{(C.9)}$$

$$Y_V = -\sum_{mn'} \frac{\coth(\gamma_{Vmn} b_g)}{\sin^2 k_0 l} \frac{1}{k_{cVmn}^2} \frac{\varepsilon_{mn}}{a_g c} \left\{Y_{hVmn}\left(\frac{(2n'+1)\pi}{c}\right)^2 + Y_{eVmn}\left(\frac{m\pi}{a_g}\right)^2\right\}$$

$$\pi^2 \left\{J_0\left(\frac{m\pi}{a} w\right)\right\}^2 \frac{4k_0^2}{\left[k_0^2 - \left\{\frac{(2n'+1)\pi}{c}\right\}^2\right]^2} \left[\cos\left\{\frac{(2n'+1)\pi}{c} l\right\} - \cos k_0 l\right]^2 \cos^2 \frac{m\pi}{a_g}\left(\frac{a_g}{2} - d\right)$$

$$(n = 2n'+1) \qquad \text{(C.10)}$$

$$Y_P = \frac{1}{2} \sum_{m,n} \frac{1}{\sinh \gamma_{Pm,n} c} \frac{k_{cPm,n}^2}{\gamma_{Pm,n}^2} Y_{hMm,n} \frac{\varepsilon_{m,n}}{a_g b_g} \pi^2 \left\{J_0\left(\frac{m\pi}{a_g} w\right)\right\}^2$$

$$\frac{4k_0^2}{(k_0^2 + \gamma_{Pm,n}^2)^2} \cos^2 \frac{m\pi}{a_g}\left(\frac{a_g}{2} - d\right) \left\{\cosh(\gamma_{Pm,n} l) - \cos k_0 l\right\}^2 \left(1 - e^{-\gamma_{Pm,n} c}\right) \qquad \text{(C.11)}$$

$$Y_H = -\frac{8}{a_r b_r} \frac{\pi^2}{\sin^2 k_0 l} \frac{1}{Z_0 k_0^2} (1 - \cos k_0 l)^2$$

$$-\sum_{m,n} \frac{4}{\sin^2 k_0 l} \frac{\pi^2}{k_{cHm,n}^2} \frac{\varepsilon_{m,n}}{a_r b_r} \left\{J_0\left(\frac{2m\pi}{a_r} w\right)\right\}^2$$

$$\frac{k_0^2}{\left\{k_0^2 - \left(\frac{2n\pi}{b_r}\right)^2\right\}^2} \left(\cos\frac{2n\pi}{b_r} l - \cos k_0 l\right)^2 \qquad \text{(C.12)}$$

$$\left\{1 + \cos\left(\frac{4m\pi}{a_r} d\right) \cos\left(\frac{2n\pi}{b_r} s\right)\right\} \left\{Y_{hm,n}\left(\frac{2n\pi}{b_r}\right)^2 + Y_{em,n}\left(\frac{2m\pi}{a_r}\right)^2\right\}$$

$$k_{cWm,n} = \sqrt{\left(\frac{m\pi}{2l}\right)^2 + \left(\frac{n\pi}{2w}\right)^2},\ \gamma_{Wm,n} = \sqrt{k_{cWm,n}^2 - \varepsilon_r k_0^2},\ Y_{hWm,n} = \frac{\gamma_{Wm,n}}{jk_0 Z_0},\ Y_{eWm,n} = \frac{jk_0 Y_0}{\gamma_{Wm,n}}$$

$$k_{cVm,n} = \sqrt{\left(\frac{m\pi}{a_g}\right)^2 + \left(\frac{n\pi}{c}\right)^2},\ \gamma_{Vm,n} = \sqrt{k_{cVm,n}^2 - \varepsilon_r k_0^2},\ Y_{hVm,n} = \frac{\gamma_{Vm,n}}{jk_0 Z_0},\ Y_{eVm,n} = \frac{jk_0 Y_0}{\gamma_{Vm,n}}$$

$$k_{cPm,n}=\sqrt{\left(\frac{m\pi}{a_g}\right)^2+\left(\frac{n\pi}{b_g}\right)^2},\ \gamma_{Pm,n}=\sqrt{k_{cPm,n}^2-\varepsilon_r k_0^2},\ Y_{hPm,n}=\frac{\gamma_{Pm,n}}{jk_0Z_0},\ Y_{ePm,n}=\frac{jk_0Y_0}{\gamma_{Pm,n}}$$

$$k_{cHm,n}=\sqrt{\left(\frac{m\pi}{a_r}\right)^2+\left(\frac{n\pi}{b_r}\right)^2},\ \gamma_{Hm,n}=\sqrt{k_{cHm,n}^2-\varepsilon_r k_0^2},\ Y_{hHm,n}=\frac{\gamma_{Hm,n}}{jk_0Z_0},\ Y_{eHm,n}=\frac{jk_0Y_0}{\gamma_{Hm,n}}$$

$$\varepsilon_{m,n}=\begin{cases}4 & (mn\neq 0)\\ 2 & (mn=0)\end{cases}$$

I_1 is the contribution of the incident magnetic field of TE_{10} mode. Y_{WS} and Y_{WM} are self and mutual admittance in the wall thickness, respectively. Y_V and Y_P are self admittance in the waveguide and are the contribution of the waves propagating toward the *y*- and *z*-directions, respectively. Y_H is the self admittance including the contributions from the surrounding slots in half free space. Z_0 is the intrinsic impedance and equals to 120π. *c* is the length of virtual cavity [3-11] which is chosen by about 3/4 guide wavelength.

Appendix D: The Euler equation for calculus of variations

As the problem of the calculus of variations, the maximum of the integral

$$J(u) = \int_{z_2}^{z_1} F(z, u, u')dz \tag{D.1}$$

is determined where the value z_0, z_1, $u(z_0)$ and $u(z_1)$ are given. The function $J(u+\varepsilon\tau)$ may be regarded as a function $\Phi(\varepsilon)$ of ε, thus

$$\Phi(\varepsilon) = \int F(z, u + \varepsilon\tau, u' + \varepsilon\tau')dz \tag{D.2}$$

where ε is a parameter and $\varepsilon\tau$ is known as the variation of the function u. $t(z)$ is a arbitrary function which satisfies $\tau(z_0) = \tau(z_1) = 0$. $\Phi(\varepsilon)$ must have a extremum at $\varepsilon = 0$ in a sufficiently small neighborhood of 0, and therefore $\Phi'(0) = 0$. If we differentiate the integral $\Phi(\varepsilon)$ with respect to ε under the integral sign, we obtain;

$$\Phi'(0) = \int_{z_0}^{z_1}\left(\frac{\partial F}{\partial u}\tau + \frac{\partial F}{\partial u'}\tau'\right)dz = 0 \tag{D.3}.$$

We transform the second part of the integral by partial integration, and we obtain the equation;

$$\int_{z_0}^{z_1}\tau\left(\frac{\partial F}{\partial u} - \frac{d}{dz}\frac{\partial F}{\partial u'}\right)dz = 0 \tag{D.4},$$

valid for every one of the functions τ. Therefore

$$\frac{\partial F}{\partial u} - \frac{d}{dz}\frac{\partial F}{\partial u'} = 0 \tag{D.5}$$

Appendix E: Design of the leaky waveguide array antenna

In the design of the antenna, we referred the parameters of the Japanese DBS and COMETS antennas, since the slot analysis of the cross slot is difficult due to the complicated structure.

The broad wall width of the waveguide a_g determines the wavelength of the dominant TE_{10} mode, which reflects the beam direction. Since all the slots are identical, the phase differences between the radiating waves and the input waves are constant on the aperture. Therefore, including the slow wave effect of a slot, the following equation is obtained as;

$$\frac{2\pi}{\lambda_g} d + \phi_s = \frac{2\pi}{\lambda_0} d \sin\theta_t \qquad \text{(E.1).}$$

The phase delay ϕ_s can be approximately compensated by the beam scan angle θ_s, so

$$\frac{\lambda_0}{\lambda_g} \cong \sin(\theta_t - \theta_s) \qquad \text{(E.2).}$$

This equation is the formula of the leaky wave theory. Hence, the broad guide width can be obtained by

$$a_g = \frac{\lambda_0}{2\sqrt{1-\sin^2(\theta_t - \theta_s)}} \qquad \text{(E.3)}$$

The slot offset determines the phase difference of the excitations between the two crossed slots, which reflects the axial ratio. The optimum offset depends on the required beam direction and the waveguide broad wall width a_g. The offset d is determined so that the ratio between d and a_g equals to that for the COMETS antenna, because the beam tilting angle is the same with it.

Slot length is determined to realize the required coupling obtained in Sec. 5.2. The coupling factor corresponds to the termination loss of 8.1 %. The Japanese DBS antenna has 16 slots on a waveguide. Provided that all the input power radiate out from 16 slots with uniform aperture distribution, the coupling of each slot is expressed by

$$C_n = \left(1 - \left|S_{21}^{[n]}\right|^2\right) \times 100 \quad [\%] \quad (n = 1, 2, 3, \cdots\cdots, 16) \qquad \text{(E.4)}$$

where we assume as $\left|S_{11}^{[n]}\right| = 0$. The propagating power T_n in the waveguide which has N slots with constant coupling C satisfies following equation;

$$\begin{cases} T_n = (1-C)T_{n-1} \\ T_0 = 1 \end{cases} \qquad (n = 1, 2, \cdots\cdots, N) \qquad \text{(E.5).}$$

Therefore, the termination power is expressed by

$$T_N = (1 - C)^N \qquad \text{(E.6).}$$

In order to obtain the termination power T_{26} of 8.1 % for $N = 26$, C equals to 9.21 % which is close to C_6 of the Japanese DBS antenna. The equivalent slot length with the sixth slot of the Japanese DBS antenna should be obtained.

The radiation power of a straight slot for these parameters are calculated by using the straight slot analysis including the mutual couplings from other slots mentioned in Chap. 3. We use the slot length of 9.67 mm which radiates the same amplitude of power with the Japanese one.